FINAL REPORT - DEVELOPING MODEL ASPHALT SYSTEMS USING MOLECULAR SIMULATION

Michael L. Greenfield and Liqun Zhang
Dept. of Chemical Engineering
University of Rhode Island
Kingston, RI 02881
greenfield@egr.uri.edu

initial draft: 11/21/2005
revised draft: 9/1/2009

URITC PROJECT NO. 000216

PREPARED FOR
UNIVERSITY OF RHODE ISLAND
TRANSPORTATION CENTER

Technical Report Documentation Page

1. Report No.	2. Government Accession No.	3. Recipient's Catalog No.
000216	N/A	N/A

4. Title and Subtitle	5. Report Date
Developing Model Asphalt Systems using Molecular Simulation	September 1, 2009
	6. Performing Organization Code: N/A

7. Author(s)	8. Performing Organization Report No.
Michael L. Greenfield and Liqun Zhang	N/A

9. Performing Organization Name and Address	10. Work Unit No. (TRAIS)
University of Rhode Island, Dept. of Chemical Engineering, 205 Crawford Hall, Kingston, RI 02881	N/A
	11. Contract or Grant No.: URI 2301 0000216, 2301 0000259

12. Sponsoring Agency Name and Address	13. Type of Report and Period Covered
URI Transportation Center, Carlotti Administration Building, 75 Lower College Rd., Kingston, RI 02881 *and* RI Department of Transportation, Research & Technology Division, Two Capitol Hill, Providence, RI 02903	Final , 1/2004 – 11/2005
	14. Sponsoring Agency Code

15. Supplementary Notes
None

16. Abstract

Computer based molecular simulations have been used towards developing simple mixture compositions whose physical properties resemble those of real asphalts. First, Monte Carlo simulations with the OPLS all-atom force field were used to predict the density, heat capacity, thermal expansion coefficient, and isothermal compressibility for small molecules similar to compounds found in asphalts. Similar calculations were then performed on a 3-component mixture for which detailed property measurements were available in the literature. Good agreement between simulation predictions and experiment (literature values) was found in all cases. Molecular dynamics simulations were then used to estimate the same properties for two asphalt-like mixtures. Different molecules were chosen to reflect the maltene, resin, asphaltene components of an asphalt, with each mixture based on a different asphaltene structure taken from the literature. Different density, glass transition, and bulk modulus properties were found for the mixtures, indicating the effects of different asphaltene structures. Distributions in molecular orientation between molecules were also calculated, to learn the extent of predicted parallel vs. perpendicular ordering in the mixture. A key finding is that molecules tend to order randomly over 3 nm length scales. A literature review of related asphalt chemistry is included in the report as well.

17. Key Word	18. Distribution Statement
asphalt, asphalt chemistry, asphalt composition, asphalt model, glass transition, molecular simulation, molecular dynamics, Monte Carlo, asphalt speciation	No restrictions. This document is available to the Public through the URI Transportation Center, Carlotti Administration Building, 75 Lower College Rd., Kingston, RI 02881

19. Security Classif. (of this report)	20. Security Classif. (of this page)	21. No. of Pages	22. Price
Unclassified	Unclassified	109	N/A

Form DOT F 1700.7 (8-72) Reproduction of completed page authorized

Abstract

Computer based molecular simulations have been used towards developing simple mixture compositions whose physical properties resemble those of real asphalts. First, Monte Carlo simulations with the OPLS all-atom force field were used to predict the density, heat capacity, thermal expansion coefficient, and isothermal compressibility for small molecules similar to compounds found in asphalts. Similar calculations were then performed on a 3-component mixture for which detailed property measurements were available in the literature. Good agreement between simulation predictions and experiment (literature values) was found in all cases. Molecular dynamics simulations were then used to estimate the same properties for two asphalt-like mixtures. Different molecules were chosen to reflect the maltene, resin, asphaltene components of an asphalt, with each mixture based on a different asphaltene structure taken from the literature. Different density, glass transition, and bulk modulus properties were found for the mixtures, indicating the effects of different asphaltene structures. Distributions in molecular orientation between molecules were also calculated, to learn the extent of predicted parallel vs. perpendicular ordering in the mixture. A key finding is that molecules tend to order randomly over 3 nm length scales. A literature review of related asphalt chemistry is included in the report as well.

Keywords: asphalt, asphalt calculation, asphalt composition, asphalt model, bitumen, density, molecular dynamics, molecular simulation, Monte Carlo, OPLS, orientation

Contents

List of Figures

List of Tables

Executive Summary

Computer simulations have been conducted in order to calculate the physical properties of mixtures of molecules, with their concentrations chosen so they serve as a simplified model of asphalt. Different molecules were chosen to reflect the maltene, resin, and asphaltene components of an asphalt. The energies and forces originating from each molecule are represented using classical mechanics-based equations for the contributions from each atom, with the underlying parameters taken from established studies in the chemistry literature. The outcomes of the simulations are predictions of how model asphalts behave over length scales of 1-5 nm and 1-10 ns (1 nm = 10^{-9} m, 1 ns = 10^{-9} s). For properties such as density and heat capacity, which lead to predicting glass transition, these small scales are sufficiently large for predicting macroscopic behavior of the mixture.

One long-term use of model asphalts is to assist with interpreting experimental measurements on real asphalts. For example, why are particular experimental trends observed, such as an increase in the upper temperature of the glass transition range when the asphaltene content in an asphalt is artificially increased? (This was observed in studies at the Western Research Institute in the 1990's.) The mixtures created in this study form a starting point for addressing such questions on the molecular level. Ongoing work is addressing such questions for polymer-modified asphalts.

Another long-term use of the model asphalt mixtures is to use them to address molecular-scale questions about asphalts that are difficult or impossible to answer experimentally. How do different kinds of molecules work together to achieve the overall response of asphalts to physical, chemical, or environmental stresses? The challenge with model asphalts will be to recognize the extent that subtle chemical nuances among molecules can be combined into larger amounts of few molecules.

In this study, the Monte Carlo simulation technique was first used to test the literature parameterizations by predicting properties of asphalt-like small molecules, such as naphthalenes and phenanthrenes. The same method was then applied to an asphalt-like mixture for which detailed property measurements were available in the literature. Good agreement between predictions and literature values was found in all these cases.

Selected molecules from the parameterization tests were combined with asphaltene molecules selected from the literature in order to constitute the asphalt-like model mixtures. Molecular dynamics simulations were found to be more effective than Monte Carlo for reaching equilibrium states with these mixtures. The resulting predictions of density and heat capacity showed qualitative trends that were consistent with known experimental characterizations of real asphalts. Quantitatively, the model asphalt density was too low due

to saturate alkane in the mixture being overabundant; this was recognized only when the project was being completed. The densities and heat capacities suggested a sub-zero ∘C glass transition, but noise in the simulation prevented a more precise determination. Calculations of the orientations between different parts of the same molecule suggested that asphaltenes may buckle slightly more than smaller aromatic molecules, even under low load conditions; this is being quantified further in follow-up work. Orientations between different molecules that fall within a 30 Å center-of-mass separation were largely equivalent to those of randomly packed molecules. This counters hypotheses that aromatic molecules would all orient parallel to one another. Within this overall random orientation, some weighting towards parallel configurations was found in the mixture based on asphaltene molecules with a large aromatic core and small side chains. Asphaltenes with a smaller core and longer side chains, which are shapes consistent with fluorescence depolarization data, were not oriented parallel to a large extent.

In total, this report documents the simulation methods employed, method verifications using simple molecules and mixtures, and the application of those methods to asphalt-like mixtures. A literature search describing different measurements related to the underlying chemistry and structure of asphalts is included as well. The mixtures developed are predicted to display properties that are similar to those of real asphalts but are not exactly the same. Refinements to these models are being undertaken in followup studies.

Chapter 1

Introduction

Asphalts used in road construction are complicated, poorly defined, and inexpensive mixtures of hundreds of chemical compounds [1]. Consequently asphalt physical properties measured under extreme conditions, such as hot or cold temperatures, can span wide ranges, depending on the material source and its physical, thermal, and chemical treatments during processing [1]. Within pavement and roadway design, predictive modeling tools developed for chemical mixtures are then poorly equipped for guiding improvements to asphalt properties.

What if simplified, chemically well-defined mixtures were known that could replicate the different behaviors of asphalts under conditions of interest? They would be useful for developing and testing methods for modifying asphalts in order to obtain targeted physical properties. Careful experimentation, which is today's standard, could then be supplemented by accurate, predictive modeling tools. Ultimately this combination of tools could create engineering opportunities for high-performance highway asphalts to be produced at near-commodity prices.

Projects sponsored by the Strategic Highway Research Program (SHRP) took a first step in this direction by creating a library of so-called "core" asphalts [1–4]. These asphalts are well-defined from a highway engineering perspective, and they have provided a context for subsequent research studies into asphalt modification strategies, the different contributions to physical properties from different asphalt components, etc. [5]. While tremendous amounts of knowledge have been obtained, and recommendations for improved asphalt binders have already been put in place [6], the question of which chemical process or procedure provides the best modification strategy remains an open question. The SHRP core asphalts provide a good starting point and excellent data, but in themselves they are not sufficiently well-defined on a chemical basis for answering all molecular-level asphalt research questions that may be of interest.

1.1 Research Project

The goal of this research has been to use several chemical engineering modeling techniques to develop — on the computer — idealized combinations of chemicals that form mixtures whose physical properties

are predicted to be representative of SHRP core asphalts. Such mixtures would not replace asphalts in engineering applications. Instead, they would provide inputs for fundamental studies in order to elucidate why different asphalts exhibit different physical properties, and how those properties could be tuned to more desirable values. Analogous techniques based on solution thermodynamics have been developed in fuel science [7, 8]. The fuel research results were mixtures (also called "recipes") of 5-10 chemicals that exhibit physical properties, such as temperature-dependent volatility, that resemble those of real fuels.

The calculations in this project were performed using molecular simulations. The overall ideas and methods involved in molecular simulations are described in chapter 3.

1.2 Overall Chemical Description of Molecules in Asphalt

An overall chemical description of the molecules in asphalt is important for predicting additive solubility and for assessing possible chemical reaction mechanisms. Measurements such as nuclear magnetic resonance (NMR) spectroscopy can reveal the balance among aromatic, linear alkane, and branched alkane chemical groups within an asphalt [9]. We consider it important for a model asphalt to capture this approximate balance in order to make reasonable estimates of how additives, such as polymers or plasticizers, will modify an asphalt material. An advantage of using mixtures in simulations is that not all NMR features have to be placed in a single, "average" molecule. Contrasting molecular features, such as polar vs. nonpolar, aliphatic vs. aromatic, or linear vs. branched, can be placed on different molecules in the mixture in order to provide both an appropriate composition and a correct balance of properties.

Existing asphalt chemical models provide some guidance about the size and polarity of different compounds found in asphalts. Traditionally asphalts have been described using a "micellar model," in which polar compounds with aromatic functional groups (benzene rings, etc.) are dispersed in less polar, "solvent"-type molecules of lower aromatic content. (See ref [1] for the history of this model.) The dispersed molecules also contain heteroatoms (atoms other than carbon or hydrogen) and have a larger molecular weight compared to the solvent phase. Comparing among asphalts, differences have been reported in the size of the polar domains: smaller packets of polar molecules (better solvation) vs. larger ones (poorer solvation, with larger interfacial energies). Turner and Branthaver [10] found that the mixture comprising the polar phase can be separated from the remainder of the nonpolar asphalt mixture via size exclusion chromatography, confirming the appreciable difference in molecular weight. This overall polar/nonpolar description provides a useful hierarchy for interpreting composition studies and mechanical properties. The results from the proposed research will differ in that simplified, molecularly specific compositions will become available as part of the results.

1.3 Physical Properties

The focus here is to create mixtures that replicate several physical properties of asphalts that strongly affect overall highway performance and durability. The research focused on properties that are well-defined in a laboratory setting and, preferably, that are realizable on the molecular level (also called the "nanoscale" in recent research trends). Examples of physical properties amenable to molecular-level chemical modeling tools are density, coefficient of thermal expansion, viscosity, and modulus. It is recognized that these properties are not of primary interest (or perhaps much interest at all) in asphalt binder specification and/or pavement design. They are chosen here because they are the properties predicted in the most straightforward manner from a molecule simulation. Macroscopic-level highway-level properties, such as cracking or rutting, require additional information about road design and structure that isn't accessible from the tools planned for use in this study. In follow-up work to this project [11], methods are discussed for estimating the shear viscosity of a model asphalt and its temperature dependence. Those methods, results, and relationships to real asphalt binders will be available in the final report from that project.

Which properties of interest to highway usage of asphalts may be investigated on the molecular level? The glass transition defines the range of temperatures over which an asphalt changes from a hard, brittle, high modulus material (low temperature) to a softer, more elastic, moderate modulus material (warmer temperatures). Below the glass transition, molecules are essentially locked in place and execute only slow, local motions [12]. This potentially could benefit highway rutting resistance, since little asphalt flow can occur. However, little energy can be absorbed, making the asphalt brittle. Above the glass transition, molecules move freely and can reach new equilibrium arrangements (or "configurations") after an imposed physical perturbation, such as experiencing shearing forces from a vehicle. This more facile mechanical response allows an asphalt system to resist cracking. However, the various moduli decrease as an asphalt is heated through the glass transition, potentially making a road more prone to rutting. Clearly an appropriate balance must exist in a successful roadway material. The glass transition behaviors of core asphalts are available from both fundamental studies [2] and later research studies [10], for comparison purposes. For SHRP core asphalts, the glass transition begins at low temperatures of -45 to -25°C (-49 to -13°F) and ends over -6 to 10°C (21 to 50°F) [10].

Asphalt stiffness is a measure of its stress-strain behavior. The larger the modulus (Young's modulus, shear modulus, or bulk modulus for tension, shear, or compression respectively), the smaller the deformation in response to an imposed stress [13]. Similarly, the maximum stress as a function of strain equals the material strength. In relation to highway performance, Kluttz and Dongre [14] have reported that a low-temperature binder stiffness of greater than 300 MPa, measured after 7200 seconds of load, is correlated with pavement cracking at that same temperature [3]. This was the motivation for specifying the stiffness (equivalent via time-temperature superposition) after 60 s at 10°C above the lower specification temperature. Correlations have also been made between pavement cracking and properties such as viscosity and ductility [3, 15]. The time-dependence is a consequence of viscoelasticity: the ability of a material (such as asphalt) to generate stress in response to both imposed strain (like an elastic solid) and imposed strain rate (like a

viscous liquid). The temperature-dependent viscosity is related to the shear modulus at small deformations via the methods of oscillatory shear [12]. Property data for asphalts are again available for core asphalts [2], providing another target for the calculations.

1.4 Project Objectives

The key objective of this 12-month project was a model asphalt composition that is predicted to display physical properties similar to those of Strategic Highway Research Program (SHRP) core asphalts. These compositions can then be used in subsequent asphalt property prediction studies, using both modeling and experiments to study length scales that range from molecular to macroscopic. A long-term objective is to use the model asphalts to look as asphalt modification. While many chemical processes and/or procedures are currently used to modify asphalt properties, the question of how *best* to improve asphalts and *why* such methods work or fail remains an open question. One goal of the current project is to take a step towards a molecular modeling platform in which such questions can be addressed.

Several specific tasks must be accomplished in order to accomplish these goals:

- Propose simplified asphalt mixtures based on asphalt characterizations in the literature.
- Conduct molecular simulations on model mixtures to explore and interpret the "whys" of asphalt function.
- Compare physical property predictions from simulation to literature data. Use results and new knowledge to improve and optimize model compositions.
- Each molecular simulation could require days to weeks of computer time, so there is a limit on the number of iterations that can be conducted.

A desirable stretch objective that is probably not achievable within the 12-month time frame is

- Test asphalt additive strategies using molecular simulation. Keep parameters fixed so predictive capabilities can be tested. One example would be to analyze how polymers and plasticizers affect asphalt modulus as a function of temperature.

Such questions are being addressed during a subsequent project in the current year.

While conducting the work, it was recognized that the mismatch between the properties that are easest to calculate first and the properties of most interest in practice (to asphalt chemists and pavement engineers) created a situation in which extensive, direct comparisons with the same properties of SHRP core asphalts were not possible. Comparisons with "typical" asphalt properties found in any source have been made instead. Details of the materials being compared represent an attempt to make the comparisons useful for readers of various interests.

1.5 Task Descriptions

Determining a chemical mixture that replicates asphalt properties requires answering two overall modeling questions. 1) What physicochemical modeling approach yields sufficiently accurate property predictions for asphalt-like mixtures, while maintaining molecule-level detail? 2) Within such a model, what sets of chemical compounds lead to good agreement with the desired properties? Both questions rely on knowing values and ranges of the asphalt physical properties that are to be replicated by the models discussed above.

The following specific tasks were chosen for this project:

Task 1. Method Validation

The first task is to validate the overall approach using pure compounds that are similar in size, shape, and chemical functionality to those found in asphalts. An example is predicting the glass transition of alkyl-substituted naphthalene molecules, which have structures shown in Figure 4.1. Molecules will be chosen for which experimental glass transition data are available in the literature. The intent of this task is to demonstrate that molecular simulation approaches using parameterized force fields are sufficiently accurate for moderate molecular-weight compounds, such as found in asphalts.

Task 2. Initial Mixture Simulations

The second task is to choose small sets of molecules whose presence in asphalt and relative concentrations are consistent with NMR asphalt speciation data [9, 16]. Preliminary asphalt mixture simulations will be conducted using these compositions. Specifically, Monte Carlo and/or molecular dynamics simulations will be used to determine equilibrium densities, expansion coefficients, glass transition ranges, and moduli for the proposed mixture. These results will then be compared to literature data for a SHRP core asphalt. Differences will be quantified between the predicted results for the model composition and the measured results for the core asphalt. Differences in glass transition that result from small changes in molecular structure will assist with interpreting the glass transition behavior of complete asphalt mixtures.

Task 3. Mixture Composition Iteration

The third task is to modify the model mixture composition in order to achieve different physical properties. Based on the results from Task 2, relative concentrations will be changed and new simulations will be conducted. The goal is to obtain predicted results from the model system that are comparable to those of the desired experimental system. This process will iterate until convergence is as good as possible. It is expected that many iterations will be required.

Task 4. Other SHRP Core Asphalts

The steps in Task 3 will be repeated, using the properties of another SHRP core asphalt as the target. This task will be repeated for each core asphalt of high interest.

1.6 Outline of this report

This report documents the first steps of the overall research project in developing model asphalts. Chapter 2 summarizes related scientific literature in the fields of asphalt characterization and asphalt chemistry. Chapter 3 explains the kinds of modeling tools used in this report and illustrates examples of intermediate results. Chapter 4 applies these methods systematically to small molecules that have chemistries similar to those in asphalts. Chapter 5 shows how the same methods can be applied to a well-defined mixture, in order to predict mixture properties accurately. Chapter 6 describes the model asphalt mixtures and compares their predicted properties with those of real asphalts. Molecular scale properties and ideas that can be inferred from the model systems are discussed as well. Finally, chapter 7 concludes the report by relating the modeling findings to the original tasks.

Chapter 2

Literature Survey

The objective of this chapter is to summarize information available in the scientific literature about the molecular nature of asphalt. No works were found that seek the exact goals of this project. The many works available instead provide context and guidance for the choice of molecules and relative concentrations to use in this work.

2.1 Project Context

Several projects sponsored by the Strategic Highway Research Program (SHRP) of 1987-1992 addressed the challenge of characterizing and evaluating asphalt binders. Within SHRP, the "Binder Characterization and Evaluation" project was conducted by the Western Research Institute (WRI), the Pennsylvania Transportation Institute (at Penn. State University), SRI International, and the Texas Transportation Institute (at Texas A&M University), with the goal of understanding asphalt properties and their relationship to asphalt composition and composition changes [1]. The Volume 1 report [1] provided an overall summary of asphalt properties. Subsequent volumes focused on the specifics of asphalt chemistry [2], physical characterizations (particularly mechanical tests such as rheology) [3]), and experimental details of new/improved test methods [4]. Studies by Jennings and co-workers within SHRP focused on NMR characterization of asphalts [9]. Tremendous amounts of knowledge have been obtained through SHRP, and the "Superpave" asphalt specifications for improved asphalt binders were recommended as a result [6, 17].

Part of the SHRP project involved creating a library of so-called "core" asphalts. These asphalts are well-defined from a highway engineering perspective, and they have provided a context for subsequent research studies into asphalt modification strategies, the different contributions to physical properties from different asphalt components, etc. [5]. The SHRP core asphalts provide a good starting point and excellent data, but in themselves they are not sufficiently well-defined on a chemical basis for answering all molecular-level asphalt research questions that may be of interest.

2.2 Transportation Databases

To ensure that the problem and questions being considered in this research have not been solved already, literature searches were first conducted using the databases TRIS (Transportation Research Information Services) and RIP (Research In Progress). General-purpose research books in the asphalt area were also searched. These sources were then supplemented with literature references obtained from ArticleFirst, a general-purpose research database.

2.2.1 TRIS Search Term: Asphalt Composition

54 studies appear using these keywords. Titles and references of all the studies are listed in Appendix 1, grouped into the following categories:

- Aggregates and Adsorption
- Aging
- Characterization
- Design
- Performance
- Polymer
- Rheology
- Roadway
- Safety

Many studies tend to be experimental characterizations of asphalt properties and composition effects. Some are interim and final reports from funded transportation projects. Others appear in journals, such as the Journal of the Association of Asphalt Paving Technologists (ISSN 0270-2932).

The data reported are useful in defining typical ranges of physical properties of asphalts, providing specific cases of additive enhancement (which can be used to test predictive abilities), and collecting lists of additive strategies already employed. The SHRP reports and Superpave descriptions prescribe the high and low temperature properties of interest — $|G^*|/\sin\delta$ and (s and m), respectively. Connections grounded in polymer science between storage modulus G', loss modulus G'', and viscosity η provide a crucial connection to $|G^*|$, the magnitude of the complex shear modulus; δ, the loss tangent ($\tan\delta = G''/G'$); and m, the slope of strain vs. time (creep). Papers that report connections between highway properties and asphalt rheology [18, 19] are useful as well. Rheological properties can be extracted from molecular dynamics simulations or laboratory experiments, while highway performance provides a direct connection to the desired applications.

2.2.2 TRIS Search Term: Asphalt Additive

117 studies appear with these keywords. Most papers are experimental characterizations of asphalts, using lab tests or roadway data. Some look at additive modeling strategies. Combinations of experiment and modeling [20, 21] will be useful for simultaneously testing simulation predictions and comparing them with expectations from modeling studies.

Papers and reports that combine the results of both of these searches [22,23] will help to relate the macroscopic properties accessible via molecular simulation to properties of interest for highway engineering, such as roadway durability.

Additional papers concerning additives in asphalts can be found in journals specific to the field. For example, several articles in Journal of the Association of Asphalt Paving Technologists that address additive issues can be located via the Association of Asphalt Paving Technologists (AAPT) web site at

http://www.asphalttechnology.org/journals/Additives.html

Specific articles available from the ArticleFirst database and the book Asphalt Science and Technology [5] will help with devising model compositions for asphalt mixtures.

2.2.3 TRIS Search Term: Molecular Simulation

No papers were listed in the TRIS database with the keywords "Molecular Simulation."

2.2.4 RIP Searches on Related Terms

RIP keyword searches using "asphalt* AND additive" or "asphalt* AND composition" led to several studies looking at experiments with different additives in asphalt: lime, liquids, or polymers for anti-stripping; crumb rubber or carbon black (from rubber) for improved physical properties. Titles, dates, and funding sources are listed in Appendix 2 (asphalt* and additive) and Appendix 3 (asphalt* and composition). Based on the project summaries, none appear to have been modeling studies. Instead, their results could be useful as input test cases for the next stages of this research project. A RIP search on "molecul*" had no results, confirming the TRIS finding that no current transportation research can be described with keywords such as "molecule" or "molecular."

2.2.5 Additional Searches

The papers and reports obtained from the TRIS and RIP searches are useful regarding highway-relevant properties and overall asphalt descriptions. They are lacking, however, in the fundamental aspects of asphalt chemistry that are necessary for simulating model asphalts on the molecular level.

To extend the search in this direction, books in the University of Rhode Island (URI) library were studied and a database of published scientific literature, ArticleFirst, was searched. It contains approximately 13,000 literature citations from many published sources in science and engineering. For a description of ArticleFirst, see http://www.oclc.org/firstsearch/; for on-site URI access see the link from "URI library, general reference" at http://www.uri.edu/library/reference_databases/ref.html. This process, supplemented by citations from the papers found, led to numerous publications that assisted with conducting the current project.

2.3 Books

Several books contain useful information for asphalt research. This survey will describe only a subset of the books available at URI. *Hot Mix Asphalt Materials, Mixture Design, and Construction* [24] provides

an overall introduction from a civil engineering perspective; it is used as the textbook in the URI Civil Engineering graduate course CVE 531 Bituminous Materials. Concerning asphalt chemistry, Roberts et al. write

> the importance of asphalt chemical composition, although not well understood, cannot be disputed. The performance of asphalt as a binder ... is determined by its physical properties ... which in turn are determined directly by chemical composition [24].

The Chemistry and Technology of Petroleum [25], which is available on-line, provides an overall description of petroleum, its components, and their processing. *Asphalt Science and Technology* [5], edited by Usmani, contains papers authored by numerous researchers funded by the Strategic Highway Research Program (SHRP). The topics range from molecular characterizations, such as nuclear magnetic resonance (NMR) spectroscopy and rheology of SHRP "core" asphalts, to polymer modifications and performance-modification relationships. *Chemistry of Asphaltenes* [26] is an analogous 1981 collection of papers presented at the September 1979 American Chemical Society meeting. It contains numerous interesting characterizations about asphalt structure. 1990's characterization techniques (described below) may have outdated many of the contributors' hypotheses and conclusions, however.

These different sources [24, 25] provide an overall description of the make-up of asphalt cement. Crude oil distillation residue can be fractionated, based on *n*-pentane or *n*-heptane solubility, into insoluble *asphaltenes* and soluble *maltenes* (sometimes called *petrolenes*). The asphaltenes can be subsequently dissolved into an aromatic solvent, such as toluene. The maltenes can be further subdivided by a variety of procedures based on adsorption and/or chromatography. One subdivision leads to *resins* and *oils*; the latter resemble more volatile paraffinic (waxy) crude oil components but are of higher molecular weight. An alternate process leads to a more detailed subdivision into *saturates*, *naphthene aromatics*, and *polar aromatics*. Within the asphalt cement, it had been thought (this is now a matter of debate in the literature) that asphaltenes cluster into larger shapes ("colloids"), which are soluble because resins mediate the interactions between asphaltenes and saturates. This activity is analogous to that of surfactants in soap solutions. The size of these colloids is often a topic of research interest. More recent studies (e.g. within SHRP [1]) have suggested that asphalts contain molecules with a range of solubilities. This idea is discussed further in chapter 6. In this project it is necessary to include molecules that reflect properties of each of these chemical families.

2.4 Journal Articles

Initial papers were identified by ArticleFirst, and subsequent papers were found by tracking citations from papers already identified. The resulting set of journal articles are divided here into the following topics:

2.4.1) Molecular spectroscopy characterizations

RICO NMR scattering

2.4.2) Thermal and mechanical characterizations

DSC rheology

2.4.3) Performance and molecular characteristics

2.4.4) Molecular simulation of asphalt

structure elucidation	molecular dynamics	molecular thermodynamics

Note that acronyms are defined as terms arise in each subsection. Each section contributes a complementary perspective to the overall project.

2.4.1 Molecular Spectroscopy Characterizations

Several researchers have conducted molecular-level investigations of asphalt structure. Strausz and co-workers published a 1992 review [27] that describes their significant efforts in deciphering asphaltene chemistry. Most significant was their findings, via a novel catalyzed chemical reaction "RICO" (ruthenium-ion-catalyzed oxidation), that extended aromatic domains are not present in asphaltenes! Instead, alkyl-substituted sections of two to five fused aromatic rings were connected by sparse, short to moderate length alkyl branches. Extended naphthenic domains (i.e. alkane rings, such as substituted cyclohexane) also played a major role. Later RICO studies [28, 29] focused on characterizing minor products and found a large array of naphthenic-related compounds. Experimental protocols for these studies were also more effective procedures (due to improvements in the analytical chemistry) and thus were "expected to yield more accurate quantitative data" [28]. Table 3 of ref [28] contains an especially useful compilation regarding asphaltene composition; it lists relative concentrations of many compounds. In a related study [30], broad similarities in composition were found for asphaltenes from different sources, with the exception of more "immature" (i.e. less ancient) petroleum sources. RICO studies have also been combined with analyses based on ^{13}C nuclear magnetic resonance (NMR) spectroscopy [31]. The data from each method assisted with interpreting the other, and a four-compound model asphaltene molecule mixture was proposed. It can't be assumed that all asphalts contain asphaltenes with this precise composition. Instead, these results provide guidance about *reasonable* compositions, particularly in light of asphaltenes from many different sources showing similar RICO results.

Storm et al. [32] of Texaco proposed a data analysis technique for assessing molecular weight estimates measured via mass spectroscopy. They estimated maximum molecular weights of approximately 700-1000 g/mol for the oil, resin, and asphaltene components in different crude oil fractions.

Storm et al. [33] also studied asphaltenes via ^{1}H and ^{13}C NMR spectroscopy. These experiments yielded ratios for the distribution of molecular environments in oils, resins, and asphaltenes. Their results suggested smaller molecular structures than often postulated in the literature, e.g.

> we believe ... the PNA (polynuclear aromatic) cores contain about 4 to 6 rings, instead of

25, and only a few PNA cores are bridged together, instead of many, as in the polymer-like representations suggested by other work [33]

These sizes are consistent with the findings of Strausz and co-workers. From the perspective of this project, they enable the chemistries of proposed asphalt mixtures to be compared with the compositions of measured asphalts.

Gillet et al. [34] discussed the ^{1}H and ^{13}C NMR spectral shifts observed for the different environments for hydrogen and carbon atoms that are present in crude oil and its derivatives. They also discussed the use of an additional molecule (1,4-dioxane in their case) as an internal standard, which allowed for a (C area):(H area) ratio to be calculated; such a calibration enables quantitative estimates of the fraction of carbon and hydrogen found in each kind of chemical environment. In a follow-up study [35], they quantified the distributions of carbon and hydrogen environments in a synthetic oil (of known composition) and in the higher boiling ends of an Arabian Light crude oil. The asphalt fraction was highest in aromatics, with approximately one in five aromatic carbons attached to an alkane chain and the same number attached to hydrogen. Alkanes were in chains, rather than rings, by a ratio of approximately 7:3.

Jennings et al. [9] applied NMR techniques to numerous SHRP core asphalts. They found different fractions of aromatic vs aliphatic, different extents of branching and aromaticity, and different molecular mobilities among the different core asphalts. Their report provides an excellent source for comparing molecular compositions with data for those core asphalts most of interest to the project sponsors. In a later study [16], they used NMR to quantify oxidation that occurs at carbon atoms bonded to aromatic rings.

Pekerar et al. [36] used solid-state ^{13}C NMR to assess asphaltene and resin mobility. They found rigid domains among both the aromatic and aliphatic carbons. The aromatic contribution is expected, since fused aromatic rings (e.g. naphthalene) largely constrain atom positions in a solid phase. The aliphatic results indicate contributions from naphthenic rings.

Characterization studies have also measured heteroatoms (i.e. atoms other than carbon and hydrogen) in asphaltenes. Frakman et al. [37] focused on oxygen-containing compounds, using a set of chromatography experiments to find fluorenones, alkylfluorenones, and alkylbenzylfluorenones. Fluorenone is a 5-membered ring in which one carbon atom is double bonded to an oxygen atom (this is a carbonyl group) and the remaining carbon atoms are fused in pairs to phenyl rings. (Despite the name, it does not contain any fluorine.) Their chromatography measurements also yielded approximate concentrations of these compounds in an Athabasca asphaltene. (Note that Athabasca asphaltenes are not necessarily the same compounds as found in paving asphalts. Instead, the compounds found in paving asphalt depend on the crude oil source.) Green et al. [38] used exchange reactions to study sulfur compounds. Each sulfur-containing molecule was chemically converted to a methylsulfur salt; the methyl group chemical environment was then determined via ^{13}C NMR. Several thiophenes were identified, but the process was ultimately only semi-quantitative.

Several characterization studies have found results consistent with the long-standing idea [25] that asphalts contain micelles of asphaltenes surrounded (or solubilized or "peptized") by resins. Such structures are sufficiently stable that they remain clustered together within characterization experiments that "count"

individual molecular-scale entities. For example, small angle neutron scattering studies have been conducted to study asphaltene polydispersity effects [39] and temperature effects [40] in solution. Rod-like particles were found in the latter, with radii that dropped from 18 Å at room temperature to 13 Å at 150°C. Lengths ranged from 20–150 Å, with both the maximum and average lengths decreasing with increasing temperature. Dielectric measurements [41] also support the idea of asphaltene-resin clusters of radius ca. 30 Å. Storm et al. [42] also found that the measured size was the same in toluene solution and in vacuum residue, based on solution rheology. This was consistent with their finding [42] that the sizes in small angle neutron scattering and X-ray scattering (room temperature and 93°C, respectively) were similar.

Miller et al. [43] compared the compositions of maltenes, asphaltenes, and hydrocracked derivatives from a Mayan crude oil. They found that asphaltenes could be further extracted into soluble (i.e. non-colloidal) and insoluble (colloid structure forming) fractions. Characterizations via vapor-phase osmometry, size exclusion chromatography, and small angle neutron scattering revealed average sizes (in solution or suspension) of 50 Å in maltene and noncolloidal asphaltene and of 150 to 850 Å in colloidal asphaltene [43]. The molecular weights of 300-600 g/mol, from laser desorption mass spectroscopy, indicate that the particle sizes represent sets of particles, since an object of even 50 Å radius has a molecular weight much greater than 600 g/mol. (A 23 Å edge cube of hydrocarbon material has a molecular weight of 6000 g/mol, for example.)

Fluorescence depolarization studies by Mullins and co-workers [44, 45] focused on asphaltenes. They imposed very dilute conditions and a preparation method that was expected to create individual asphaltene molecules surrounded by solvent. The depolarization rate of asphaltene fluorescence was consistent with each asphaltene molecule having only 1 or 2 aromatic cores. The frequency in the fluorescence spectrum suggested that each aromatic core consisted of a small number (4–10) of fused rings. They also observed significant overlaps in size between resins and asphaltenes.

Detailed composition data have been measured for overall crude oil mixtures by Pedersen et al. [46]. Their results cannot be transferred directly to asphalt studies because the measurements were made prior to the crude oil distillation process.

These characterization papers assist the present research in that they provide guidelines about which kinds of molecules are present at higher concentrations in asphalt. Additional papers will be introduced and discussed in more detail in later chapters. In total, these works facilitate choosing molecules and concentrations that are consistent with asphalt speciation data from NMR, RICO, etc. Model asphalt mixtures described already (see below) are of particular interest for preliminary simulations.

2.4.2 Thermal and Mechanical Characterizations

The glass transition behaviors of core asphalts are available from both fundamental studies [2] and later research studies [10], for comparison purposes. Turner and Branthaver [10] used differential scanning calorimetry (DSC) to study the glass transition behavior in different SHRP core asphalts. They then measured the change in glass temperature after each asphalt was chemically modified by adding or remov-

ing various amounts of waxes, maltenes (oil/resin mixtures), and/or asphaltenes. Other specific alkane and aromatic molecules were also considered. For SHRP core asphalts, the glass transition begins at low temperatures of -45 to -25°C (-49 to -13°F) and ends over -6 to 10°C (21 to 50°F) [10]. Increasing asphaltene concentration tended to increase the end point of the T_g region, while the starting (i.e. lower) temperature remained unchanged. This behavior was common among several core asphalts. This behavior is consistent with the later findings of Glover et al. (see below).

Shenoy has presented a rheology approach that adapts the melt flow index (of polymer engineering) to characterization of unmodified [47] and modified asphalts [20]. Under the usual simplifying assumptions about melt flow index employed in polymer flow analyses [13], shear stress and shear rate (which convert to storage and loss modulus data required in Superpave measurements [3, 17]) are predicted to lie on a unified curve. In follow-up work using SHRP core asphalts [21, 48], Shenoy showed that these guidelines were largely followed over moderate ranges of frequency for both unmodified asphalts and for asphalts combined with polymer additives. He later showed [49] that aging effects can be correlated via a shift factor that depends on temperature and load conditions. Melt flow index was not used in this simulation project. While it is straightforward to define experimentally (mass that flows over a specified time while under a specified load, in a specified geometry), it is not possible to calculate it using the simulation tools available in this work.

2.4.3 Asphalt Performance and its Molecular Characteristics

A few authors have looked at aspects that relate overall performance qualities of asphalts to their underlying molecular behavior. Netzel et al. [50] looked, using NMR and cross polarization effects, at the dynamics of several SHRP core asphalts and found differing underlying molecular mobilities. They also related their NMR findings to rheological studies of SHRP core asphalts [51].

In relation to highway performance, Kluttz [14] has claimed that a modulus of greater than 300 MPa, measured after 7200 seconds of load, is correlated with cracking [3]. Correlations have also been made between pavement cracking and properties such as viscosity and ductility [3, 15].

Glover and co-workers [52] have specifically measured the effects of asphaltene, saturate, and aromatic concentration on asphalt performance, using Superpave measurables. They found that increasing asphaltene concentration (at constant saturates concentration) increased the high-temperature performance grade while the low-temperature performance increased only slightly (often an increase within a single grade). In contrast, increasing saturates concentration (at constant asphaltene concentration) decreased both the low- and high-temperature performance grades by a similar amount. These data provide good tests for the calculations underway. The only disadvantage discussed [52] was significant increases in hardening susceptibility with increasing asphaltene or saturates content, which limited the immediate applicability of the results.

The properties of entire asphalt–aggregate mixtures need to be addressed using techniques applicable over longer length scales. Molecular simulations cannot be extended to such scales because the number of atoms becomes much too large. One method for longer length scales is finite element modeling. Examples

of finite element modeling of asphalt–aggregate mixtures include those of Sadd et al. [53] (performed at URI) and of You and Buttlar [54]. Other articles from the same journal issue could be useful in later project stages.

2.4.4 Molecular Simulation of Asphalt

This search was begun by using the term "Molecular Simulation Asphalt*" in ArticleFirst. Only one paper was found that contained "Molecular Simulation" and any string including "asphalt" [55]. Similar searches using the names of particular molecular simulation techniques in the keywords list yielded less than 10 additional papers [50, 56–62]. These papers, described below, provide a collective starting point for simulating model asphalt mixtures. Advances in so-called "force fields" (equations and parameters for estimating the strength of physical and chemical interactions among molecules) since 1996 should help with furthering these studies. While those papers do provide guidance, there is little overlap with the proposed work. Several papers do propose either a single "asphaltene" molecule or a set of molecules that reproduce the statistics of molecular environments. The search for particular sets of model mixture compositions that replicate desired **asphalt thermal and mechanical properties** is a new idea.

Structure elucidation in asphaltenes and related molecules

Michael Klein and co-workers [56, 60, 63–65] employed multiple data sources to create statistical approximations of "resid" — the petroleum residue after crude oil distillation is complete. The resid was represented by a collection of 10^3 to 10^4 noninteracting molecules, with the model system having molecular characteristics, such as atomic ratio, that matched those of real resids as reported from experiments. Model system properties were calculated via structure/property relationships [65]. The range of different molecular size distributions was used as a parameter in optimizing the predictions from these relationships [65]. Allowing for chemical reactions among species did not improve accuracy; instead the required computer time is better spent on simulating a larger system without reactions [64]. Average molecular compositions, molecular weights, and atomic ratios calculated from the simulations were reasonably consistent with experiment, as should be expected since they were simulation inputs. The resulting distributions provide useful inputs for the work in the current project, especially when combined with the more recent composition findings discussed above.

Kowalewski et al. [55] characterized the asphaltene fraction precipitated from a "Boscan" crude oil fraction. They then used so-called "structure elucidation" programs to create an asphaltene "molecule", based on available experimental data such as the measurements described above. In their case, a single $C_{618}H_{722}O_{10}N_{12}S_{20}$ molecule represented measured molecular properties — C:H ratio, C:O ratio, relative sizes of aromatic vs aliphatic components — on a statistical level. (Such a molecule is now viewed as being much larger than a single asphaltene, however.) Finally, they simulated this molecule with molecular dynamics, finding little change in the energy of conformation. Similar approaches have been applied in coal research, as reviewed by Carlson and Faulon [66].

The ongoing work here differs in that asphalt will be represented as a mixture of smaller compounds. Ironically, this should provide a closer representation to the measured data reported by Kowalewski et al. (and of Strausz and co-workers and of Storm et al.) than does their own single molecule.

Direct molecular dynamics of asphaltenes and related molecules

Several studies have analyzed asphaltene and resin interactions via molecular simulation, with a focus towards phenomena that impact solid precipitation during crude oil processing. Murgich et al. [67] emphasized the three-dimensional shapes taken on by resins and asphaltenes within crude oil. They chose large molecules with fused aromatic rings and extended alkane branches in order to represent the resin and asphaltene. In the latter, polar groups (acid, amine, thiophene) were located at the edges of extended aromatic regions. They found nonplanar distortions of the extended aromatic regions, with clusters of 4 asphaltene molecules being less favorable than clusters of 2 or 3 asphaltenes. The extended aromatic domains were inconsistent with the characterizations [27] of Strausz and co-workers, however.

In follow-up work, Murgich et al. [57] used molecular dynamics to simulate asphaltene and resin adsorption onto the mineral kaolinite, which is representative of rocks in petroleum reservoirs. Aromatic rings were planar to the surface. In the adsorbed phase, as in the asphaltene-asphaltene and asphaltene-resin cases, van der Waals forces dominated the interactions.

In still later work, Murgich et al. [68] modified their model asphaltene molecule in light of Strausz et al.'s findings regarding molecular composition (see above). The net result was a three-dimensional shape that showed significant van der Waals interactions with model resin molecules; these interactions were more favorable than those with *n*-octane (alkane) or toluene (aromatic) solvents of low boiling point [68]. The shapes of each molecule were described as "constant", but this is likely due to the simulations being relatively short — of order 25-100 ps.

Rogel and Léon [61] simulated low and high concentration adsorption of ethoxylated dodecylphenol amphiphiles (also called surfactants) on representative asphaltene molecules. They found more favorable adsorption at high surface concentrations (20 vs 1 adsorbed molecule) and noted that the thickness of the polar head group layer was independent of the size of the head group; the amphiphile apparently packed such that the entire head group could remain close to the surface.

Molecular thermodynamics of precipitation

More molecularly coarse "molecular thermodynamics" models have been developed to address the conditions under which asphaltene precipitation occurs. (These researchers' motivation is to enhance crude oil processing towards products more valuable than asphalt cement.) Wu et al. [58] developed a molecular thermodynamics framework for asphaltene-oil phase equilibria and applied it [59] to asphaltene precipitation. With this model they predicted regions of single or multiple phases among crude oil components, i.e. asphaltenes, resins, and oils. The asphaltenes and resins were each represented as a single component; the oils were treated as a continuous medium [58].

Victorov and co-workers [69, 70] proposed an asphaltene precipitation model based on self assembly of asphaltenes and resins. The resin-stabilized asphaltene micelle geometry was related to shape parameters. They obtained parameters that led to good agreement with precipitation data.

The paper by Li et al. [62] that arose in the initial search is appropriate to consider but is not actually in the area of molecular simulation. They used a Monte Carlo approach to determine the effects of a range of pavement parameters on predicted pavement performance. They chose the Present Serviceability Index (PSI) as the objective function; it was a function of Equivalent Single Axle Load (ESAL) application, within a standard roadway model. They found that their predictions showed trends consistent with those measured via accelerated aging.

Due to the absence of papers in the direct area of this proposal, we can be confident that the research here has not been performed before.

Appendix A: TRIS Search, "Asphalt Composition"

Note: The *Journal of the Association of Asphalt Paving Technologists* is found most easily by searching its ISSN number, 0270-2932. URI has a complete collection. The journal *Transportation Research Record* is found most easily by its ISSN number, 0361-1981.

Subtopic: Aggregates and Adsorption

- AN #: 00936359, "INFLUENCE OF THE SURFACE ENERGY STATUS OF AGGREGATES ON THE PERFORMANCE OF ASPHALT HOT MIX," Conference: Ninth International Conference on Asphalt Pavements, AUTHOR(S): Harders, O; Noesler, I, 08/2002.
- AN #: 00936054, "SURFACE ENERGY MEASUREMENT OF ASPHALT AND ITS APPLICATION TO PREDICTING FATIGUE AND HEALING IN ASPHALT MIXTURES," Journal: Transportation Research Record No: 1810, AUTHOR(S): Cheng, D; Little, DN; Lytton, RL; Holste, JC 2002.
- AN #: 00756177, "EFFECT OF FILM THICKNESS ON THE RHEOLOGICAL PROPERTIES OF ASPHALTS IN CONTACT WITH AGGREGATE SURFACE," Journal: Transportation Research Record No: 1638, AUTHOR(S): Huang, S-C; Branthaver, JF; Robertson, RE; Kim, S-S 1998. (ref [19])
- AN #: 00214305, "ASPHALT CEMENT DURABILITY AND AGGREGATE INTERACTION," 04/1973.
- AN #: 00127324, "MECHANICAL BEHAVIOR AND REINFORCEMENT OF MINERAL FILLER-ASPHALT MIXTURES," Journal: Association of Asphalt Paving Technologists Proc Vol: 42, AUTHOR(S): Anderson, DA; Goetz, WH 1973.
- AN #: 00210367, "FLOW IN AGGREGATE-BINDER MIXTURES," AUTHOR(S): Tons, E 02/01/1967.
- AN #: 00210371, "STUDY OF THE ELECTRO-CHEMICAL REACTIONS IN AN AGGREGATE- ASPHALT SYSTEM," AUTHOR(S): Wellman, RP 10/1966.
- AN #: 00210332, "THE TENSILE BEHAVIOR OF A BITUMINOUS CONCRETE MODEL," AUTHOR(S): Lavoie, RP 09/1965.

Subtopic: Aging

- AN #: 00756179, "ASPHALT AGING: DUAL OXIDATION MECHANISM AND ITS INTERRELATIONSHIPS WITH ASPHALT COMPOSITION AND OXIDATIVE AGE HARDENING," Journal: Transportation Research Record No: 1638, AUTHOR(S): Petersen, JC; Harnsberger, PM 1998.
- AN #: 00626696, "DESIGN AND USE OF SUPERIOR ASPHALT BINDERS. FINAL REPORT," AUTHOR(S): Davison, RR; Bullin, JA; Glover, CJ; Jemison, HB; Lau, CK; Lunsford, KM; Bartnicki, PL 08/1992.
- AN #: 00626092, "INFRARED STUDY OF THE AGING OF ASPHALTS IN CONTACT WITH AGGREGATES." IN: AMERICAN CHEMICAL SOCIETY SYMPOSIUM ON CHEMISTRY AND CHARACTERIZATION OF ASPHALTS, AUGUST 1990, WASHINGTON, D.C., Journal: FUEL SCIENCE & TECHNOLOGY INTERNATIONAL Vol: 10 No: 4, AUTHOR(S): McKay, JF; Wolf, JM 05/1992.

- AN #: 00750413, "RELATING ASPHALT AGING AND DURABILITY TO ITS COMPOSITIONAL CHANGES (WITH DISCUSSION)," Journal: Association of Asphalt Paving Technologists Proc Vol: 58, Conference: Asphalt Paving Technology 1989, AUTHOR(S): Tuffour, YA; Ishai, I; Craus, J 1989.
- AN #: 00450691, "CHEMICAL COMPOSITION OF ASPHALT AS RELATED TO ASPHALT DURABILITY: STATE OF THE ART," Journal: Transportation Research Record No: 999, AUTHOR(S): Petersen, JC 1984. (ref [22])
- AN #: 00210850, "RELATION BETWEEN ASPHALT COMPOSITION AND HARDENING BY VOLATILIZATION AND OXIDATION," Journal: Assoc Asphalt Paving Technol Proc, AUTHOR(S): Traxler, RN 1961.
- AN #: 00210948, "MICROBES AS CAUSE OF BITUMINOUS INSULATION DETERIORATION," Journal: Bitumen, Terre, Asphalte, Peche /Ger/, AUTHOR(S): Temme, T 1955.

Subtopic: Characterization

- AN #: 00930589, "DEVELOPMENT OF STIRRED AIR-FLOW TEST (SAFT) FOR IMPROVED HMAC PLANT BINDER AGING SIMULATION AND STUDIES OF ASPHALT AIR BLOWING," AUTHOR(S): Glover, CJ; Davison, RR; Vassiliev, N; Hausman, T; Williamson, SA 09/2001.
- AN #: 00482287, "THE USE OF HIGH PERFORMANCE LIQUID CHROMATOGRAPHY TO MONITOR PERFORMANCE AND STUDY CHANGES IN ASPHALT CEMENTS. FINAL REPORT," AUTHOR(S): Caylor, L; Sharp, T 07/1988.
- AN #: 00739812, "LIME TREATMENT OF ASPHALT TO REDUCE AGE HARDENING AND IMPROVE FLOW PROPERTIES (WITH DISCUSSION)," Journal: Association of Asphalt Paving Technologists Proc Vol: 56, Conference: Asphalt Paving Technology 1987, AUTHOR(S): Petersen, JC; Plancher, H; Harnsberger, PM, Skok, EL, Jr 1987.
- AN #: 00454797, "RELATION OF ASPHALT CHEMISTRY TO PHYSICAL PROPERTIES AND SPECIFICATIONS," AUTHOR(S): Halstead, WJ 05/1984.
- AN #: 00479286, "USE OF HIGH PRESSURE LIQUID CHROMATOGRAPHY TO DETERMINE THE EFFECTS OF VARIOUS ADDITIVES AND FILLERS ON THE CHARACTERISTICS OF ASPHALT. FINAL REPORT," AUTHOR(S): Jennings, PW; Pribanic, JA; Dawson, KR 06/1982.
- AN #: 00322720, "HIGH PRESSURE LIQUID CHROMATOGRAPHY AS A METHOD OF MEASURING ASPHALT COMPOSITION," AUTHOR(S): Jennings, PW; Pribanic, PW; Campbell, W; Dawson, K; Shane, S; Taylor, R 03/1980.
- AN #: 00210627, "INVERSE GAS-LIQUID CHROMATOGRAPHY, A NEW APPROACH FOR STUDYING PETROLEUM ASPHALTS," Journal: Analytical Chemistry, AUTHOR(S): Davis, TC; Petersen, JC; Haines, WE 02/1966.
- AN #: 00210316, "CHARACTERISTICS OF BITUMINOUS MATERIALS SUPPLEMENT TO BIBLIOGRAPHY NO. 35," Journal: Highway Research Board Bibliography, AUTHOR(S): Traxler, RN; Schweyer, HE 1966.

- AN #: 00211334, "ASPHALT COMPOSITION AND PROPERTIES," Journal: Highway Research Board Bulletin, AUTHOR(S): Schweyer, HE 1958.
- AN #: 00211341, "CONSTITUTION AND CHARACTERIZATION OF PAVING ASPHALTS," Journal: Highway Research Board Bulletin, AUTHOR(S): Havens, JH; Daniels, WF 1956.

Subtopic: Design

- AN #: 00666154, "CONTRACTOR'S PERSPECTIVE OF ASPHALT RESEARCH, WITH EMPHASIS ON PERFORMANCE BASED MIX DESIGN AND SPECIFICATIONS," Conference: Strategic Highway Research Program (SHRP) and Traffic Safety on Two Continents, Proceedings of the Conference, AUTHOR(S): Gormsen, H 1994.

Subtopic: Performance

- AN #: 00758885, "RELATIONSHIPS BETWEEN ASPHALT RUT RESISTANCE AND BINDER RHEOLOGICAL PROPERTIES," Journal: Journal of the Association of Asphalt Paving Technologists Vol: 67, Conference: Asphalt Paving Technology 1998, AUTHOR(S): Oliver, JWH; Tredrea, PF 1998. (ref [18])
- AN #: 00616491, "RUT-RESISTANT COMPOSITE PAVEMENT DESIGN. FINAL REPORT," AUTHOR(S): Harmelink, DS 07/1991.
- AN #: 00620387, "DESIGN AND MANUFACTURE OF SUPERIOR ASPHALT BINDERS. FINAL REPORT," AUTHOR(S): Davison, RR; Bullin, JA; Glover, CJ; Stegeman, JR; Jemison, HB; Burr, BL, Jr; Kyle, ALG; Cipione, CA 06/1991.
- AN #: 00602680, "EFFECTS OF ASPHALT PROPERTIES ON INDIRECT TENSILE STRENGTH," Journal: Transportation Research Record No: 1269, AUTHOR(S): Garrick, NW; Biskur, RR 1990.
- AN #: 00475995, "EFFECTS OF ASPHALT COMPOSITION AND COMPACTION ON THE PERFORMACE OF ASPHALT PAVEMENT MIXTURES. EXECUTIVE SUMMARY," AUTHOR(S): Wood, LE; Altschaeffl, AG 05/23/1988.
- AN #: 00475996, "EFFECTS OF ASPHALT COMPOSITION AND COMPACTION ON THE PERFORMACE OF ASPHALT PAVEMENT MIXTURES. FINAL REPORT," AUTHOR(S): Wood, LE; Altschaeffl, AG 05/23/1988.
- AN #: 00472636, "ASPHALT COMPOSITION TESTS: THEIR APPLICATION AND RELATION TO FIELD PERFORMANCE," Journal: Transportation Research Record No: 1096, AUTHOR(S): Goodrich, JL; Goodrich, JE; Kari, WJ 1986.
- AN #: 00454802, "A REVIEW OF RESEARCH PERTAINING TO ASPHALT COMPOSITION AND ITS RELATION TO QUALITY," AUTHOR(S): Halstead, WJ 12/1984.
- AN #: 00308027, "A TWO-CONTINUOUS-PHASE SULFUR-ASPHALT COMPOSITE-DEVELOPMENT AND CHARACTERIZATION," Journal: Canadian Journal of Civil Engineering Vol: 6 No: 3, AUTHOR(S): Beaudoin, JJ; Sereda, PJ 09/1979.

- AN #:, "CHEMICAL COMPONENTS OF ASPHALT: PHASE III, PREPARATION AND TESTING OF BLENDS OF COMPONENTS," AUTHOR(S): California Division Highways, Materials Research & Development Inc, Bureau of Public Roads (no publication date).

Subtopic: Polymer

- AN #: 00743249, "PRODUCTION OF ASPHALT-RUBBER BINDERS BY HIGH-CURE CONDITIONS," Journal: Transportation Research Record No: 1586, AUTHOR(S): Billiter, TC; Davison, RR; Glover, CJ; Bullin, JA 1997.
- AN #: 00737055, "UTILIZATION OF RECYCLED TIRE RUBBER IN ASPHALT PAVEMENTS," AUTHOR(S): Zanzotto, L; Svec, O 11/1996.
- AN #: 00643714, "CONCRETE BRIDGE PROTECTION AND REHABILITATION: CHEMICAL AND PHYSICAL TECHNIQUES. CORROSION INHIBITORS AND POLYMERS," AUTHOR(S): Al-Qadi, IL; Prowell, BD; Weyers, RE; Dutta, T; Gouru, H; Berke, N 07/1993.
- AN #: 00129927, "THERMOPLASTIC ASPHALT COMPOSITIONS FOR ALL-WEATHER PERMANENT STREET PATCHING," Journal: American Assn of State Hwy & Transp Office Proc No: 59, AUTHOR(S): Siemens, WD 11/1973.
- AN #: 00133967, "RUBBER-ASPHALT BINDER FOR SEAL COAT CONSTRUCTION," AUTHOR(S): Olsen, RE 02/1973.
- AN #: 00218081, "RUBBER-ASPHALT BINDER FOR SEAL COAT CONSTRUCTION," AUTHOR(S): Olsen, RE 1973.

Subtopic: Rheology

- AN #: 00472623, "RELATIONSHIP BETWEEN HIGH-PRESSURE GEL PERMEATION CHROMATOGRAPHY DATA AND THE RHEOLOGICAL PROPERTIES OF ASPHALTS," Journal: Transportation Research Record No: 1096, AUTHOR(S): Garrick, NW; Wood, LE 1986.
- AN #: 00931142, "RELATIONSHIP BETWEEN ASPHALT FLOW PROPERTIES AND ASPHALT COMPOSITION (WITH DISCUSSION)," Journal: Association of Asphalt Paving Technologists Proceedings Vol: 53, Conference: Asphalt Paving Technology 1984, AUTHOR(S): Dukatz, EL; Anderson, DA; Rosenberger, JL, Skok, EL, Jr 1984.
- AN #: 00082887, "INFLUENCE OF ASPHALT COMPOSITION ON ITS RHEOLOGICAL BEHAVIOR," AUTHOR(S): Marvillet, J 11/08/1974.
- AN #: 00127326, "SHEAR SUSCEPTIBILITY OF ASPHALTS IN RELATION TO PAVEMENT PERFORMANCE," Journal: Association of Asphalt Paving Technologists Proc Vol: 42, AUTHOR(S): Kandhal, PS; Sandvig, LD; Wenger, ME 1973.
- AN #: 00210760, "THE RHEOLOGICAL PROPERTIES OF ASPHALTS IN RELATION TO DURABILITY AND PAVEMENT PERFORMANCE," Journal: Assoc Asphalt Paving Technol Proc, AUTHOR(S): Sisko, AW; Brunstrum, LC 02/1968.

- AN #: 00210973, "SOME CORRELATIONS OF ASPHALT COMPOSITION WITH PHYSICAL PROPERTIES," Journal: Assoc Asphalt Paving Technol Proc, AUTHOR(S): Hughes, EC; Hardman, HF 02/1951.

Subtopic: Roadway

- AN #: 00387301, "FIELD STUDIES OF A SULPHUR/ASPHALT COMPOSITE POTHOLE REPAIR SYSTEM," AUTHOR(S): Beaudoin, JJ; Sereda, PJ 1983.
- AN #: 00097487, "BENEFICIAL USES OF SULPHUR IN SULPHUR-ASPHALT PAVEMENTS. VOLUME 2: TASK 2: LITERATURE SEARCH AND PATENT REVIEW," AUTHOR(S): Gallaway, BM; Saylak, D 08/1974.
- AN #: 00265350, "EVALUATION OF THERMOPLASTIC ASPHALT COMPOSITIONS FOR STREET PATCHING, Journal: Transportation Research Record No: 506," AUTHOR(S): Siemens, WD; Amstock, JS 1974.
- AN #: 00210386, "ROADWAY FAILURE STUDY NO. II - LATERAL CRACKING OF ASPHALTIC CONCRETE," AUTHOR(S): Lamb, DR; Scott, WG; Gietz, RH; Armijo, JD 08/1967.
- AN #: 00206320, "SUMMARY ROADWAY FAILURE STUDY NO. II-FINAL REPORT," AUTHOR(S): Lamb, DR; Scott, WG; Gietz, RH; Armijo, JD 08/1967.

Subtopic: Safety

- AN #: 00419379, "ASPHALT COMPOSITION AND HEALTH EFFECTS: A CRITICAL REVIEW," AUTHOR(S): KING, RW; PUZINAUSKAS, VP; HOLDSWORTH, CE 1984.

Appendix B: RIP Search, "Asphalt* and Composition"

1. "A Study of Physical and Chemical Characteristics of Superpave Binders Containing Air Blown Asphalt," Start date: 2003/7/1, Source Organization: Arkansas State Highway and Transportation Department
2. "DEVELOPMENT OF APPROACHES FOR ESTIMATING SOURCE TERM LEACHING BEHAVIOR, FATE & TRANSPORT, AND RISK," Start date: 2000/6, TRB Accession Number: 797321, Source Organization: Recycled Materials Resource Center
3. "PREPARATION OF CHEMICALLY MODIFIED POLYMER AND CRUMB RUBBER ASPHALTS," Start date: 1999/3/31, TRB Accession Number: 799086, Source Organization: Federal Highway Administration

Appendix C: RIP Search, "Asphalt* and Additive"

1. "Bridge Deck Resurfacing Using Rosphalt 50," Start date: 2002/6/1 End date: 2007/6/1, Source Organization: Maine Department of Transportation
2. "Quantative Determination of Asphalt Antistripping Additive," Start date: 2003/7/1 End date: 2004/6/30, Source Organization: Virginia Transportation Research Council

3. “Quantifying Anti-Strip Additive in Asphalt (Binder & Mixes),” Start date: 2003/7/1 End date: 2004/12/31, Source Organization: North Carolina Department of Transportation

4. “Stabilized Base Under Asphalt Surface,” Start date: 2002/1/1 End date: 2002/9/30, Source Organization: Alaska Department of Transportation and Public Facilities

5. “USING PYROLIZED CARBON BLACK FROM SCRAP RUBBER TIRES IN ASPHALT PAVEMENTS,” Start date: 1993/9/1, TRB Accession Number: 731869, Source Organization: Indiana Department of Transportation

6. “ASPHALT CONCRETE ANTI-STRIPPING TECHNIQUES,” Start date: 1999/7/1, TRB Accession Number: 801079, Source Organization: South Dakota Department of Transportation

Chapter 3

Molecular Simulation Methods

This research has strived to develop appropriate models for asphalts using "molecular simulations": research-level tools based on statistically tracking the mechanics and dynamics of interacting atoms and molecules. The output of such large-scale computer simulations are predictions of macroscopic-level properties and activities. Required inputs are the chemical identity and relative concentrations of the simulated molecules. Parameters are based on molecular-level chemical identity and, if well-chosen, can lead to predictive methods.

Molecular simulation has become a common computational research tool in the chemistry, physics, and chemical engineering communities. Several books describe the different kinds of simulation methods [71–73], and a variety of computer programs are available. The two most common molecular simulation approaches — Monte Carlo and molecular dynamics — have been applied in this work. The goal of this chapter is to familiarize readers with basic ideas of what these simulation methods entail. Sample intermediate results are presented for illustration. This chapter is not meant as a complete primer for running simulations, however. Readers are referred instead to the standard books cited above.

The idea of molecular simulation is that certain arrangements of molecules are more or less likely than others. Each arrangement makes it own contribution to the overall physical properties, with the more likely arrangements contributing more strongly. The overall value of a macroscopic property is defined in terms of **statistical mechanics** through two different equations:

$$\langle M \rangle = \int \cdots \int M(\mathbf{x}, \mathbf{p}) \exp\left(\frac{\mathcal{K} + \mathcal{V}(\mathbf{x}, \mathbf{p})}{k_B T}\right) d\mathbf{x}^N d\mathbf{p}^N / Q \tag{3.1}$$

$$\langle M \rangle = \frac{1}{\tau} \int_0^\tau M(\mathbf{x}, \mathbf{p}) d\tau \tag{3.2}$$

M stands for the property of interest (density, heat capacity, etc.), and the *partition function* Q serves as a normalization factor defined by the numerator with $M = 1$. (In practice, the partition function has many more uses than mere normalization.) The first equation for the average of M is based on the *probability* of a particular set of atom positions $\mathbf{x}$ and momenta $\mathbf{p}$. The particular form of this exponential depends on the

kinetic energy $\mathcal{K}$ and potential energy $\mathcal{V}$ and is specific to conditions of constant number of particles, volume, and temperature (so-called *canonical ensemble*). Conditions of constant pressure instead of constant volume lead to equation 3.1 being replaced by

$$\langle M \rangle = \int_0^\infty \int \cdots \int M(\mathbf{x}, \mathbf{p}) \exp\left(\frac{\mathcal{K} + \mathcal{V}(\mathbf{x}, \mathbf{p})}{k_B T}\right) \exp\left(-\frac{PV}{k_B T}\right) d\mathbf{x}^N d\mathbf{p}^N dV / Q^{NPT} \tag{3.3}$$

Still other conditions (variable number of particles, for example) lead to slightly different formulas. The second equation is based on the average time spent at a particular set of atom positions and momenta. The two equations are related by a concept called *ergodicity*: the more probable the state, the longer the time that will be spent in it. The methods used for these formulas are called *Monte Carlo* and *molecular dynamics*, respectively.

Monte Carlo simulation was named after the European city because it relies on random events, as do games of chance. In Monte Carlo (MC) simulation [72], random motions and configuration changes, or "moves", are applied to molecules in order to average across the different arrangements and molecular organizations that are consistent with a specified energy, temperature, and applied stress. Each proposed move has a corresponding probability, based on its energy change. Not all proposed moves are carried out. Instead, each consecutive proposed move is accepted or rejected by comparing its corresponding probability to a random number between 0 and 1. The smaller the probability p of the move, the less likely the random number ξ will lie within $0 \leq \xi \leq p$, and the less likely the move will be accepted. The name "Monte Carlo" refers to an analogy in which games of chance are won or lost based on a (hopefully) random result (such as in a Lotto game). Each individual molecular configuration provides a single estimate of a physical property, and macroscopic predictions arise from millions of such individual contributions. Moves to more likely states are accepted more often than those to unlikely states, so the more likely states contribute more significantly to the average.

In molecular dynamics simulation [72], individual molecular arrangements and orientations are probed by following how molecules move in response to intermolecular forces through a numerical solution to Newton's equations of motion:

$$F(\mathbf{x}) = ma = \frac{1}{m}\frac{d\mathbf{p}}{dt} \tag{3.4}$$

The forces arise from the potential energy $\mathcal{V}$ between molecules, which depends on the local molecule arrangements. The resulting accelerations cause changes to the molecule velocities (or momenta), which then lead to new arrangements. As in Monte Carlo, each set of molecular arrangements leads to a physical property estimate, and the macroscopic prediction emerges from a large number of contributions. The differential equation 3.4 is integrated numerically via discrete time steps, each of order 1 fs (10^{-15} s). Trajectories of order 1 to 10 ns (10^{-9} to 10^{-8} s) are possible using significant computing resources (days to weeks of run time). Appropriate facilities in the principal investigator's research lab were used in this work.

Both simulation approaches require parameterized equations for the energies and forces between molecules; each set is called a **force field**. Good agreement exists in the chemistry community about the types of energy contributions that approximate the true quantum mechanical energies. Details are explained in standard

books [71, 72]. Briefly, stretching of bond lenghts and bending of bond angles are represented using harmonic forms,

$$V_\ell = k_\ell(\ell - \ell_0)^2 \tag{3.5}$$

$$V_\theta = k_\theta(\theta - \theta_0)^2 \tag{3.6}$$

The prefactors (k_ℓ, k_θ) and minimum energy geometries (ℓ_0, θ_0) are parameters that are typically calculated by fits to quantum mechanics results and are available in the published literature. Parameters are specific to the pair/triplet of atoms in the bond/angle. Rotations about torsion angles ϕ are expressed as a polynomial in $\cos\phi$, requiring 2 to 5 parameters per torsion angle; these are available in the literature as well and depend on the 4 atoms that define the torsion angle. A set of 4 consecutive atoms on a chain define a proper torsion angle (usually just called a torsion angle). A set of 3 atoms bonded to a common atom constitute an "improper" torsion angle. In some cases a potential energy term is applied to keep these 4 atoms in a specified geometry, such as the same plane. Interactions between pairs of atoms separated by a distance r are usually represented with a Lennard-Jones form,

$$V_{nb} = 4\epsilon\left[\left(\frac{\sigma}{r}\right)^{12} - \left(\frac{\sigma}{r}\right)^{6}\right] \tag{3.7}$$

The parameters ϵ and σ depend on the types of both atoms in the pair. Energies between charges have a Coulomb form,

$$V_{Coul} = \frac{1}{4\pi\epsilon_0}\frac{q_i q_j}{r} \tag{3.8}$$

Many atoms have "partial" charges (i.e. noninteger values of q) that approximate the distribution of how electrons are shared among covalently bonded atoms. Calculating the V_{nb} and V_{Coul} terms requires the largest amount of computation time, since parts of the calculation scale with the square of the number of atoms present. The Coulomb term also requires special treatment to converge the integral of $1/r$ (which converges conditionally because there are positive and negative charges q).

A force field is used each time that the potential energy of a system is calcualted (i.e. $\mathcal{V}$ in equations 3.1 and 3.3). Without a force field, it is impossible to run a meaningful molecular simulation. In the extreme case of the potential energy $\mathcal{V}$ always equalling zero (i.e. noninteracting atoms), the statistical mechanics can be done analytically and the ideal gas law results. Needless to say, a vapor phase system is ineffective as a pavement binder.

Many research groups devote their efforts towards developing force fields and quantifying accurate force field parameters. Force fields differ in their numerical complexity (number of atom types, number of terms that arise in each energy contribution), with increased complexity typically achieving increased accuracy at a higher overall computational cost. In this research, the force field "Optimized Parameters for Liquid Simulations" (OPLS) has been used [74]. Additions [75] to this force field include heteroatoms (O, N, S, etc.), which are found in some components of asphalts.

3.1 Software Employed

Two open source computer programs were used for running the molecular simulations. *Towhee*, available via `http://towhee.sourceforge.net`, is used for Monte Carlo. It contains a variety of ensembles (constant number of molecules, volume, and temperature, or NVT; constant number, pressure, and temperature, or NPT; etc.), force fields, and possible MC step types to use. New versions are released frequently, and most calculations in this report were performed using version 3.12.5 (August 20, 2003). Towhee runs in serial on one computer processor at a time. *Lammps*, available via `http://www.cs.sandia.gov/~sjplimp/lammps.html`, is used for molecular dynamics. It contains great flexibility for simulating different molecules, but all force field parameters are required as input. Towhee is able to write a Lammps input file as part of its output, so in practice this does not cause difficulty. Lammps has three different versions available. Lammps99 is programmed using Fortran 77 and C. Lammps 2001 is an upgrade based on Fortran 90 and C that adds some new force field and ensemble capabilities. Lammps 2005 is based on C++ and C. The first two were used in the calculations described here. A strength of Lammps (all versions) is its capability to run efficiently in parallel. Typically 4 or 8 processors were used for each molecular dynamics simulation. In other projects we have found that the speedup compared to one processor is just under the number of processors used. The Lammps web page cites calculations that show this to be the case for up to thousands of processors.

3.2 Initial Configurations

An initial position for the atoms in each molecule must be specified in order to start the simulation. This set of positions, and therefore the shape of the molecule, is called its *configuration*. Preferably the initial configuration will have a low energy, and thus a high probability, so the later simulation steps can focus on intermolecular packing and energy, rather than on single molecules.

For most molecule types, the "template" feature of Towhee was employed. Positions were chosen for the atoms in one molecule, using a method as simple as drawing its structure on graph paper and reading the coordinates. The single molecule was then simulated at 2 K (–271°C) until the potential energy stabilized near a minimum value. An example is shown in Figure 3.1 for 2-methylnaphthalene. MC moves that translate individual atoms were used in these steps, and the simulation is very fast because the system contains only one molecule. The final configuration provides a set of atom positions that lead to low intramolecular energy. These positions are then translated and rotated in order to define the initial positions of all molecules of this type in later simulations. ("Template" refers to this process.) Images of template geometries are shown in later chapters (Figures 4.1, 6.1,6.2), as molecule types arise.

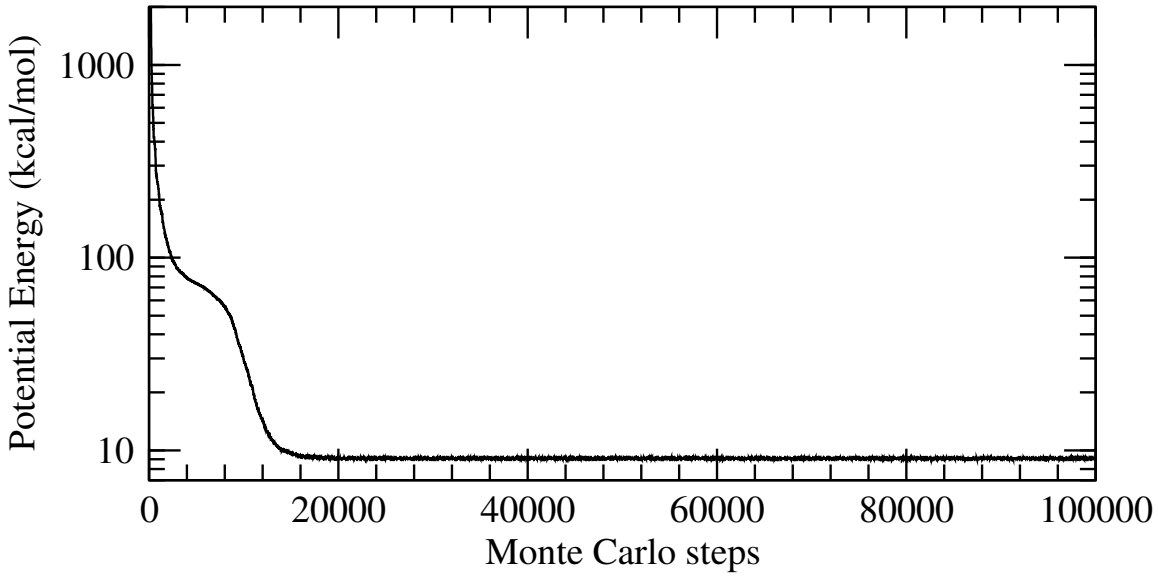

Figure 3.1: Total potential energy for a single molecule of 2-methylnaphthalene, beginning with a set of random atom positions. The energy decreases as more stable positions are found, during a Monte Carlo simulation at 2 K. The final configuration was used as a basis for all molecules of this type in subsequent simulations. The procedure and results for other molecules was analogous.

3.3 Equilibration of system of molecules

The simulations begin by putting the chosen number of molecules in a box at a chosen size. The particular ordering of atoms (crystal or random) is not too important for a fluid system, because the iniital arrangement is not likely to be a high-probability state. The simulation (MC or MD) begins, and initially the system moves away from this initial state towards a set of more likely positions. This process is called *equilibration*. The system then fluctuates about many such positions of similar probability. Estimates of properties are calculated by then *sampling* from these states, i.e. averaging according to their relative probability.

Different properties reach steady values at different rates. The overall pressure equilibrates relatively quickly, meaning that after a short amount of simulation (number of attempted moves or amount of time) it fluctuates about the ultimate long-term average value. The volume requires much more simulation in order to reach a plateau value. Examples are shown in figures 3.2 and 3.3 for 125 molecules of naphthalene. The pressure reaches a steady average value almost immediately, while the volume requires many more steps in order to contract (or expand in other cases) to a steady value.

The physical reason for this difference is that small shifts in atom position can lead to large changes in intermolecular force, and thus in pressure. Volume changes require more significant molecular motions: in order to decrease the volume, molecules must rearrange their orientations and positions so they can pack together more tightly. Consequently the volume is a useful property to monitor for equilibration of small

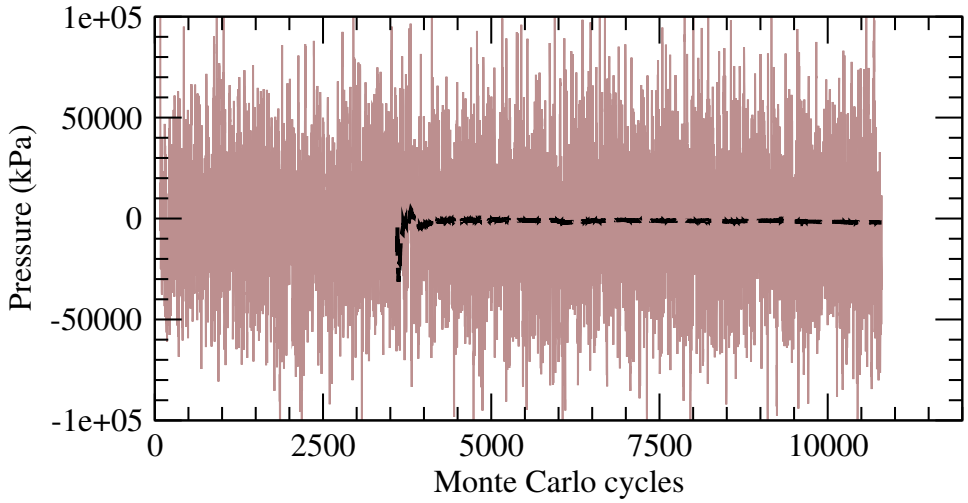

Figure 3.2: Instantaneous pressure values (light line) and running average (i.e. average up to that point in time, heavy dashed line) for a system of 125 naphthalene molecules at 65°C. No average is shown for the first batch (0-3600 cycles) since high values in the initial configuration swamped any future contributions. The average in the second batch reaches a steady value very quickly.

molecules. For long chain molecules, the overall shape of the molecule (analogous to the extent of coiling in a string, compared to a long stick) takes even longer to equilibrate. In such cases there are special methods that can be used for polymers [73]. Work conducted since the research described in this report has indicated that the time required for a molecule to rotate in the system can provide a good estimate of the equilibration time [11]. This is also called the *rotational relaxation time*.

Pressure results are large since they result from the sum of many large attractive and repulsive forces. The fluctuations are large in magnitude, compared to the average value, because the systems are small compared to macroscopic amounts, i.e. to Avogadro's number. The ratio of the fluctuations to the average varies with $1/\sqrt{N}$, where N equals the number of molecules [72]. For 10^{24} molecules this makes the fluctuations negligible on a macroscopic scale. For of order 10^2–10^4 molecules, as used in molecular simulations, they are much more noticeable.

3.4 Properties from Molecular Simulation

The isothermal compressibility (units 1/Pa) is calculated from the fluctuations in volume within a simulation at constant temperature and pressure as [71, 72]

$$\beta \equiv -\frac{1}{V}\left(\frac{\partial V}{\partial P}\right)_T = \frac{1}{Vk_BT}\langle \delta V^2 \rangle = \frac{1}{Vk_BT}\left(\langle V^2 \rangle - \langle V \rangle^2\right) \tag{3.9}$$

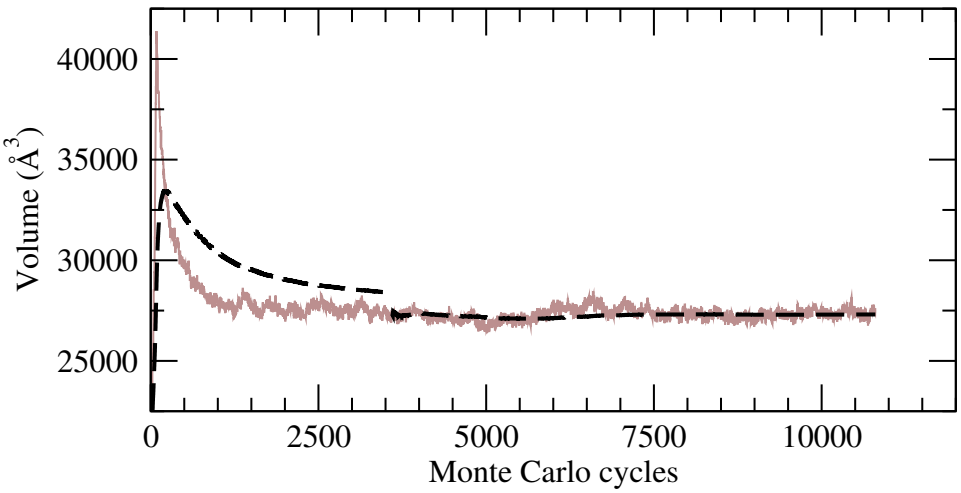

Figure 3.3: Instantaneous volume values (light line) and running average (i.e. average up to that point in time, heavy dashed line) for a system of 125 naphthalene molecules at 65°C. The instantaneous volume fluctuates about a slow drift towards a steady value. There is a step change in the running average at 3600 cycles, where the averaging process was restarted after reaching the sampling stage.

The subscript T indicates a partial derivative at constant temperature, and a quantity in angle brackets $\langle\rangle$ indicates its average value, as calculated in a simulation under the simulation constraints. Specifying the constrained variable is important for macroscopic thermodynamic derivatives since different constraints lead to different values of the derivative. (Constant temperature vs. constant density lines on a thermodynamic $P - V$ diagram provide a good visual example.)

Equation 3.9 itself can be derived by setting $M = V$ in equation 3.3 and differentiating with respect to pressure P at constant temperature T. The quotient rule of differential calculus applies since both the numerator and denominator depend on V, and the two terms in equation 3.9 (i.e. $\langle V^2\rangle$ and $\langle V\rangle^2$) are a consequence. This combination is equivalent to the average of the squared deviations from the mean,

$$\langle (V - \langle V\rangle)^2\rangle = \langle V^2 - 2V\langle V\rangle + 2\langle V\rangle^2\rangle = \langle V^2\rangle - \langle V\rangle^2$$

which leads to the label "fluctuation formula" for equation 3.9 and related equations. Physically, the thermodynamic derivative used to derive the equation (i.e. $-1/V\,(\partial V/\partial P)_T$) implies an assumption that expansions and contractions in response to natural fluctuations in pressure are equivalent to the effect on volume of a step change in pressure (this is called the fluctuation-dissipation theorem [72]). The bulk modulus (units of MPa) is then calculated as the inverse of the isothermal compressibility. Both properties relate to the change in system density with increasing pressure or stress. The thermal expansion coefficient is related to the temperature dependence of density and is calculated within a simulation at constant temperature

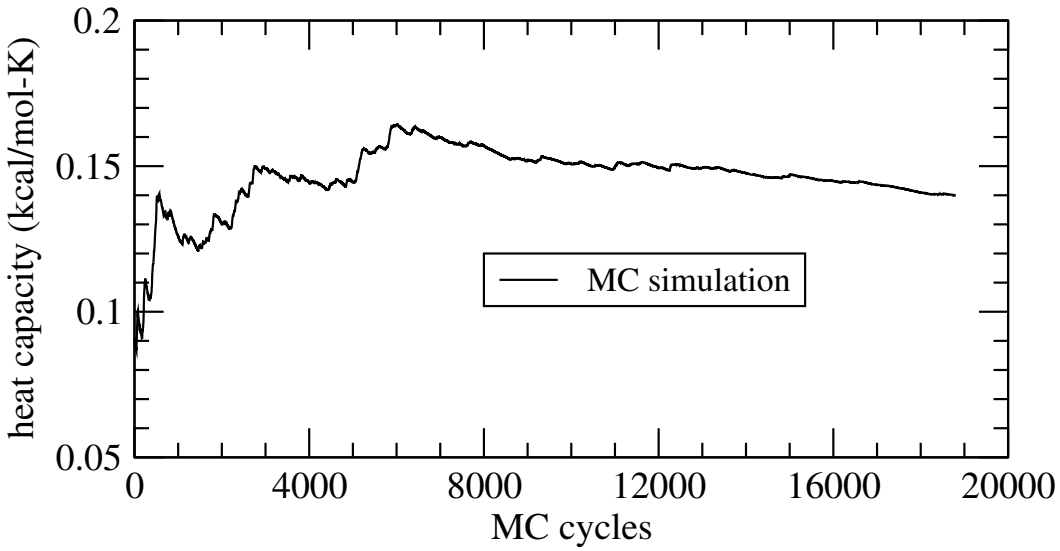

Figure 3.4: Running average heat capacity prediction for methylcyclohexane at 70° from Monte Carlo (MC) simulations.

and pressure as [71, 72]

$$\alpha \equiv \frac{1}{V}\left(\frac{\partial V}{\partial T}\right)_P = \frac{1}{k_B T^2 V}\langle \delta V \delta(E+PV)\rangle = \frac{1}{k_B T^2 V}\left(\langle VE\rangle - \langle V\rangle\langle E\rangle + P(\langle V^2\rangle - \langle V\rangle^2)\right) \quad (3.10)$$

The subscript P refers to a derivative at constant pressure. Derivation of this equation from equation 3.3 follows in a similar way but is more complicated mathematically [72].

The heat capacity equals the rate of total energy change with respect to temperature, under conditions of constant volume (C_v) or constant pressure (C_p). These quantities differ by approximately the gas constant $R = 8.314$ J/mol-K for gases but are similar in liquids and solids, due to their higher density. The heat capacity can be calculated from the energy fluctuations during the sampling stage of a constant temperature and pressure simulation as

$$C_p \equiv \left(\frac{\partial H}{\partial T}\right)_P = \left(\frac{\partial (E+PV)}{\partial T}\right)_P = \frac{1}{k_B T^2}\left(\left\langle (E+PV)^2\right\rangle - \langle E+PV\rangle^2\right) \quad (3.11)$$

where E is the sum of the kinetic and potential energy. Derivation of this equation is similar as well. Figure 3.4 shows how the prediction of heat capacity can evolve as a simulation proceeds. In this example (for methylcyclohexane), the predicted heat capacity fluctuates a bit before reaching a plateau that is near the value known from experiment.

The glass transition is calculated by simulating the model asphalt mixture over a range of temperatures, while maintaining a constant pressure (1 atmosphere). Within the simulation box, the positions of the 10^3 to 10^4 different molecules change with number of Monte Carlo steps or with time. Simultaneously, the simulation box expands or contracts in response to intermolecular forces. After sufficient averaging, the predicted

specific volume (the equivalent of 1 divided by the mass density) stabilizes at a temperature-dependent value (see Figure 3.3). Above or below the glass transition, this specific volume should increase linearly with increasing temperature. This behavior corresponds to a constant thermal expansion coefficient, with expansion being larger (with respect to temperature) above the glass transition. The glass transition is then defined by the region over which the thermal expansion coefficient changes from its glassy to its rubber/melt value. Essentially this simulation procedure corresponds to a molecular-level dilatometry experiment [13]. In fact, all three properties calculated from fluctuations (α, β, C_p) are expected to undergo a shift in value at a glass transition [12]. This provides a consistency check on T_g estimates.

Mechanical properties are calculated through simulations in which the volume remains constant and the instantaneous stresses fluctuate. A proper statistical-mechanical formulation leads to several possible expressions for the instantaneous and averaged stress tensor [76]. The time dependence of stress correlations can then be used to predict the stress relaxation modulus $G(t)$ and ultimately the real G' and imaginary G'' components [77] observable via oscillatory shear experiments [78]. Both of these approaches are valid in the low-strain region.

The glass transition and the mechanical properties are expected to vary with mixture composition. Multiple iterations, in which the composition is varied and the simulations are repeated, are expected before a mixture is found that has predicted properties comparable to those of a core asphalt. A tangential outcome of the project, useful for the molecular simulation community, will likely be methods for using the property predictions from such intermediate simulations to improve the choice of compositions that lead to a desired or targeted set of properties.

Chapter 4

Single Molecules

The first step in the research project was to simulate small molecules that contain chemical functionalities representative of different subsets of an overall asphalt mixture. These calculations served several purposes:

1. define appropriate simulation steps for obtaining an equilibrated ensemble of molecules,
2. quantify the accuracy of the chosen force field for asphalt-related chemistries through comparisons with experimental data,
3. familiarize the students with molecular modeling methods and techniques.

All these purposes were achieved, as shown below, though the procedure defined in (1) was not found to be sufficiently general for mixtures of larger molecules (see chapter 6). These calculations and their results comprise the work product for task 2.

The small molecules simulated are visualized in Figure 4.1 and listed in Table 4.1. Substituted aromatic compounds were chosen as an emphasis for several reasons. NMR studies [9, 16, 33] have found them to be present at high concentrations in asphalts. There have also been many fewer simulations conducted on aromatic compounds than on alkanes, especially straight chain alkanes. The TraPPE (Transferable Potentials for Phase Equilibria) force field development [79–83] is just one of many examples of accurate simulations of alkanes. Simulation results for all pure compounds are listed in tables 4.2 to 4.4.

4.1 Density results

The first property to be considered is the specific density (mass per volume, equal to specific gravity if in units of grams per cubic centimeter). This property is an important starting point because the overall system volume takes the longest time to equilibrate for a fixed number of small molecules (see section 3.3). It also provides a convenient method to compare results to an easily measured property. Density results for all pure compounds are listed in Table 4.2; results for other properties are listed in other tables in this chapter.

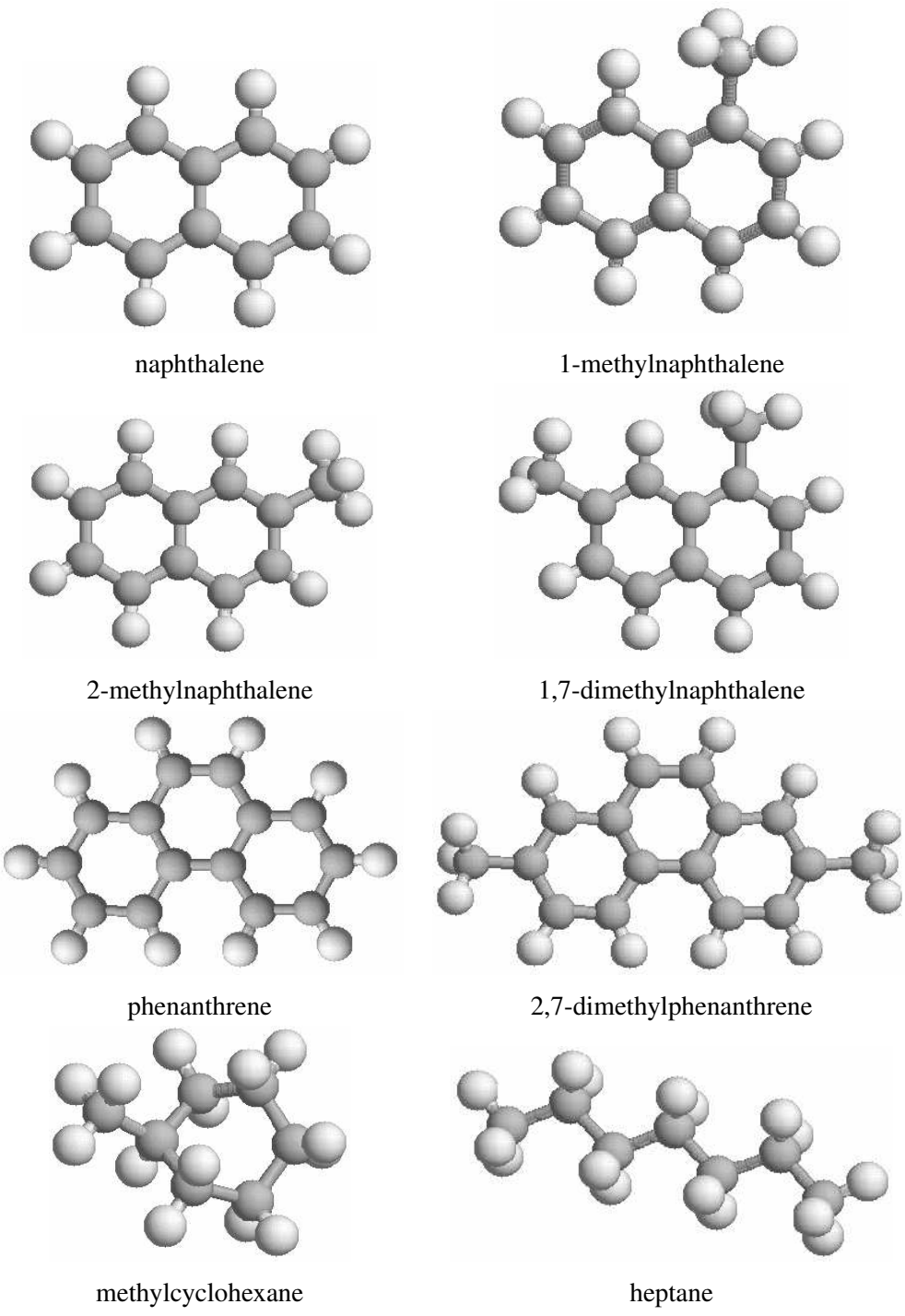

Figure 4.1: Small molecules simulated in this work as pure compounds. Gray and light spheres indicate carbon and hydrogen atoms, respectively. The configurations shown were used as templates when combining many molecules in the same simulation box.

Table 4.1: Molecular weight and simulation temperatures for small molecules studied in this work as pure compounds.

molecule	molecular weight (g/mol)	temperatures simulated (°C)
naphthalene	128.17	25, 45, 65, 85, 105, 125, 145, 165, 185
1-methylnaphthalene	142.20	0, 15, 25, 35, 50, 65, 80, 100
2-methylnaphthalene	142.20	0, 25, 40, 80, 100, 120, 170
1,7-dimethylnaphthalene	156.22	0, 25, 40, 80, 100, 120, 170
phenanthrene	178.23	0, 40, 80, 105, 125, 170
2,7-dimethylphenanthrene	206.28	-5, 25, 50, 80, 100, 120, 170
methylcyclohexane	98.19	70

4.1.1 Naphthalene and Substituted Naphthalenes

Figure 4.2 compares predicted and experimentally measured density of naphthalene as a function of temperature at atmospheric pressure. The predictions (open circles) were made via "NPT" Monte Carlo simulations (specified number of molecules N, pressure P, and temperature T); experimental values (filled circles) were taken from compilations [84, 85] of various literature sources. The predictions, based on 125 molecules, are in reasonable agreement with experiment over the range of temperatures for which data are available. The simulations describe both the density itself and its variation with temperature (i.e. thermal expansion coefficient). For each method, the change in density with respect to temperature for naphthalene (i.e. the slope of figure 4.2) remains approximately constant across the temperatures simulated. This suggests that it does not pass through a glass transition under these conditions. Everyday experience with naphthalene (i.e. mothballs) confirms that it is soft and waxy at room temperature, rather than hard and glassy.

Comparable simulations using the same parameters were also conducted using molecular dynamics, with two system sizes (125 and 343 molecules). The results are shown in 4.2 by empty or slightly filled squares. Surprisingly, the MD led to results that differed from those using Monte Carlo. The overall density is lower by approximately 5–10%, and the thermal expansion coefficient is slightly overpredicted (density decreases too much with increasing temperature).

Three substituted naphthalenes that resemble part of the resins in a model asphalt have been simulated as pure compounds. Figures 4.3, 4.4, and 4.5 compare predicted and experimentally measured density of 1-methylnaphthalene, 2-methylnaphthalene, and 1,7-dimethylnaphthalene as a function of temperature at atmospheric pressure. As for naphthalene, the predictions were made via NPT Monte Carlo simulations, and again the experimental values were taken from various literature sources [84, 85]. For all three compounds, the predictions are in reasonable agreement with experiment over the range of temperatures for which data are available. The simulations describe both the temperature variation of each density and the

Table 4.2: Density results from molecular simulation for small molecules studied in this work as pure compounds. Results are from Monte Carlo (MC) simulation unless noted. Temperatures in parentheses indicate experimental results at nearby conditions.

molecule	temperature °C	simulation g/cm^3	experiment g/cm^3, (°C)
naphthalene	25	1.018	
naphthalene (MD, 125 molecules)	25	0.962	
naphthalene (MD, 343 molecules)	25	0.985	
naphthalene	45	0.997	
naphthalene	65	0.981	0.9877, (66.71)
naphthalene	85	0.962	0.9752
naphthalene (MD, 343 molecules)	85	0.906	
naphthalene	105	0.949	0.9632, (100.86)
naphthalene	125	0.926	0.94, (127)
naphthalene (MD, 125 molecules)	125	0.830	
naphthalene (MD, 343 molecules)	125	0.852	
naphthalene	145	0.910	
naphthalene	165	0.890	0.912, (164.8)
naphthalene	185	0.868	0.889, (187)
1-methylnaphthalene	0	1.034	1.0347
1-methylnaphthalene	15	1.018	1.025, (14.4)
1-methylnaphthalene	25	1.016	1.0163
1-methylnaphthalene	35	1.009	1.010, (30)
1-methylnaphthalene	50	1.002	0.9979
1-methylnaphthalene	65	0.991	
1-methylnaphthalene	80	0.982	0.9771, (78.3)
1-methylnaphthalene	100	0.966	0.9604
2-methylnaphthalene	0	1.021	
2-methylnaphthalene	25	1.003	1.0043, (22)
2-methylnaphthalene	40	0.987	0.99047
2-methylnaphthalene	80	0.958	0.9718
2-methylnaphthalene	100	0.941	0.9491, (99.4)
2-methylnaphthalene	120	0.923	0.93
2-methylnaphthalene	170	0.877	0.891

Table 4.2 (continued) Density results from molecular simulation for small molecules studied in this work as pure compounds.

molecule	temperature °C	simulation g/cm^3	experiment g/cm^3, (°C)
1,7-dimethylnaphthalene	0	1.010	1.0115
1,7-dimethylnaphthalene	25	0.989	0.999
1,7-dimethylnaphthalene	40	0.982	
1,7-dimethylnaphthalene	80	0.957	
1,7-dimethylnaphthalene	100	0.939	
1,7-dimethylnaphthalene	120	0.919	
1,7-dimethylnaphthalene	170	0.881	
phenanthrene	0	1.110	
phenanthrene	40	1.091	1.1648, (47.12)
phenanthrene	80	1.044	1.0514, (81.82)
phenanthrene	105	1.044	1.063, (100.5)
phenanthrene	125	1.027	1.046, (130)
phenanthrene	170	1.006	1.018
2,7-dimethylphenanthrene	-5	1.057	
2,7-dimethylphenanthrene	25	1.038	
2,7-dimethylphenanthrene	50	1.029	
2,7-dimethylphenanthrene	80	1.018	
2,7-dimethylphenanthrene	100	1.012	
2,7-dimethylphenanthrene	120	1.005	
2,7-dimethylphenanthrene	170	0.972	

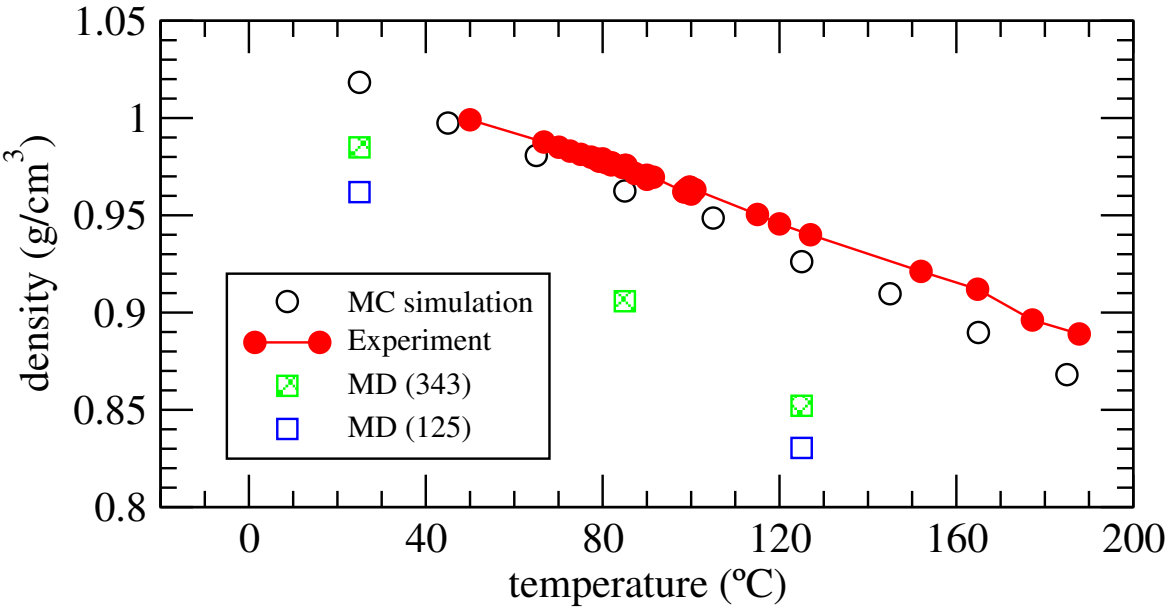

Figure 4.2: Density of naphthalene from molecular simulations, compared to experimental values [84, 85].

difference in density between the two compounds. The slight change in slope near 38° (100°F) in the 1-methylnaphthalene simulations suggests the possibility of a glass transition. This change in slope is not found in the experimental data, however, and in this case we expect that further equilibration of the simulations would lead to more smooth results. Lower temperature ranges, where asphalts exhibit glass transitions, were explored for mixtures that involved model compounds.

These results are comparable to those above for naphthalene in that predicted density is in reasonable agreement with experiment. In total, the simulations do a reasonable job at describing the differences in density among the four compounds, as shown in Figure 4.6. This provides confidence that subtleties in molecular packing details are described sufficiently accurately in the simulations.

4.1.2 Phenanthrenes

The single-molecule size was increased further by simulating phenanthrene and 2,7-dimethylphenanthrene. These molecules have a larger planar aromatic core than substituted naphthalenes (three rings instead of two). Their molecular structure is thus closer to one of the postulated forms of asphaltenes. Predicted densities are shown in figures 4.7 and 4.8. For phenanthrene, experimental data are available for comparison [84]. Agreement is adequate for the thermal expansion coefficient, but the magnitude of the density itself is a bit small (volumes predicted by simulation are too large). Subtle trends in the density plots led us to suspect that this is because the simulations were not continued for a sufficiently large number of cycles for these larger molecules. The simulations were not continued further since other molecules were chosen for use

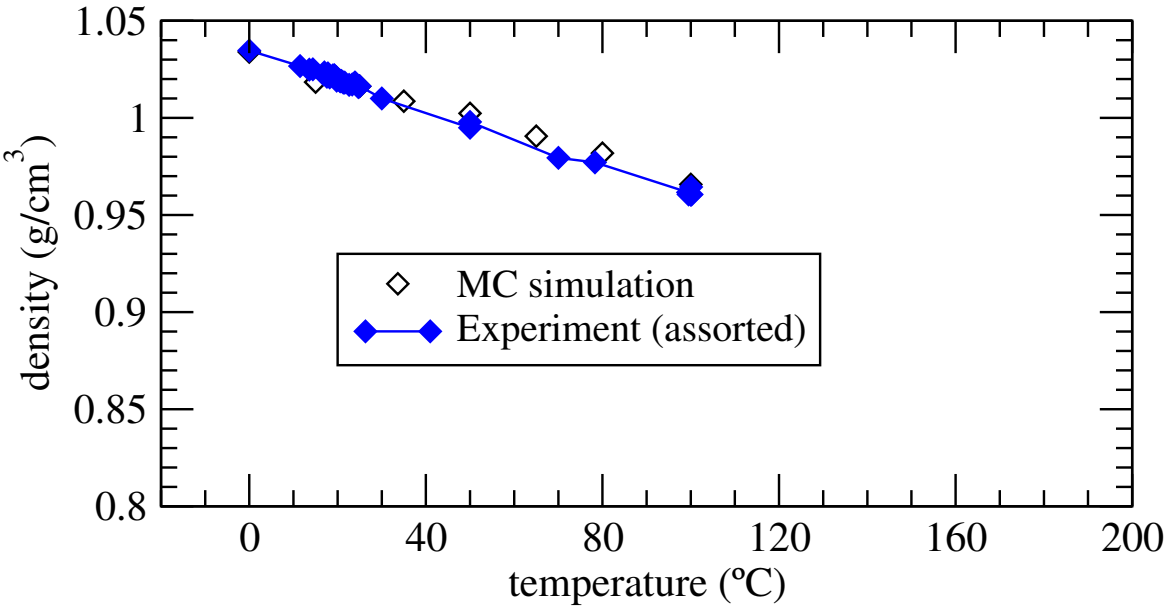

Figure 4.3: Density of 1-methylnaphthalene from Monte Carlo simulations, compared to experimental values compiled from various sources [84–86].

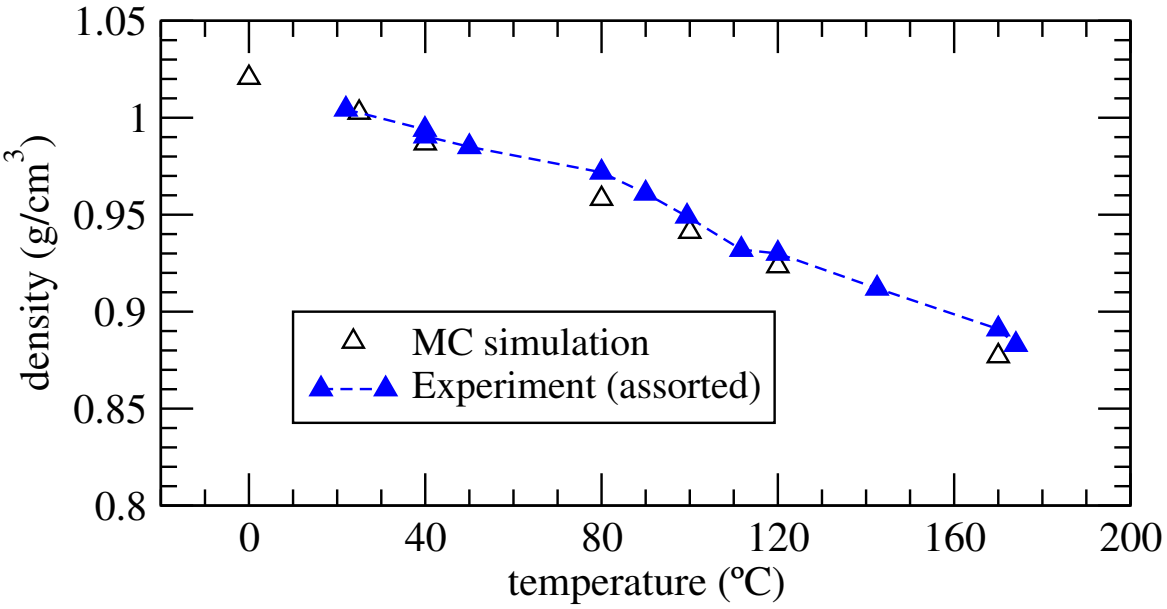

Figure 4.4: Density of 2-methylnaphthalene from Monte Carlo simulations, compared to experimental values compiled from various sources [84, 85].

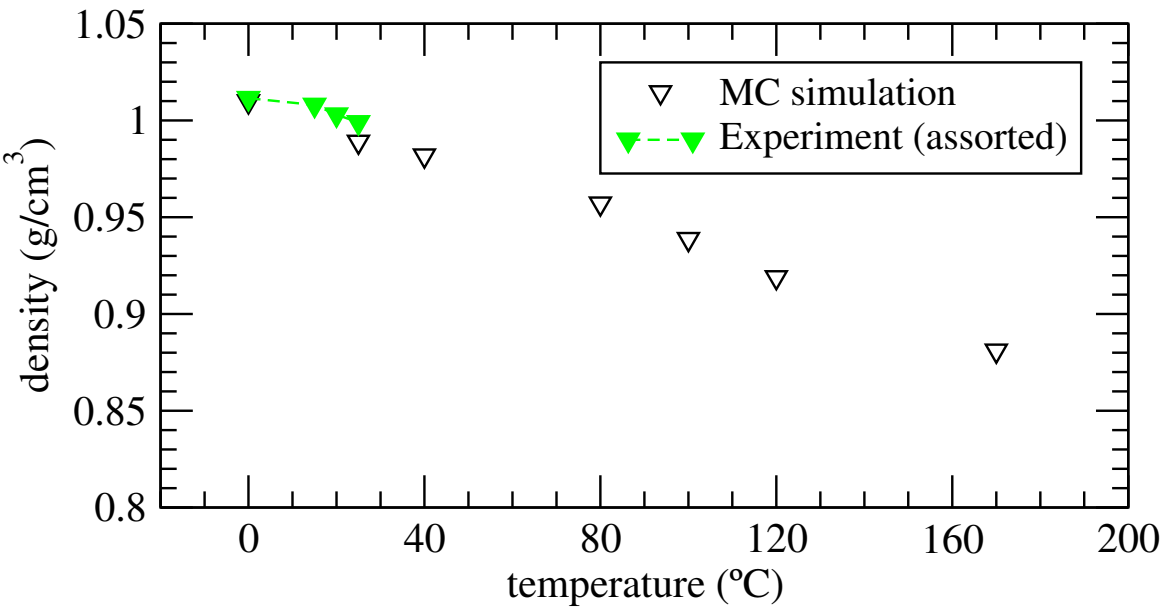

Figure 4.5: Density of 1,7-dimethylnaphthalene from Monte Carlo simulations, compared to experimental values compiled from various sources [84, 85].

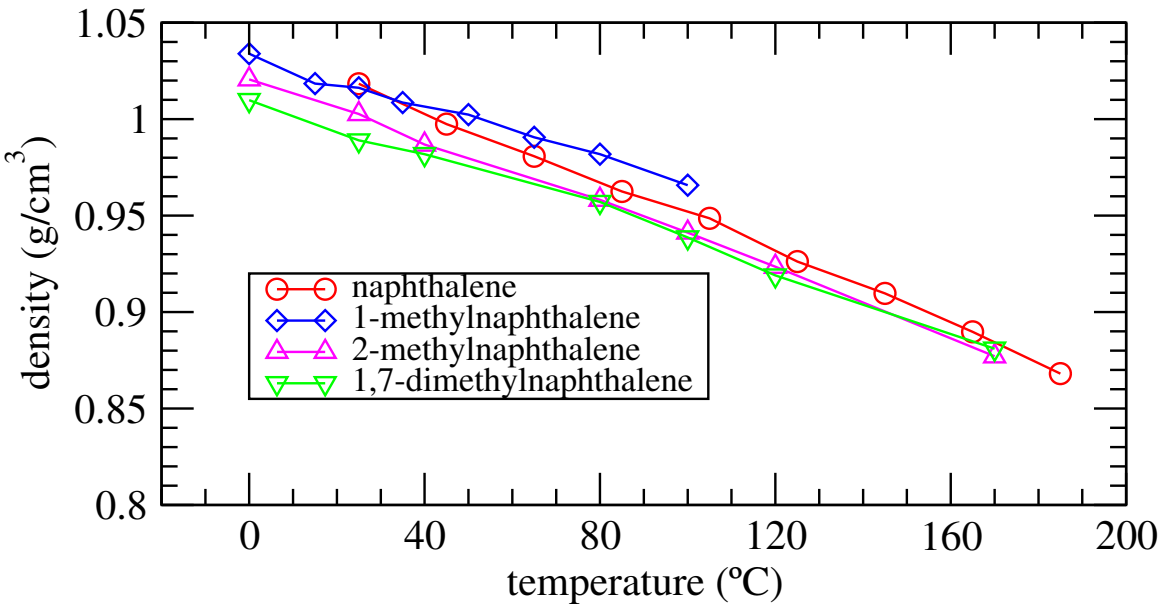

Figure 4.6: Comparison of predicted densities of naphthalene (circles), 1-methylnaphthalene (diamonds), 2-methylnaphthalene(up-pointing triangles), and 1,7- dimethylnaphthalene (down triangles) from Monte Carlo simulations.

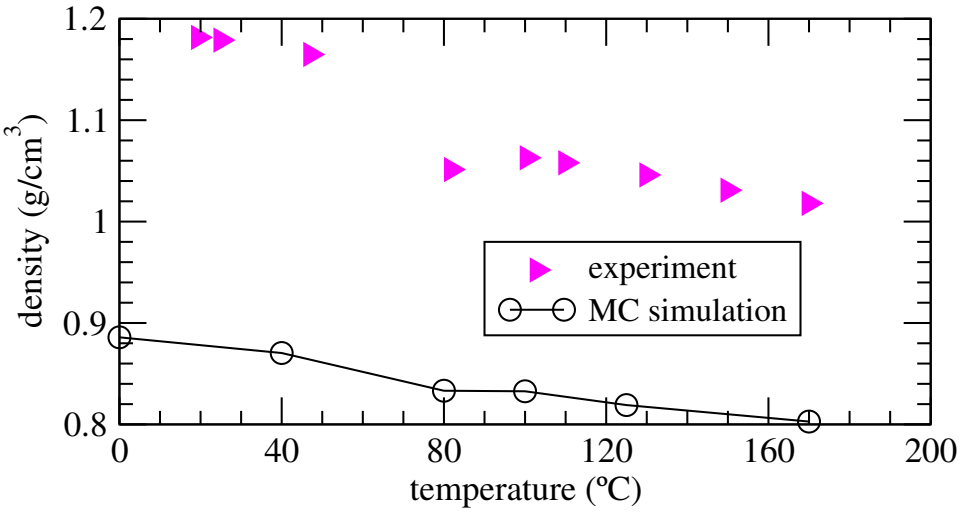

Figure 4.7: Density of phenanthrene from Monte Carlo simulations, compared to experimental values compiled from various sources [84].

in the model asphalts. In work [11] conducted since the research described in this report, we have found that rotational relaxation time (the average time for a molecule to change its orientation) provides a better measure of convergence. Physically, insufficient time to change relative molecule orientations can prevent the close packing necessary to achieve the proper density. Another possible cause of the discrepancy is insufficient accuracy of the force field.

Experimental values of density were not available from the literature for 2,7-dimethylphenanthrene. Experiments to measure the density accurately were not conducted for multiple reasons. Since 2,7-dimethylphenanthrene was not chosen for use in model asphalts, obtaining measurements was not the best use of research effort. In addition, funds for an accurate measurement effort were not available.

4.1.3 Methylcyclohexane

Methylcyclohexane was simulated because it was a component in a three-component mixture for which convenient data were available in the literature [86,87]. Those data are compared with simulation predictions in chapter 5. It is also similar to the substituted cyclic alkane molecules (so called naphthenes) that can be found in asphalt mixtures. The evolution of the estimated heat capacity was shown earlier in Figure 3.4 (p. 44). Density predictions were not made for this compound.

4.2 Additional properties

Several properties beyond density were calculated for each molecule type. Table 4.3 shows some of the heat capacity predictions, in comparison with available data. The heat capacity is within approximately a

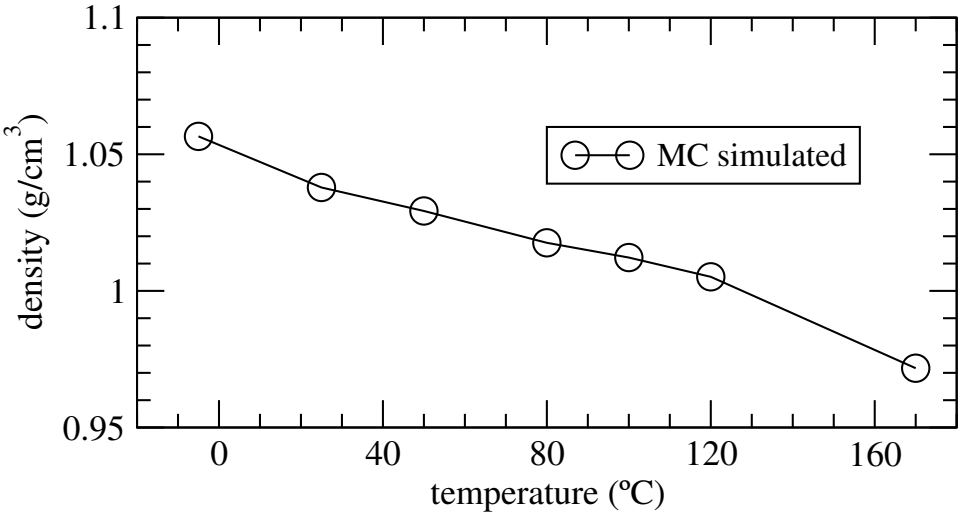

Figure 4.8: Density of 2,7-dimethylphenanthrene from Monte Carlo simulations. Experimental values were not available for comparison.

factor of two, and it is overpredicted in each case. The statistical mechanics of chemical bonds prevents a more accurate prediction, since bond vibrational frequencies are high enough that quantum mechanical effects are required for treating the details accurately. The simulations here use classical mechanics, and incorporating quantum effects is beyond the scope of the aims and needs of this project. The result is an overprediction for each vibrational mode in which quantum effects can occur. Rather than use a quantum-mechanical approach to improve the estimate, instead we assume that *qualtitative trends* in heat capacity will occur properly with temperature. Correlations [88] suggest that liquid-phase heat capacity can both decrease and increase as temperature increases, so the temperature trends listed in Table 4.3 are potentially reasonable. Results at additional temperatures would be necessary to consider if the trends in calculated results are accurate or unreasonable.

Table 4.4 shows the isothermal compressibility β and coefficient of thermal expansion α predicted for different small molecules. Experimental values could not be found for the specific molecules simulated here, and conducting measurements of these properties was beyond the scope and budget of the project, so the predictions will be compared with typical values for a variety of compounds. A range of alkanes (pentane, octane, decane) have values of order $\alpha \times 10^3 \approx 0.9$ to 1.3 K^{-1} and $\beta \approx 1.0$ to 1.3 GPa^{-1} [89], with higher molecular weight liquids (e.g. petroleum) having even lower values of β (typical range of 0.7 to 2 GPa^{-1}), i.e. being less compressible with increased pressure. The predicted expansion coefficients α are slightly smaller than this range at room temperature but are near it at elevated temperatures. The predicted isothermal compressibilities show a similar trend. The increase in β with increased temperature is consistent with the reported values for petroleum [89], which increase by approximately 50% over a 100°C rise. Experimental data for α and β across wide temperature ranges are difficult to find, precluding more

Table 4.3: Heat capacity from simulation and experiment (when available) for small molecules.

molecule	C_p (kcal/mol-K)		
	experiment[a]	simulation	
	(25°C)	(25°C)	(other T)
naphthalene	0.0469	0.0931	0.1275 (at 185°C)
1-methylnaphthalene	0.0536	0.144	0.131 (at 100°C)
2-methylnaphthalene	0.0468	0.139	0.118 (at 100°C)
dimethylnaphthalene	—	0.152	0.153 (at 170°C)
phenanthrene	0.073[b]	0.0701	
methylcyclohexane	0.049[c]	0.14	

a) Literature values collected in NIST webbook [90] unless noted otherwise
b) Liquid value at 110°C [91]
c) Liquid value at 70°C, extrapolated using the formula of ref [92] (Webbook contains an error)

detailed comparisons.

4.3 Discussion

From these results, a few observations can be made concerning parameters and glass transition. First, no parameters were varied in this work in order to obtain the agreement shown. Instead, parameter values were taken from literature sources [74, 75]. The same parameters are used for chemical groups that are the same in each molecule (i.e. aromatic carbon atoms, saturated carbon atoms, pendant hydrogen atoms on each). In other words, the parameters may be viewed as inputs that can be applied to a variety of model compounds. The only differences among molecules are the presence or absence of short alkane branches, and these differences affect molecular packing enough to lead to differences in density, which are predicted accurately. This provides confidence that the parameters can be used with additional alkane-substituted aromatic compounds, which are very typical of the compounds found in asphalts. Prior simulations in the literature have confirmed the same trends for alkanes. In total, we can expect the force field to be sufficiently accurate for the compounds found in asphalts.

Table 4.4: Isothermal compressibility β and coefficient of thermal expansion α predicted from molecular simulations of pure compounds.

molecule	isothermal compressibility (GPa^{-1})		expansion coefficient (K^{-1})	
	(25°C)	(other T)	(25°C)	(other T)
naphthalene	0.335	1.50 (185°C)	0.649 $\times 10^{-3}$	1.33 $\times 10^{-3}$ (at 185°C)
1-methylnaphthalene	0.308	0.652 (100°C)	0.442 $\times 10^{-3}$	0.770 $\times 10^{-3}$ (at 100°C)
2-methylnaphthalene	0.317	8.32 (100°C)	0.523 $\times 10^{-3}$	0.832 $\times 10^{-3}$ (at 100°C)
dimethylnaphthalene	0.362	1.17 (170°C)	0.491 $\times 10^{-3}$	0.545 $\times 10^{-3}$ (at 170°C)
phenanthrene	0.273	—	0.301 $\times 10^{-3}$	—
methylcyclohexane	—	3.21 (70°C)	0.202 $\times 10^{-3}$	—
typical	0.7–2		0.9-1.3 $\times 10^{-3}$	—

Chapter 5

Small Molecule Mixtures

The calculations described in chapter 4 showed that molecular simulations are capable of predicting the expansion and contraction of pure compounds that possess hydrocarbon functionalities similar to those of compounds found in asphalts. Other work in our laboratory [93] has found similar results for certain molecules with heteroatoms, such as benzophenone (carbonyl bonded to two benzene rings), anisole (methyl phenyl ether), and thiophene and its derivatives (sulfur in a 5-membered aromatic ring). Monte Carlo simulation led to quantitative predictions of the temperature-dependent density, while molecular dynamics predicted the correct thermal expansion coefficient but at a density that was systematically slightly low. (See section 4.1.1 for a discussion.)

The next logical step is to assess the performance of molecular simulations on a mixture of small molecule analogs to the compounds in asphalt. The intent of the calculations in this chapter is to demonstrate how methods similar to those applied to pure compounds are equally capable of success for mixtures of molecules. For this purpose it is necessary to look at well-defined mixtures that are simpler than asphalts.

5.1 Mixture definition

A mixture of 1-methylnaphthalene, methylcyclohexane, and heptane was chosen because high quality experimental measurements of physical properties at precisely defined compositions were reported in the literature [86, 87]. This mixture provides a reasonable test because its components represent well-defined constituent groups of asphalt. 1-methylnaphthalene exemplifies a small portion of a resin or asphaltene molecule. 1-methylcyclohexane and *n*–heptane are examples of cyclic and straight-chain saturated alkanes. Simulations were conducted at many of the reported conditions by using our normal procedure: (1) place molecules of low energy and favorable conformation (i.e. shape) into a regular arrangement, (2) equilibrate the sample via a long simulation in which the total volume evolves to a steady value, (3) accumulate ("sample") from the statistics of this steady state via another simulation to gather the results. This multi-step strategy is required to ensure that high probability molecular arrangements contribute most significantly to the results. Multiple variants of step (2) — subdivisions into multiple runs of various lengths, temperatures,

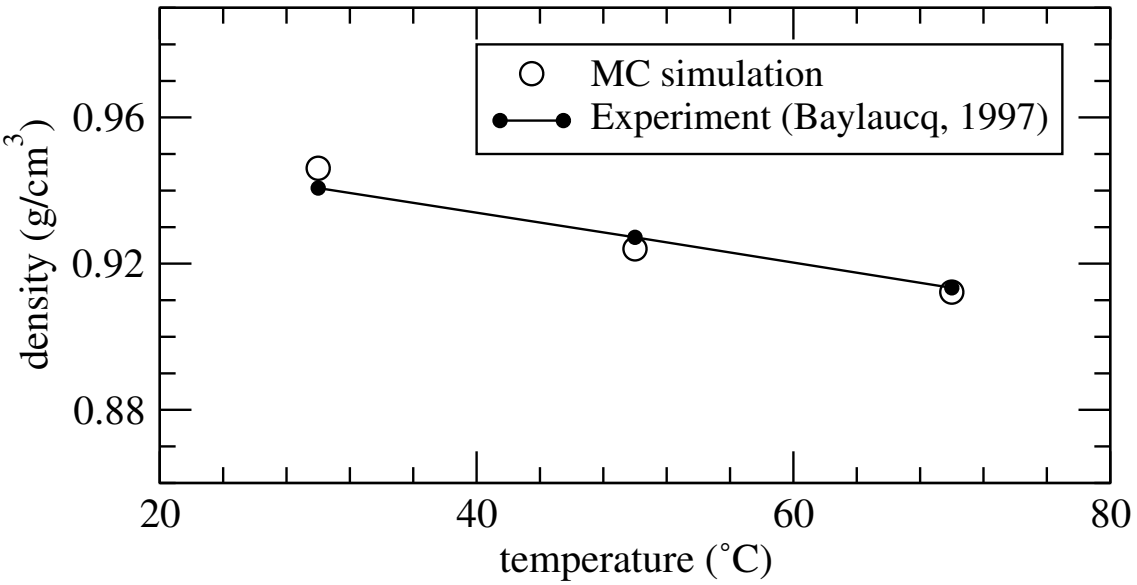

Figure 5.1: Predicted density of a ternary hydrocarbon mixture as a function of temperature, for a 1:1:6 mixture of heptane/methylcyclohexane/1-methylnaphthalene (mole fractions 0.125, 0.125, 0.750 respectively). The predicted densities follow the experimental values [87] relatively closely.

and pressures — are often required as the molecules included become more complicated (e.g. longer alkanes and large asphaltenes). The total volume (in step 2) equilibrates more slowly than the pressure but potentially more quickly than the position and orientation relaxations of the largest (and thus slowest) molecules. The precise amount of time required for relaxation depends on the molecules present in each system and on the temperature.

5.2 Results vs. temperature, composition, and pressure

Examples of the results for this 1-methylnaphthalene/methylcyclohexane/heptane mixture are shown in Figures 5.1, 5.2, and 5.3. These figures show the effects of independently varying temperature, composition, and pressure while the other settings are held fixed. The numerical values used in the figures are listed in Table 5.1.

Figure 5.1 explores temperature. Typical behavior is found: density decreases with increasing temperature. The temperature dependence of density, as calculated in the simulations, is consistent with that measured experimentally [87]. Both the density itself and its temperature derivative (which leads to the thermal expansion coefficient) show good agreement.

Figure 5.2 shows density changes as a function of chemical composition at a fixed temperature. With more cyclic alkane methylcyclohexane and less aromatic 1-methylnaphthalene, the density decreases. The

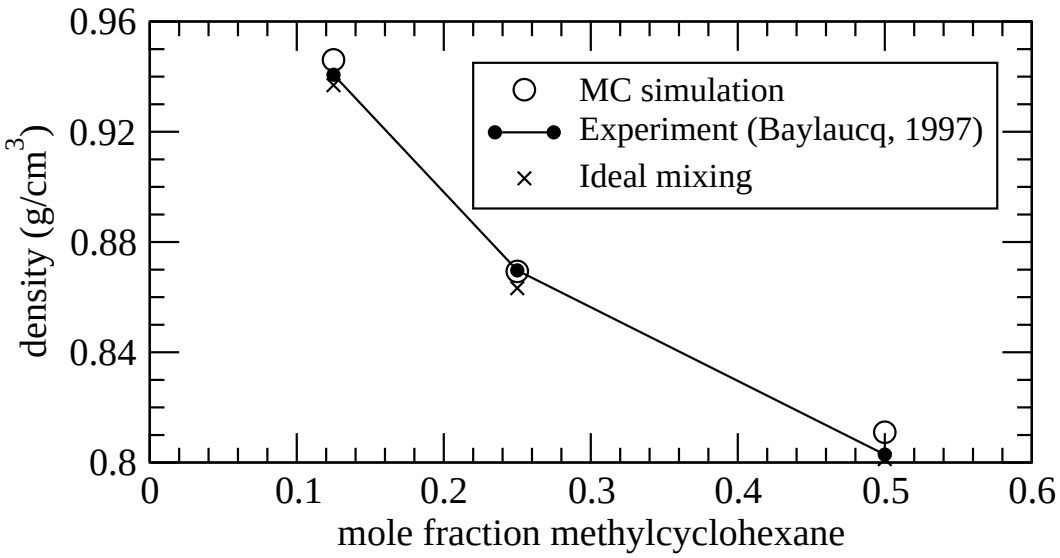

Figure 5.2: Predicted mixture densities at 303.15 K (30°C or 86°F), for specified mole fractions of methylcyclohexane. The heptane and 1-methylnaphthalene mole fractions are listed in Table 5.1. As in Figure 5.1, the experimental trends are predicted well.

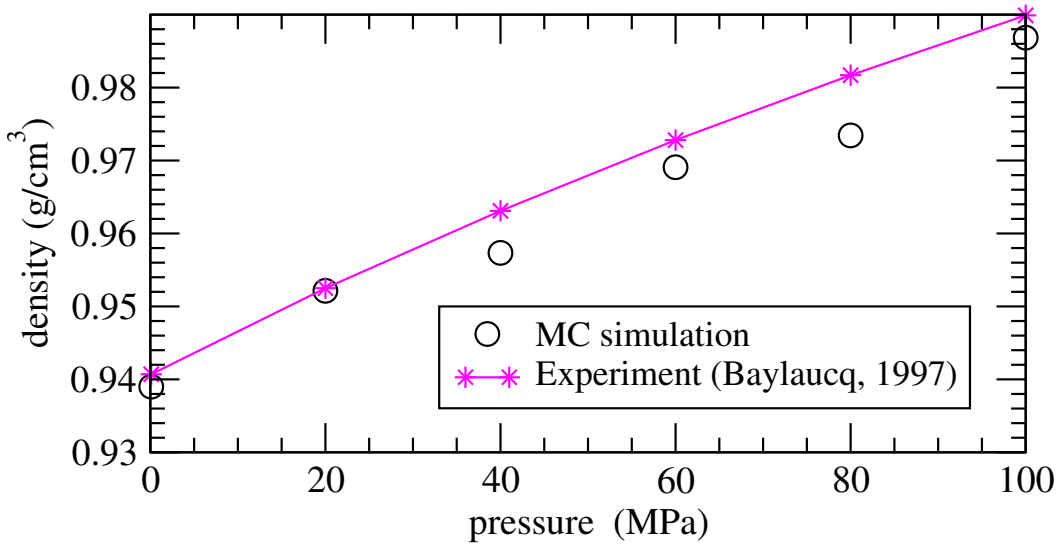

Figure 5.3: Predicted density of the same ternary hydrocarbon mixture as a function of pressure, at a specified temperature of 303.15 K (30°C or 86°F) for the same composition as in Figure 5.1.

Table 5.1: Hydrocarbon Mixture Results from Simulation (this work) and Experiment (literature)

mole fractions			conditions		density (g/cm^3)	
heptane	methyl-cyclohexane	1-methyl-naphthalene	T (°C)	P (MPa)	simulation	experiment (literature [87])
0.125	0.125	0.750	30	0.1	0.946	0.941
0.125	0.125	0.750	50	0.1	0.924	0.927
0.125	0.125	0.750	70	0.1	0.912	0.913
0.125	0.125	0.750	30	0.1	0.946	0.941
0.250	0.250	0.500	30	0.1	0.869	0.870
0.250	0.500	0.250	30	0.1	0.811	0.803
0.125	0.125	0.750	30	0.1	0.939	0.941
0.125	0.125	0.750	30	20	0.952	0.953
0.125	0.125	0.750	30	40	0.957	0.963
0.125	0.125	0.750	30	60	0.969	0.973
0.125	0.125	0.750	30	80	0.973	0.982
0.125	0.125	0.750	30	100	0.987	0.990

effect of changing the ratio among the three compounds affects the density, and the extent of this change is calculated accurately by the simulation. Densities corresponding to no volume change on mixing (so-called "ideal" mixing) are shown with $\times$ symbols. These results, in which the volume is calculated as an arithmetic average of the individual compound specific volumes, differs in two of three cases from the experimental results. It is encouraging that the simulations track better with the experimental results than with the simpler densities that follow from ideal mixing.

The trend in density with pressure (Figure 5.3) is predicted reasonably. The density increases with pressure in both the experiment and the simulation. The simulation results show some noise because the higher pressures make them more difficult to equilibrate. Longer simulations are also required to allow the liquid molecules sufficient opportunities to organize relative to one another. Absolute differences between simulation and experiment are comparable to those in Figures 5.1 and 5.2. The different value at (30°C, 0.1 MPa) shows that statistical errors upon repeating the simulation (in this case by two different students on the project) are comparable to this deviation from experiment and smaller than the general trends in density found as functions of temperature, pressure, and composition.

This three component mixture was originally studied by Baylaucq et al. because it had been proposed as a model composition for crude oil [86]. Such a mixture is incomplete from the perspective of this report, since it lacks the "heavy ends" (molecules with higher molecular weights and boiling points) that constitute asphalts. Mixtures of larger molecules are required for asphalts, as shown in the next chapter. Despite this mismatch in size, however, the results shown in this chapter are significant since they show that the methods being employed can be expected to yield accurate results for hydrocarbon mixtures that contain both

aromatic molecules, saturated hydrocarbon rings, and more linear hydrocarbon chains. Asphalt mixtures, which contain asphaltenes, resins, and saturates, fall into this general mixture category.

Chapter 6

Asphalt-like Mixtures

The asphalt characterizations present in the literature (chapter 2) have suggested chemical families and size ranges for the many kinds of molecules that are found in different asphalts. In this chapter we describe how we chose a few molecules to comprise initial asphalt mixtures. We then describe our results using these mixtures and compare them with selected asphalts.

6.1 Chemical Families in Asphalt

A classic method for separating asphalt into components is by employing solubility in a series of organic solvents, supplemented with chromatography (i.e. Corbett method) [1, 24, 25]. Molecules that are insoluble in straight-chain alkanes (such as n-heptane or n-pentane, depending on the test) are called *asphaltenes*. The alkane-soluble compounds are adsorbed (such as on a semipolar chromatography column) and are then eluted (i.e. desorbed) using a variety of solvents. Molecules that elute immediately (e.g. with n-heptane) are *saturates*. Molecules that adsorb more strongly and elute when an aromatic solvent (such as benzene) is added are called *naphthene aromatics* [24]. Molecules that elute with a more polar solvent, such as an aromatic/alcohol mixture, are called *polar aromatics* [24]. The two sets of aromatics are sometimes together called *resins* [24]. These resins are soluble in n-heptane but insoluble in n-pentane [45]. This kind of separation is somewhat indistinct, since all alkane-insoluble molecules are lumped together as asphaltenes, all molecules soluble in alkanes that weakly adsorb are saturates, and the balances are resins. Multiple different chemistries can occur within each category, as long as they have similar solubility in a solvent/resin/saturate mixture [94]. Other separations, such as via size exclusion chromatography, distinguish among chemical families defined slightly differently [1].

As a starting point, we chose to represent each broad family using one molecule type. For the saturates, we chose a straight-chain hydrocarbon, *n*–docosane (*n*–$C_{22}H_{46}$). Storm et al. [33] performed NMR studies that quantified the relative concentrations of different chemical groups in different fractions of resid obtained from two crude sources. Storm's results, shown in Table 6.1, allow for comparisons between the structures of molecules considered here and the representative values found from those crude oil sources; a basis of

100 carbon atoms is used in the comparison. (Numbers used here are shown in Table 6.1 in **boldface**.) Storm reported 72.2% (alkane C/total C) in the oil phase, with a partial subdivision of different alkane environments as listed in the table. If all CH_3 ends must be adjacent to a CH_2 (as in a straight chain), then the average chain length equals (72.2 C / 4 ends) = 18.05 carbon atoms per end and thus 36.1 carbon atoms per chain (since each chain has two ends). Using the reported value of 4.9 chain ends instead leads to a length of 29.5. Assigning all CH_2 groups to the backbone and leaving out the possible branch point leads to (4+24.3) = 28.3 carbon atoms with 4 CH_2 groups next to an end, or 14.1 carbon atoms on CH_2 groups per straight chain (16 carbon atoms in total). A chain length of 22 is in the middle of this range. *n*–C_{22} is also the normal alkane with the highest concentration in the speciation reported by Kowalewski et al. [55]. Its melting point T_m=44°C and boiling point T_b=369°C [90] are consistent with this saturate being a waxy component of an overall asphalt.

For the resin, we chose 1,7-dimethylnaphthalene. Its alkane:aromatic ratio (2:10 or 16.7:83.3) is quite a bit different from the overall resin balance (approximately 58:42, see Table 6.1) reported by NMR [33], but it does resemble some of the molecules depicted earlier for asphaltenes [26]. The number of aromatic rings and side chains makes it intermediate between saturates and asphaltenes. Its size is relatively small, however, compared to the overlap in resin and asphaltene molecular weight distribution reported by Groenzin and Mullins [45].

Two different asphaltene molecules were considered. Both have appeared in the scientific literature as examples of asphaltene molecules, based on experimental characterizations. One, taken from NMR studies by Artok et al. [31], contains a moderate-size aromatic core with very small branches. It is from a collection of sample molecules they proposed that in total represent statistics of molecular asphaltenes. A ball-and-stick model is shown in Figure 6.1. The other molecule, taken from discussions by Groenzin and Mullins [45] of their fluorescence depolarization studies, contains a somewhat smaller aromatic core and much longer alkane side branches. It is also one molecule from a collection of proposed asphaltenes. Ball-and-stick and wireframe models are shown in Figure 6.2. These models were chosen because they represent different proposed styles for the kinds of bonding patterns present in asphaltenes. Rogel and Carbognani have chosen asphaltenes with much larger pericondensed aromatic rings (8 to 20 rings fused together) for their simulations [95]. The molecular weights and other molecular characteristics of these proposed asphaltene molecules are compared in Table 6.2.

The overall mixture composition was chosen based on measurements by Storm and co-workers [33]. They applied NMR to asphalt fractions separated by the common alkane precipitation method (they used heptane), and through the different peak positions of different kinds of carbon atoms they were able to identify the balance among aromatic and alkane carbons in the asphaltene, resin, and saturate mixtures. An asphaltene mass fraction of 21% was selected, which is similar to the 22wt% they reported for Ratawi vacuum residue.

The concentrations of n-C_{22} and dimethylnaphthalene were chosen based on the alkane:aromatic carbon ratio (72.2:27.8 $\approx$ 8:3) reported by Storm et al. [33] for the oil components. This led to mixtures with

Table 6.1: Speciation reported by Storm et al. [33] for Ratawi vacuum residue and Alaska North Slope (ANS) crude oil, based on ^{1}H and ^{13}C NMR experiments. The overall division among oil, resin, and asphaltene comes from their earlier work [32]. Identifications of the missing carbon atom types (such as 39 of the 72.2% oil alkane carbon C(AL) in Ratawi vacuum residue) were not identified in those works. One possibility is that they are alkane branch points. All values are based on mole fractions, rather than weight fractions.

		Ratawi vacuum residue			ANS vacuum residue		
parameter		oil	resins	asphaltenes	oil	resins	asphaltenes
H/C atom ratio		1.6	1.53	1.22	1.6	1.4	1.0
C(AR),%		**27.8**	**41.3**	58.1	27.9	42.7	59.0
	b_3	0.0	0.4	9.8	0.0	2.0	11.0
	H	10.2	16.2	16.5	10.0	14.6	13.6
	R	9.9	11.7	14.1	10.7	14.7	18.2
	n, b_2, CH_3	7.8	31.5	17.9	7.3	11.4	16.2
C(AL),%		**72.2**	**58.7**	41.9	72.1	57.3	41.0
	a	**4.9**	3.2	2.3	2.8	3.3	2.2
	b	**4.0**	3.8	2.8	3.5	4.4	2.6
	d+*e*	**24.3**	19.7	13.1	22.6	15.9	12.4
H(AR),%		7.3	10.6	13.7	6.6	10.8	14.0
H(α),%		14.0	12.5	22.0	12.5	16.6	21.1
H(β),%		59.6	53.3	50.8	64.7	55.5	51.6
H(δ),%		19.0	23.6	13.6	16.3	17.1	13.8

C(AR) = aromatic carbon attached to H, R, CH_3, naphthenic carbon (n), 3 AR at the fusion of 2 rings as in naphthalene (b_2), or 3 AR at the fusion of 3 rings (b_3)

C(AL) = alkane carbon at end of chain (*a*), next to end (*b*), or on CH_2 group (*d*+*e*); individual definitions of *d* and *e* are not provided in the original paper

H = hydrogen attached to aromatic carbon (AR), alkane carbon bonded to aromatic carbon (α), aliphatic carbon (β), or terminal CH_3 group (δ)

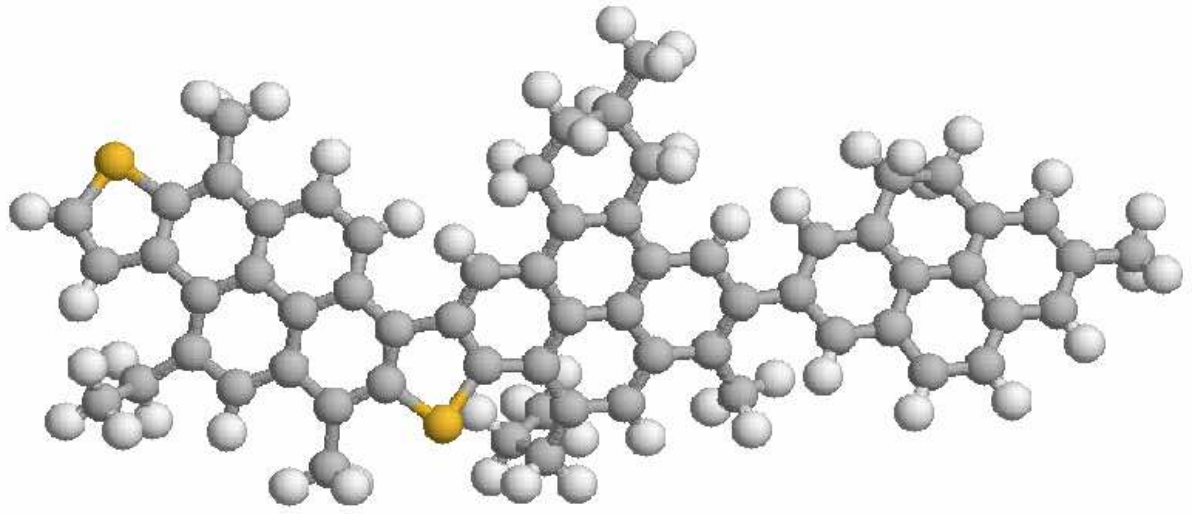

Figure 6.1: Ball-and-stick representation of asphaltene 1, $C_{64}H_{52}S_2$. This configuration corresponds to the template used when creating the mixture. It was taken from Figure 8 (upper left) of ref [31].

59wt% n-C_{22} and 20wt% 1,7-dimethylnaphthalene. If more molecules were desired for each subsection of the asphalt, an alternative would have been to use the overall oil/resin/asphaltene balance reported for this mixture (71.0/7.5/21.5, ref [32]) in conjunction with the resin and oil breakdowns of alkane and aromatic carbon. We are pursuing such a strategy in future work. An alternative interpretation of the current work is that n-C_{22} and dimethylnaphthalene represent alkane and aromatic fractions of the maltene, with no resin molecules being present.

A molecular simulation requires a precise number of molecules, rather than an overall mass fraction. This was achieved using standard chemical engineering methods for converting between mass fraction and mole fraction. First, a concentration of 5 asphaltene molecules per simulation box was chosen as a basis. The corresponding mass of resin and saturate was then calculated from the asphaltene molecular weight and the ratio of mass fractions. Finally, the corresponding number of molecules of resin and saturate were calculated using their molecular weight. The number of resin and saturate molecules were then rounded to the nearest integer values, causing a slight shift in concentration. The resulting mass fractions are listed in Table 6.3. The somewhat smaller molecular weight of asphaltene 1 causes its mixture to require somewhat fewer molecules than the mixture with asphaltene 2. Table 6.4 lists the mass fraction of each atom type, the hydrogen-to-carbon ratio, and the distribution of carbon and hydrogen between aromatic and alkane environments for each mixture. The overall mass fractions carbon in the mixtures are similar to those in asphaltenes alone (Table 6.2), while the fractions of hydrogen and sulfur in the mixtures are higher and lower respectively, compared to the asphaltenes.

We note that the model asphalts have low heteroatom content (0.7 to 1.5 mass% sulfur, and no nitrogen or oxygen) compared to typical amounts in SHRP core asphalts (1.1 to 6.9 % sulfur, 0.5 to 2.0 % nitrogen, 0.6

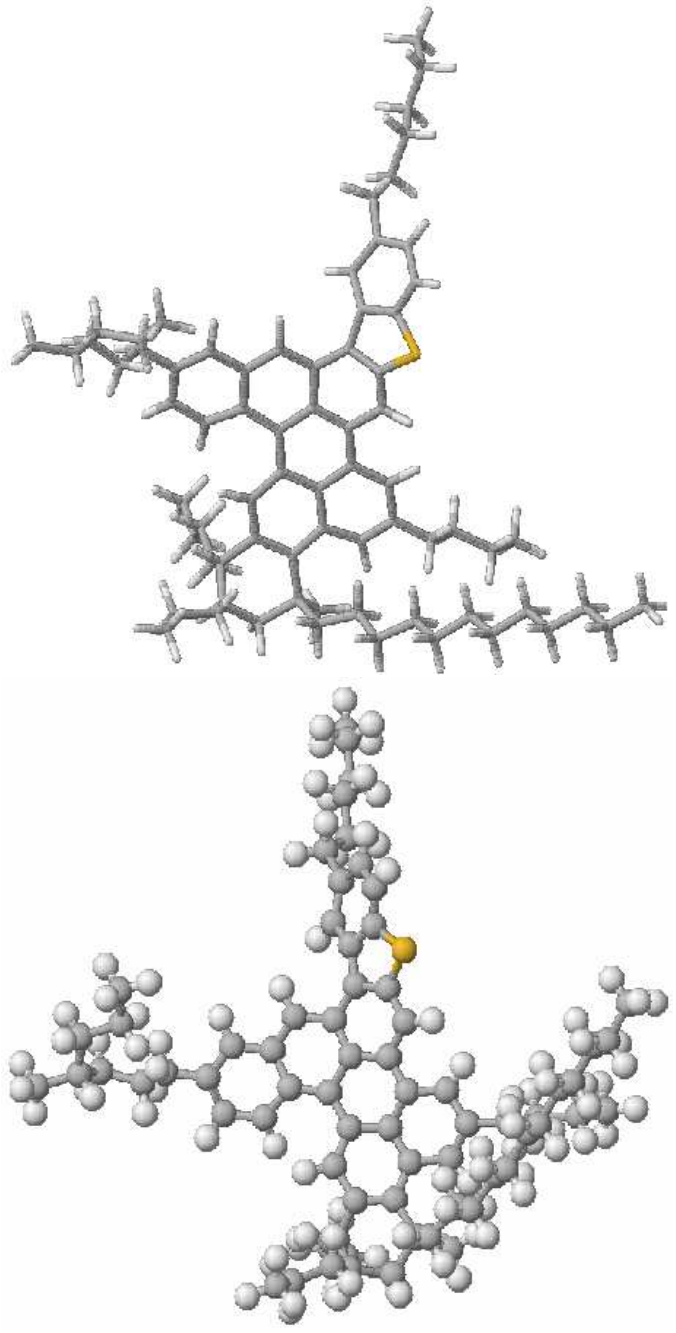

Figure 6.2: Wireframe and ball-and-stick representations of asphaltene 2, $C_{72}H_{98}S$. The ball-and-stick configuration corresponds to the template used when creating the mixture. The molecule was taken from Figure 8 (left side) of ref [45].

Table 6.2: Chemical composition of asphaltene 1 and asphaltene 2 molecules.

molecule	molec. wt (g/mol)	% C (total) (by mass)	% H	% S	% C (aromatic) (vs. total carbon)	% C (alkane)
asphaltene 1	885.25	86.8	5.9	7.2	75.0	25.0
asphaltene 2	995.6	86.9	9.9	3.2	41.7	58.3

Table 6.3: Overall composition of mixtures based on asphaltene 1 and asphaltene 2.

	number of molecules			mass fraction		
mixture	asphaltene	1,7-dimethyl-naphthalene	*n*–C_{22}	asphaltene	1,7-dimethyl-naphthalene	*n*–C_{22}
1	5	27	41	20.7	19.7	59.6
2	5	30	45	21.1	19.8	59.1

to 1.1 % oxygen) [9]. The impact on physical properties is not calculated here. Model asphalts in follow-up work [96] have higher concentrations of sulfur and nitrogen, similar to those in SHRP core asphalt AAA-1.

6.2 Volume and equilibration

An extensive set of Monte Carlo simulations was used in an attempt to equilibrate each asphalt-like mixture. Based on the ternary mixture of small molecules (chapter 5), we would expect that of order $1 - 2 \times 10^5$ Monte Carlo cycles with a combination of atom translation, molecule translation, molecule rotation, volume changes, and molecule configuration moves would be sufficient to reach an equilibrium state. Figure 6.3 shows, however, that this was not the case. The asphaltene 1-based system remained out of equilibrium even after 115,000 MC cycles, which required approximately a *month* of CPU time for each mixture. As seen in the figure, the system has not reached a sampling regime, in which it fluctuates about a long-term average. Instead the volume is slowly drifting, with no plateau in evidence. Physically, we suspect that this is because

Table 6.4: Distribution of atom types (by number unless indicated) in the asphalt-like mixtures.

	mass % by atom			H/C	Carbon (vs. total C)		Hydrogen (vs. total H)	
mixture	C	H	S	ratio	% aromatic	% alkane	% aromatic	% alkane
1	86.85	11.65	1.50	1.60	33.0	67.0	9.4	90.6
2	86.87	12.45	0.68	1.71	26.3	73.7	8.0	92.0

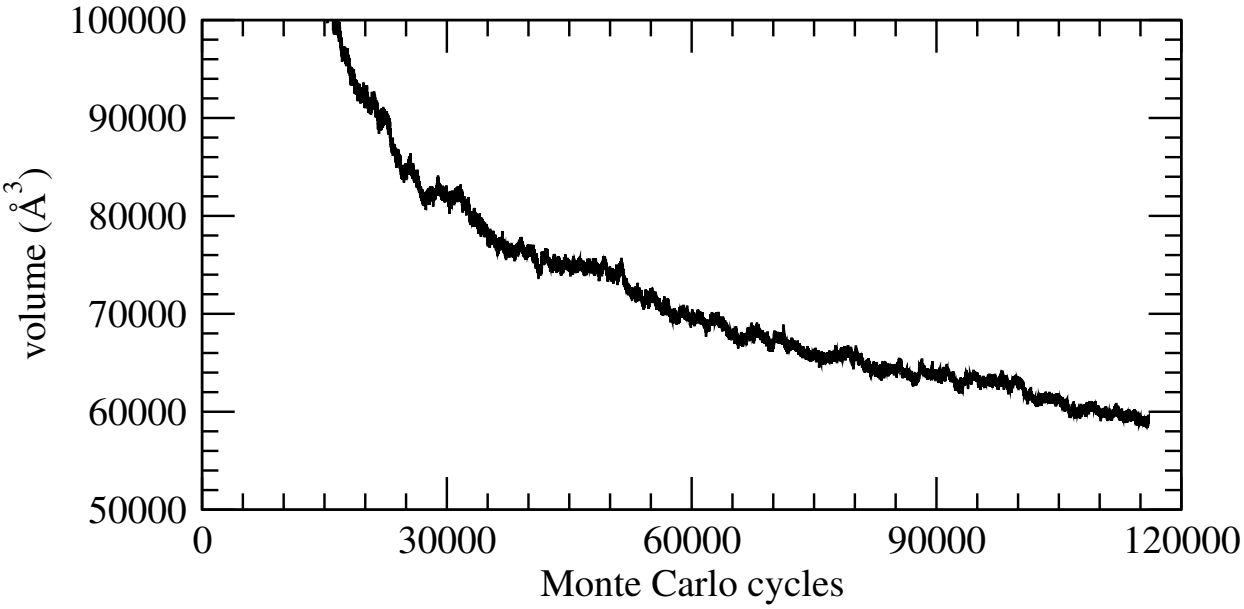

Figure 6.3: Evolution of overall volume for mixture based on asphaltene 1, as a function of Monte Carlo cycles. The volume continues to change even after significant amounts of simulation.

the larger molecular weights led to a higher viscosity and more sluggish system response.

Subsequently we turned to molecular dynamics. This method moves all atoms simultaneously according to configuration- and distance-dependent intermolecular forces. We hypothesized that molecular dynamics would facilitate the molecules moving closer together, and Figure 6.4 shows that this was indeed the case. For both asphalt-like mixtures, the volume decreased significantly after a few hundred ps and reached new steady values at each temperature. In later work [11], we have attributed the slow response to different relaxation times for each molecule type in the system. Large molecules require a longer time to reach equilibrium. For asphaltenes at the lower temperatures considered, the estimated relaxation time is much longer than any possible molecular simulation. This makes the results potentially sensitive to the initial molecule positions employed. For smaller molecules, the relaxation times are much shorter than a typical simulation. (See ref [11] for details.)

The small molecule simulations of naphthalene suggested that slightly different densities may result (between Monte Carlo and molecular dynamics), potentially due to subtle differences in how the energies between molecules are calculated in two separate standalone programs. Further comparisons of results between the two methods for small molecules were not carried out, so research efforts could be focused on model asphalt systems.

Examples of overall molecular simulation cells that result after volume equilibration are shown in Figure 6.5. Results at other temperatures are similar. Discerning packing differences among many temperatures requires averaging over many structures rather than a single image, as we show in later work [96].

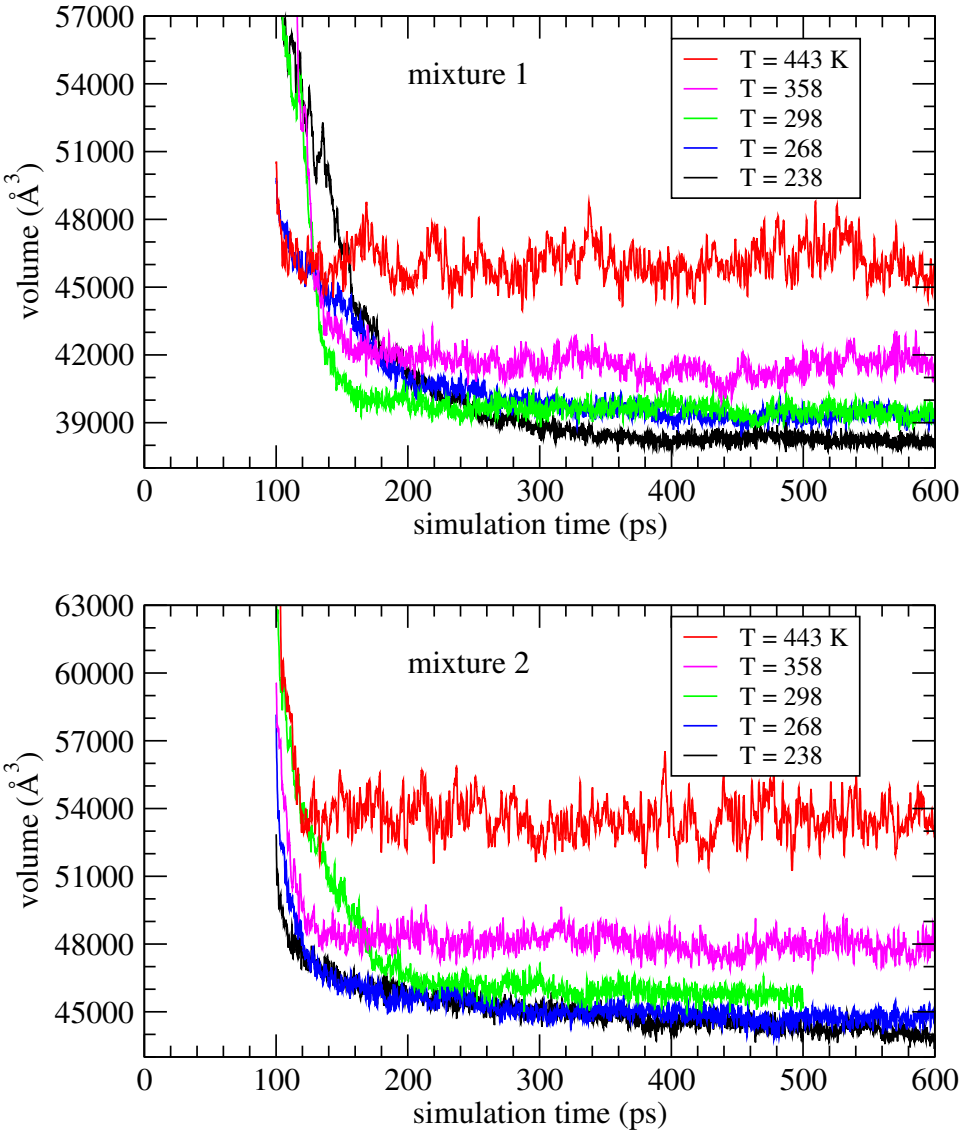

Figure 6.4: Evolution of overall volume for mixtures based on asphaltene 1 (top) and 2 (bottom), as a function of simulation time in molecular dynamics. After sufficient equilibration, volume increased monotonically with respect to temperature. Using MD instead of MC, the volume stabilized at a constant level for each temperature, allowing average properties to be estimated. Prior to 100 ps, volumes were fixed to constant values.

The molecules are close to one another, and discernable patterns are difficult to recognize. Restricting the images to only the asphaltene molecules (Figure 6.6), it can be seen that both parallel stacking and more distant, non-parallel interactions occur in each mixture. Molecules that are closely spaced with similar shapes are parallel; those pointing in different directions are non-parallel. Stacking is more predominant in the asphaltene 1-based mixture. We hypothesize that this difference is due to the side chains on the asphaltene 2 preventing closer aggregation and/or association. Since the side chains of asphaltene 2 make it more representative of NMR [33] and fluorescence [45] data, the lower image in figure 6.6 is more likely representative of the geometry of asphaltene associations in bulk asphalts.

6.3 Density results

The two different asphalt-like mixtures were simulated at 5 temperatures over the range -35°C to 170°C. Such a high upper temperature was chosen to explore the extent of liquid-like behavior; it is slightly higher than the upper temperature experienced in the rolling thin-film oven (RTFO) procedure. The volume evolution at each temperature is shown in Figure 6.4, and the sampling regions for each mixture at each temperature are magnified in Figures 6.7 and 6.8. At each temperature, the volume and its fluctuations stabilized about a different plateau. The final averages reached representative values in each case, as depicted by the horizontal lines.

The average densities of each mixture are shown in Figure 6.9. They were calculated from molecular dynamics using volume evolution curves analogous to that shown in Figure 3.3. Both mixtures show a similar temperature dependence. The highest predicted densities are at -35°C, where ρ equals 0.929 and 0.889 g/cm^3, respectively. The asphaltene 2-based mixture shows a continual change in slope as the temperature is increased. The sharpest change in slope is just above 0°C, suggesting a glass transition. The asphaltene 1-based mixture densities show some scatter in the rate of decrease. A well-defined break in slope and volumetrically defined glass transition are not clear, but there is possible evidence for a glass transition somewhere within the -35 to 25°C range. Glass transition data from experiment are not available for these systems, since they are not available in practice. (They are only theoretical models of asphalt systems.)

The densities of several real asphalts have been reported in the literature. Unfortunately Storm et al. [33] did not report densities for the asphalts used to choose the mixture compounds and compositions. Robertson and co-workers of the Western Research Institute have reported densities at 60°C that ranged from 0.99 to 1.03 g/cm^3 for different SHRP asphalts [97]. Such densities are similar to those of pure, small aromatic compounds, such as substituted naphthalenes (see Figure 4.6 on page 54). The model asphalts simulated here are approximately 10–15% too low in density. This is likely a result of a mismatch in overall asphalt composition. In the model asphalts, a high alkane maltene concentration was chosen to match portions of the NMR data (Table 6.1, see also discussion above). Compared to SHRP core asphalts, the model asphalts here (Table 6.4) have more hydrogen (11.5–12.5 mass% vs. 10.2–11.4%), more carbon (86.9 vs. 80.7–86.7%), and less sulfur (<1.5% vs. 1–7%), in comparison to NMR data [9]. The lower H and C

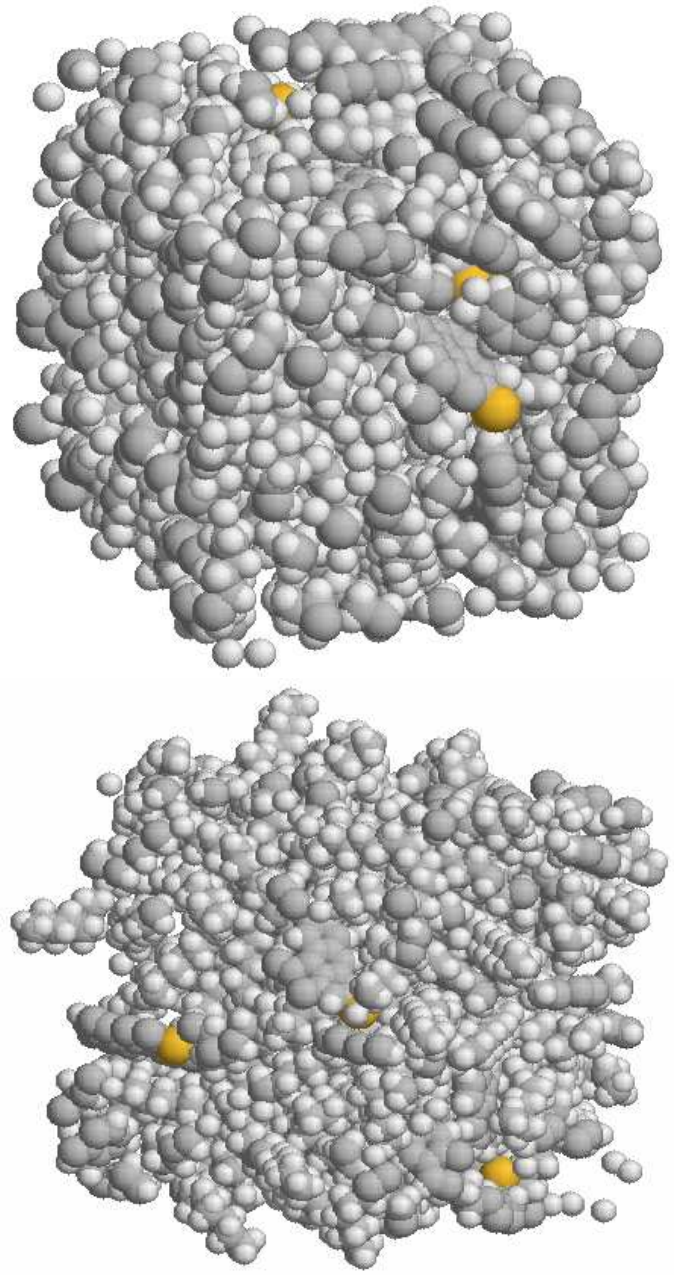

Figure 6.5: Simulation boxes after volume equilibration for mixtures based on asphaltene 1 (top, -5°C) and asphaltene 2 (bottom, 25°C). Carbon, sulfur, and hydrogen atoms are depicted in dark gray, yellow, and white, respectively. Open holes on each edge and isolated atoms are due to periodic boundary conditions, meaning that the right side of the box interlaces with a copy of the left side, etc.

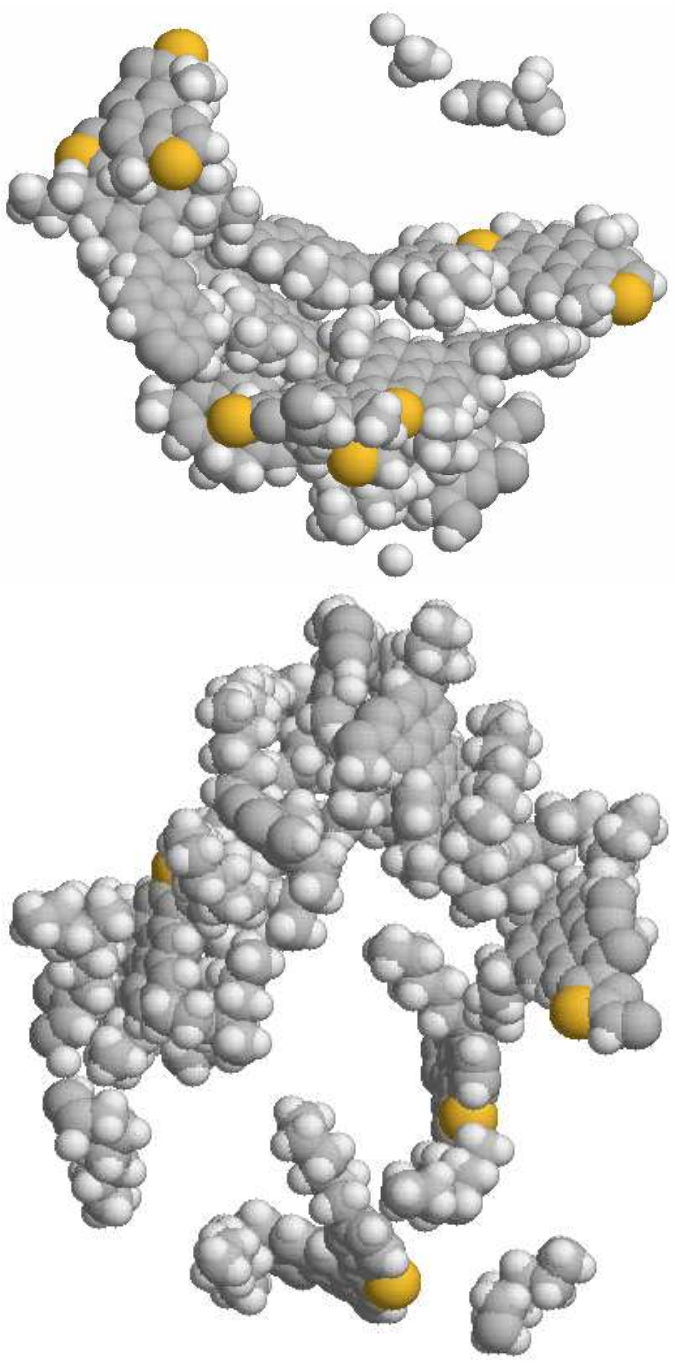

Figure 6.6: Asphaltene molecules in simulation boxes after volume equilibration for mixtures based on asphaltene 1 (top, -5°C) and asphaltene 2 (bottom, 25°C). Carbon, sulfur, and hydrogen atoms are depicted in dark gray, yellow, and white, respectively. Periodic boundary conditions are applied here as well.

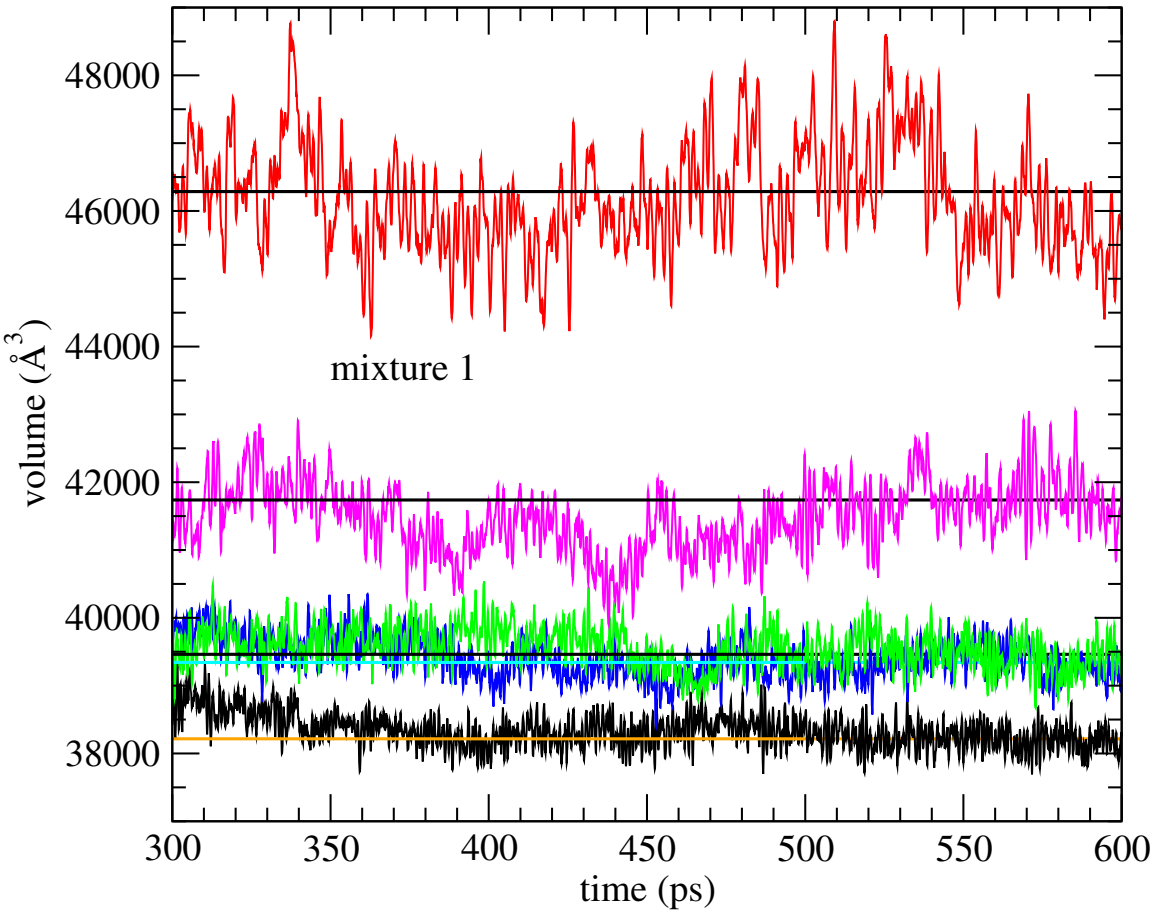

Figure 6.7: Sampling region in overall volume for mixtures based on asphaltene 1, as a function of simulation time in molecular dynamics. Horizontal lines show the final averages, which increased monotonically with respect to temperature.

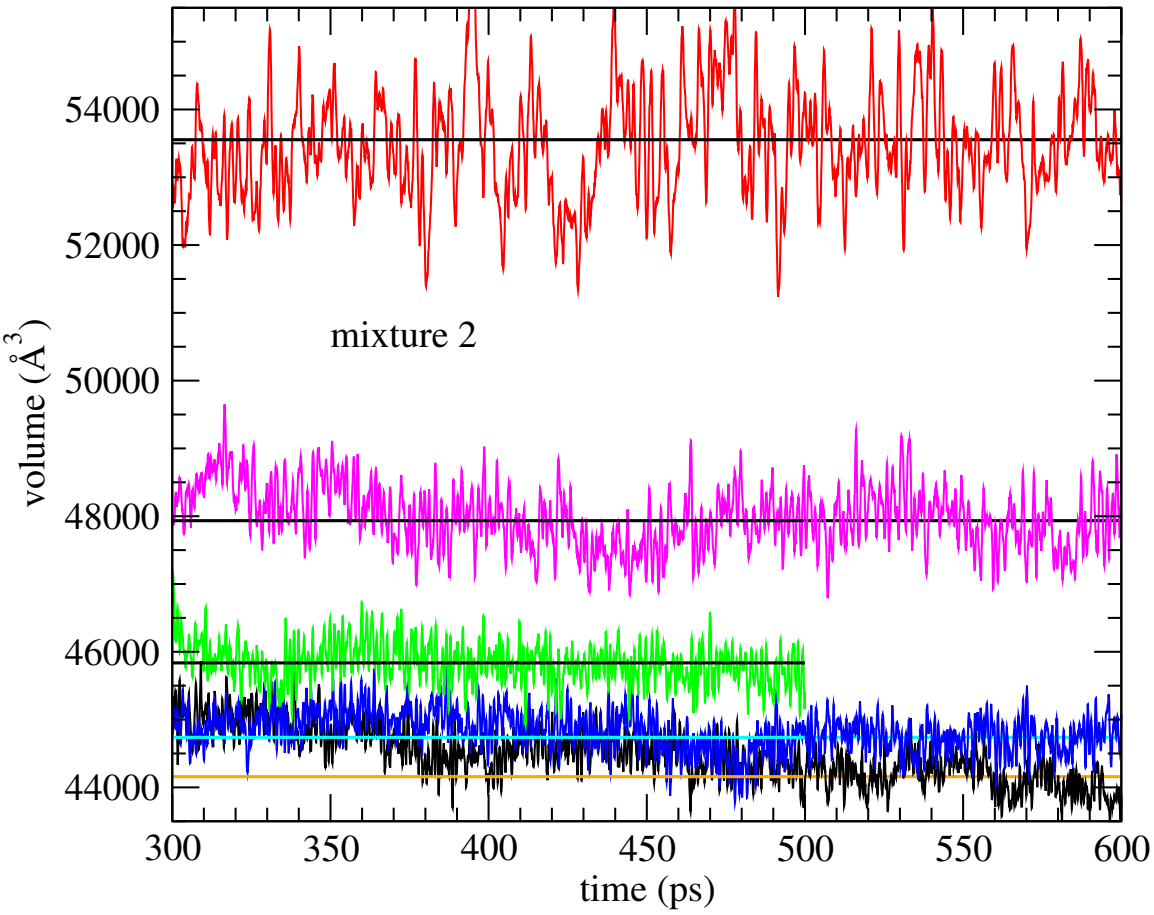

Figure 6.8: Sampling region in overall volume for mixtures based on asphaltene 2, as a function of simulation time in molecular dynamics. Horizontal lines show the final averages, which increased monotonically with respect to temperature.

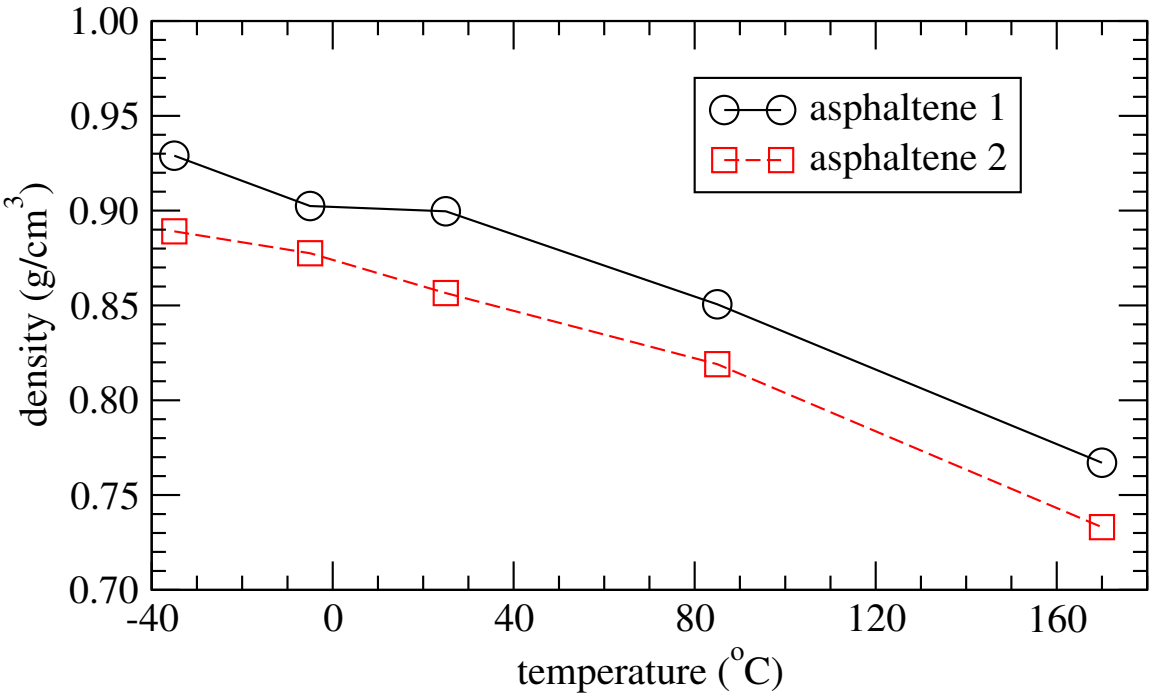

Figure 6.9: Average density calculated for each model asphalt mixture over a range of temperatures. The averages were accumulated in the sampling regions (Figures 6.7–6.8) of molecular dynamics simulations, at the temperatures shown.

limits in the experimental data correspond to asphalts with approximately 6–7% sulfur [9]. Nitrogen and oxygen were also found at 1–2 wt% [9] in real asphalts; the model asphalts lack heteroatoms besides S. Merely replacing some C and H atoms with heavier N, O, and S atoms would increase the mass density, independent of any densifying effect that such changes would cause in the molar volume. Composition refinements in future work that include such functional groups should attain mass densities more similar to those of SHRP asphalts.

6.4 Heat capacity, expansion coefficient, and isothermal compressibility

The heat capacity of each asphaltene mixture was calculated from the sampling region of most molecular dynamics simulations, using eq 3.11. The results are shown in Figure 6.10. The asphaltene 2-based mixture shows approximate rises in heat capacity between -40°C to 0°C and between 25°C to 85°C. A rise is consistent with a glass transition occurring in that temperature range. The accuracy of these results (not shown) is insufficient for drawing a firm conclusion, however. For the asphaltene 1-based mixture, calculated heat capacities are more widely scattered. The range of calculated heat capacities is larger than the range found at all temperatures for the asphaltene 2-based mixture. The relationship to a glass transition is unclear. These findings, in combination with the larger errors associated with the density, suggest that both systems (especially the asphaltene 1-based mixtures) would benefit from additional averaging, which should lead to improved statistics.

The heat capacities differ significantly from the experimental values measured by differential scanning calorimetry for SHRP core asphalts [97]. That report illustrates DSC results (see Figures 3-45, 3-46, 3-47) with increases in heat capacity when passing through T_g from 0.8 to 1.4 J/g°C for AAA-1 and from 1.0 to 1.6 J/g°C for AAB-1 and AAM-1. The heat capacities found here by molecular dynamics for the asphalt mixtures are larger than those experimental values for real asphalts; heat capacity measurements for the model systems are not available, as explained above. One likely cause of the differences in heat capacity, found while writing the final report, is that some run-time parameters in the molecular dynamics simulations were not set to the best choices, one effect being that energy fluctuations were prone to errors. This makes the results for heat capacity not very reliable. Even without this drawback, we suspect that the errors in both magnitude and trend are additionally due to insufficient sampling during the molecular dynamics simulations. Longer simulations will lead to better defined "plateau" values, indicating a converged average. These will be conducted in the future in order to investigate this hypothesis. Finally, another possible cause for the discrepancy is a fundamental limitation of classical molecular simulations in calculating heat capacity, since quantum-mechanical effects on bond length and bond angle vibrations are not accounted for. Doing so would be extremely expensive computationally and would not be worthwhile for obtaining estimates of a property not widely used in asphalt engineering.

The results for coefficient of thermal expansion (α) and isothermal compressibility (β) are shown in Figures 6.11 and 6.12. The expansion coefficients are of order $0.4 \times 10^{-3}\mathrm{K}^{-1}$, which is comparable to that

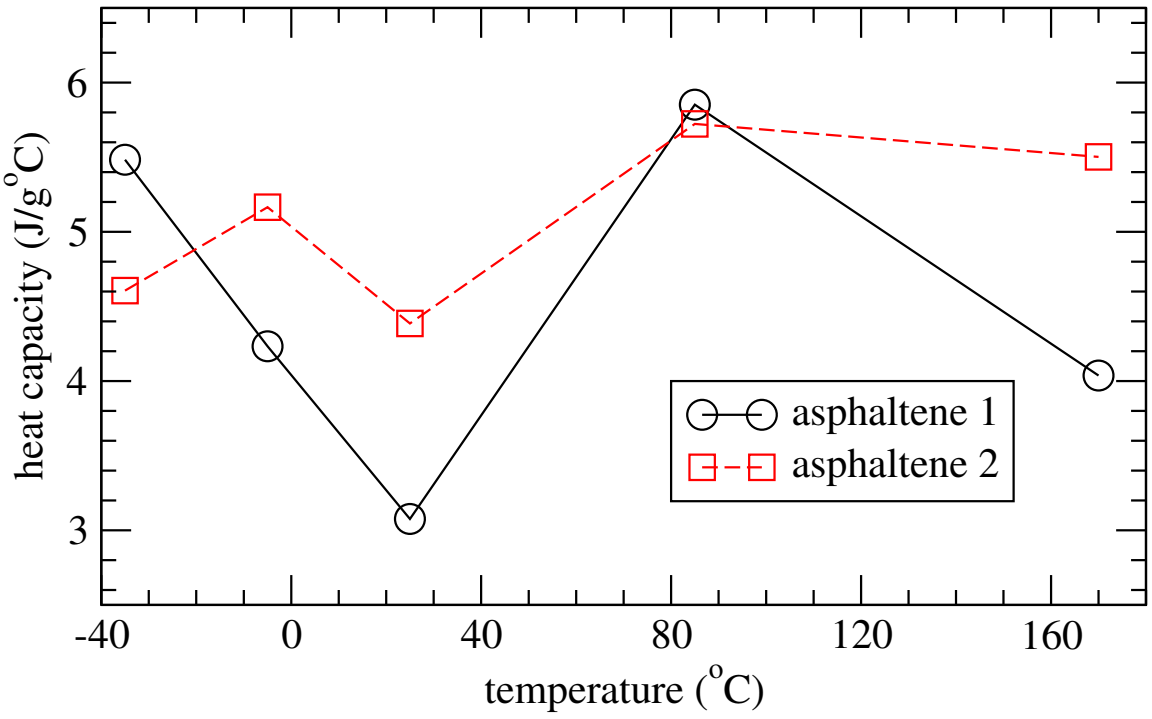

Figure 6.10: Heat capacity calculated for each model asphalt mixture from molecular dynamics.

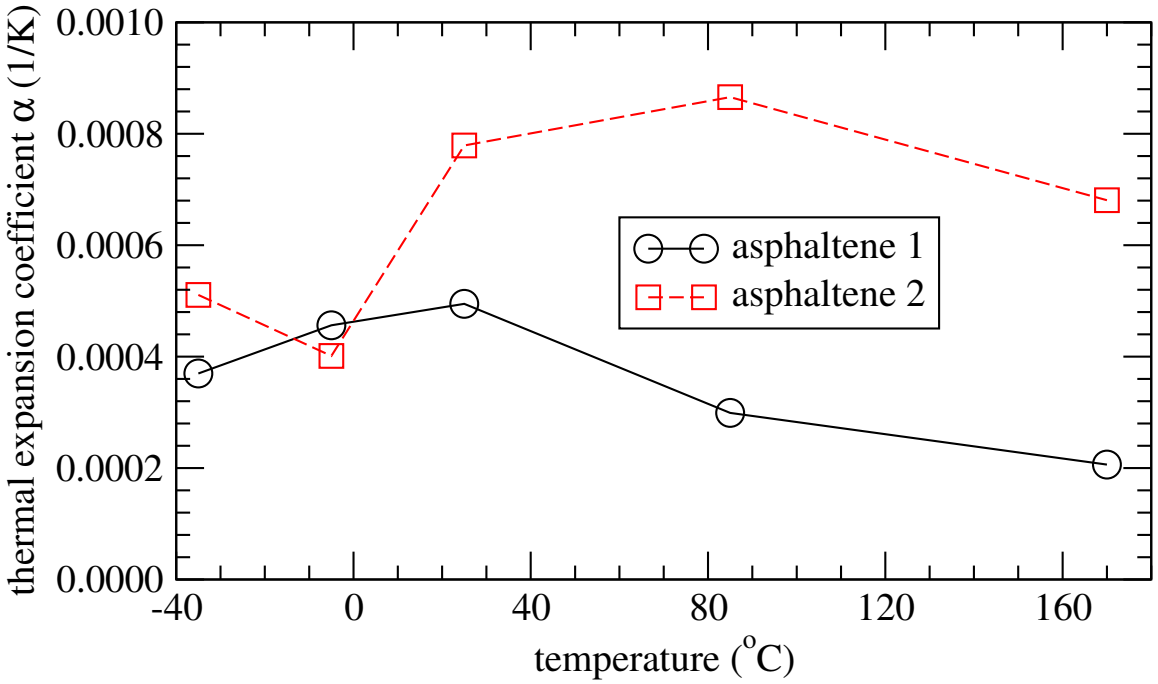

Figure 6.11: Coefficient of thermal expansion for each model asphalt mixture from molecular dynamics.

of the small molecules (Table 4.4). The rise in compressibility above 0°C for the asphaltene 2 mixture is consistent with the density plot, indicating hints of glass transition behavior. The situation is not as clear for the asphaltene 1 mixture, as was seen with the density and heat capacity. The overall rise in isothermal compressibility with temperature is consistent with literature expectations (see section 4.2 on page 55). This corresponds to a decrease in the bulk modulus from of order 2 GPa to less than 1 GPa at elevated temperatures (figure 6.13). Note that bulk modulus κ is different from complex modulus G^*. It refers to the compressibility of the material under uniform stress, while G^* refers to the stress required to deform a material under shearing conditions. Glass transition evidence is not clear from these figures for either mixture.

6.5 Molecular Orientation

The arrangement of molecules relative to one another can affect the ability of an asphalt to transmit force and respond to cyclic stresses. The non-spherical shapes of the different molecules present in the model asphalt implies that anisotropic packings may be present within the mixture, which could potentially lead to anisotropic effects that persist over longer length scales. The presence of energetic interactions related to such packings, e.g. π–π interactions between neighboring asphaltene molecules, is often postulated in regard to the overall physical and chemical properties of asphalts [9]. While one may expect that molecules

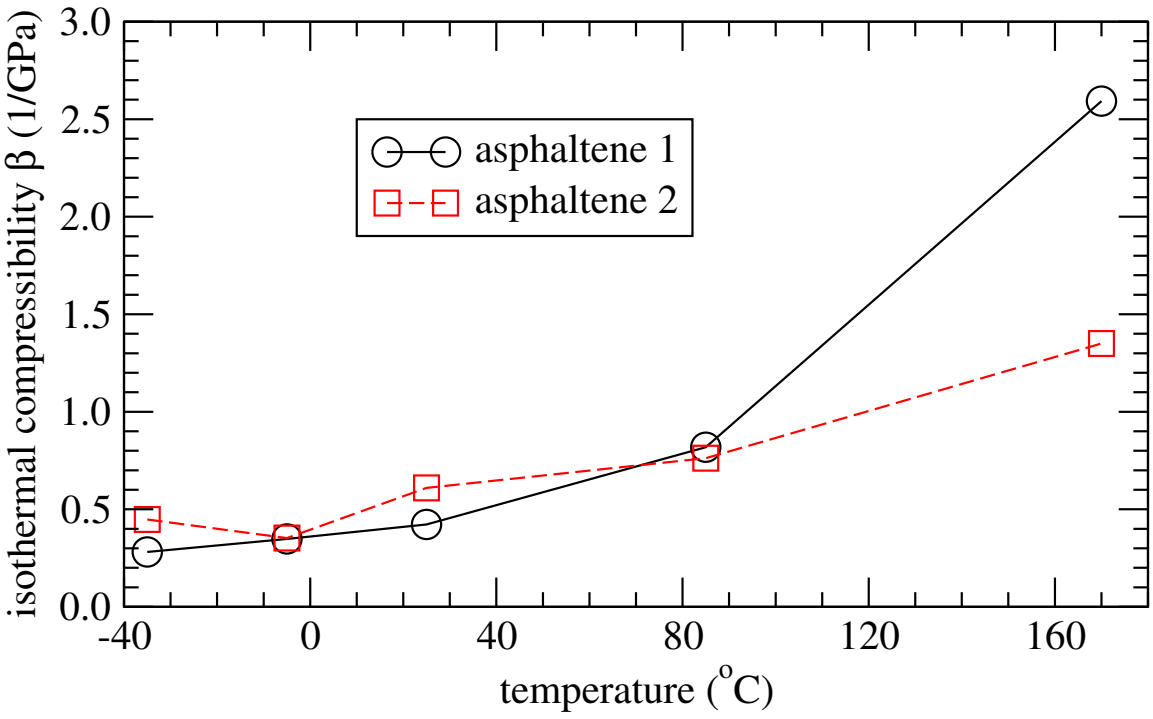

Figure 6.12: Isothermal compressibility (inverse of bulk modulus) for each model asphalt mixture from molecular dynamics.

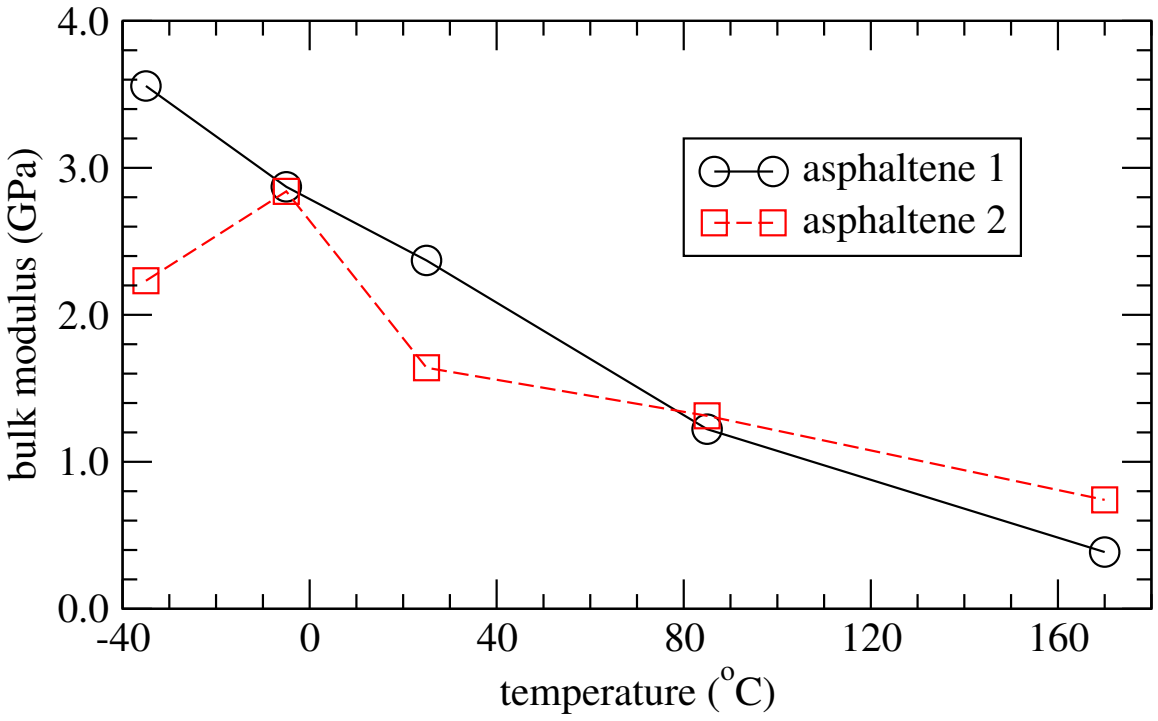

Figure 6.13: Bulk modulus for each model asphalt mixture from molecular dynamics.

with a planar tendency should preferentially occur parallel to one another (similar to how papers stacked on a messy desk are mostly parallel), this has not always been found to be the case in real molecules. For example, neighboring benzene molecules (one planar aromatic ring) have been determined both theoretically [98] and experimentally [99] to pack into perpendicular "T" configurations, rather than coplanar parallel stacks.

In order to learn more about how the different molecules arrange themselves in the model asphalt mixtures, programs were written to calculate average molecular orientations. Normal vectors were calculated for each of two fused rings on the same molecule by constructing interatomic vectors within the ring and then using their cross product. Effort was focused on molecules with planar aromatic rings (e.g. dimethylnaphthalene and the asphaltenes), since the ring provides a physically representative normal vector about which relative orientations can be assessed. Triads of carbon atoms along a C_{22} chain could also define a local plane in the same manner, but due to torsional flexibility such molecules will likely have a number of different local planes along the chain, with no net average orientation that corresponds to the entire molecule for long periods of time.

The pair of normal vectors per molecule allows three different types of orientation to be calculated. Within each molecule, the angle between the normal vectors equals the *intramolecular* orientation, i.e. the deviation from planarity between the two fused rings. At an energy minimum this angle θ should be zero, and increases beyond zero suggest local stresses on the molecule. The angle itself is calculated using the dot product of the two normal vectors, $u_1 \cdot u_2 = |u_1||u_2| \cos\theta$. Two types of *intermolecular* orientation can be defined. One type comes from comparing molecules of the same type: dimethylnaphthalene vs. dimethylnaphthalene and asphaltene vs. asphaltene. In other words, one normal vector is taken from each of two neighboring molecules, and the angle is calculated via their dot product. The other type comes from the cross comparison, i.e. an asphaltene with a nearby dimethylnaphthalene molecule. Pairs of molecules can be averaged over all possible molecule combinations, or the calculation can be limited to pairs whose centers of mass are separated by no more than a setpoint separation R. Typically R=30 Å was used in the results shown here. This size includes most of the immediate separations present in the simulations. Smaller choices of R (a value equal to the first most likely separation distance) were pursued in follow-up work [96, 100].

The intramolecular orientation for dimethylnaphthalene in mixtures 1 and 2 are shown in Figure 6.14. These distributions were calculated by averaging within the Monte Carlo simulations, after molecular dynamics brought the molecular configurations and overall volume closer to an equilibrated state. While there is some scatter, generally dimethylnaphthalene retains a near-planar configuration, with the angle between planes lower than 15°. The deviations from planarity (i.e. higher angles) occur slightly more often at higher temperatures. Within the noise, the results are similar in the two mixtures.

The same simulations led to predicted intramolecular orientations for asphaltenes, which are shown in Figure 6.15. The asphaltenes experience a wider range of angles between adjoining rings, indicated a larger deviation from planarity. Such traits could be a response to forces exerted over a larger area since asphaltenes are bigger molecules. It suggests that asphaltene bending could be one mechanism for an asphalt to absorb

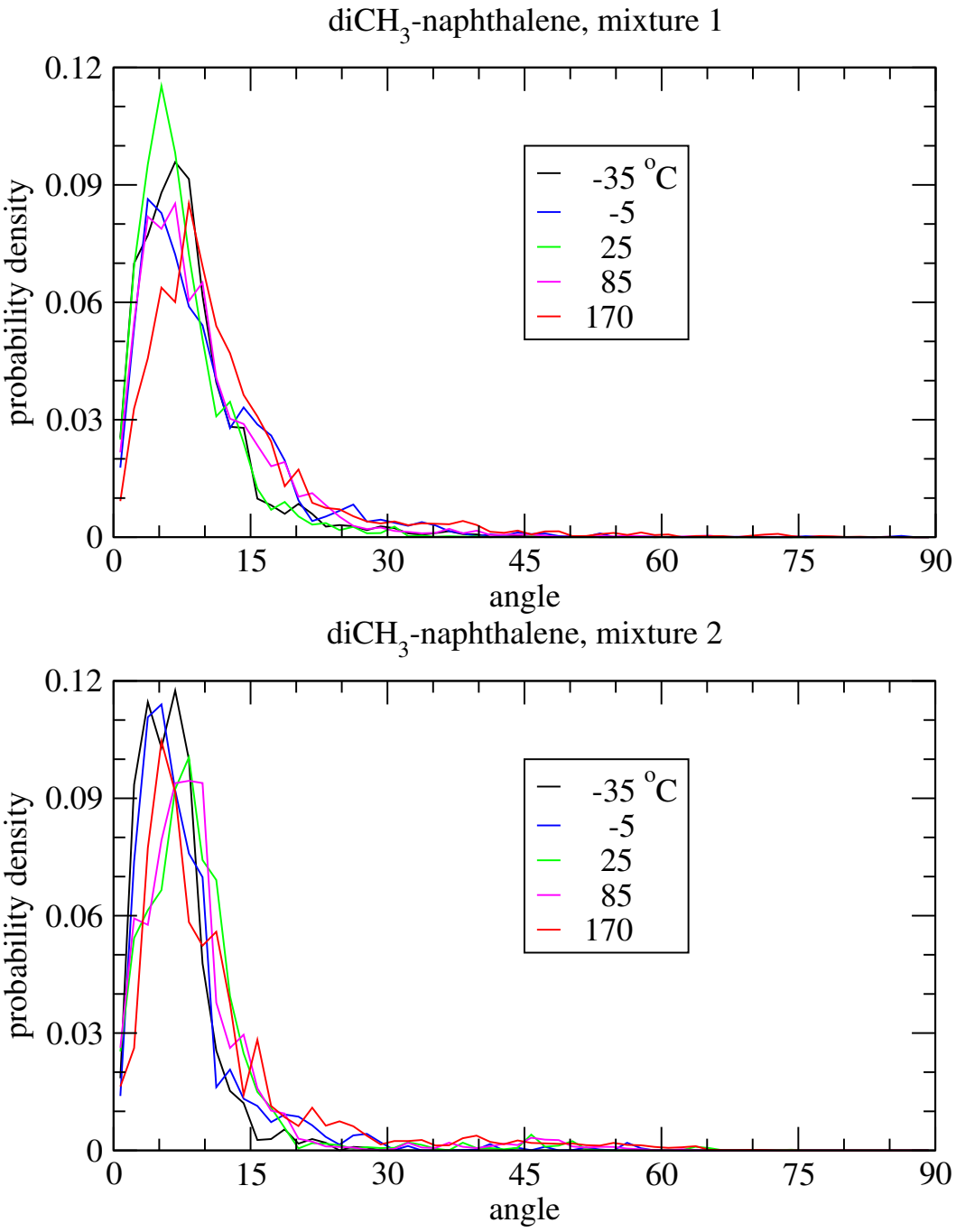

Figure 6.14: Intramolecular orientation for dimethylnaphthalene molecules in mixtures based on asphaltene 1 and 2; colors distinguish among different temperatures.

or release stress, as part of the overall viscoelastic response. Comparing asphaltenes in the two mixtures, the shape of the distribution and its temperature dependence differ. This indicates one possible underlying factor for why asphalts from different sources can exhibit different properties: their underlying asphaltenes may respond differently on a molecular level to stress. One possible source of the larger deviations from planarity, however, is the absence of improper torsion potential energy functions for the asphaltene. This assumption was only recognized at the time the report was being written, and its implications are being investigated in the next phase of the research. Another possible problem was a discovery that under certain circumstances the Monte Carlo code can lead to incorrect sampling. This bug was corrected by the code author (Marcus Martin), but some errors in sampling the average distributions may have occurred.

Intermolecular orientations were calculated by comparing all pairs of molecules whose centers of mass were closer than a setpoint distance of 30 Å. The resulting distributions are shown in Figures 6.16, 6.17, and 6.18 for dimethylnaphthalene pairs, asphaltene pairs, and dimethylnaphthalene–asphaltene. A completely random intermolecular orientation distribution would follow the function

$$P(\theta)d\theta = C\sin\theta d\theta \tag{6.1}$$

with $C = 1$ for θ in radians and $C = \pi/180$ for θ in degrees. This normalized function (integral of $P(\theta)d\theta$ from 0 to 90° equals 1) follows from choosing a random third point uniformly over (x, y) to form a triad with $(0, 0)$ and the x-axis. The $\sin\theta$ arises for the same reason that the area $dxdy$ in Cartesian coordinates becomes $\sin\theta drd\theta$ in polar or cylindrical coordinates.

Pairs of dimethylnaphthalene molecules are seen to follow this random distribution reasonably closely at most temperatures. At the coldest temperature, the dimethylnaphthalene molecules in the asphaltene 1 mixture show an enhanced tendency to be closer to parallel, while in the asphaltene 2 mixture a suppression of near-perpendicular dimethylnaphthalene molecules is more noticeable. For asphaltenes the results show much more scatter, since there are fewer pairs: a maximum of $5 \times 5 = 25$ compared to $27 \times 27 = 729$ and $30\times30 = 900$ pairs for asphaltenes and dimethylnaphthalenes, respectively. (Some pairs do not contribute to the statistics because their centers are further away.) The distributions for both mixtures indicate significant deviations from random inter-asphaltene orientations.

The distributions of orientations between molecule types show more structure than the orientations between dimethylnaphthalene molecules but less than those between asphaltene molecules. Asphaltene 1 shows a tendency to pack consistently closer to parallel with dimethylnaphthalene, compared to the random distribution. Asphaltene 2 roughly follows the random distribution more closely than asphaltene 1, except for a slightly larger suppression of the largest intermolecular angles. Both distributions appear relatively insensitive to temperature.

6.6 Solubility parameters

Redelius [94, 101] and Youtcheff (personal communication) have suggested that solubility parameters could be another useful way to compare these model asphalts with experimental data. The original Hilde-

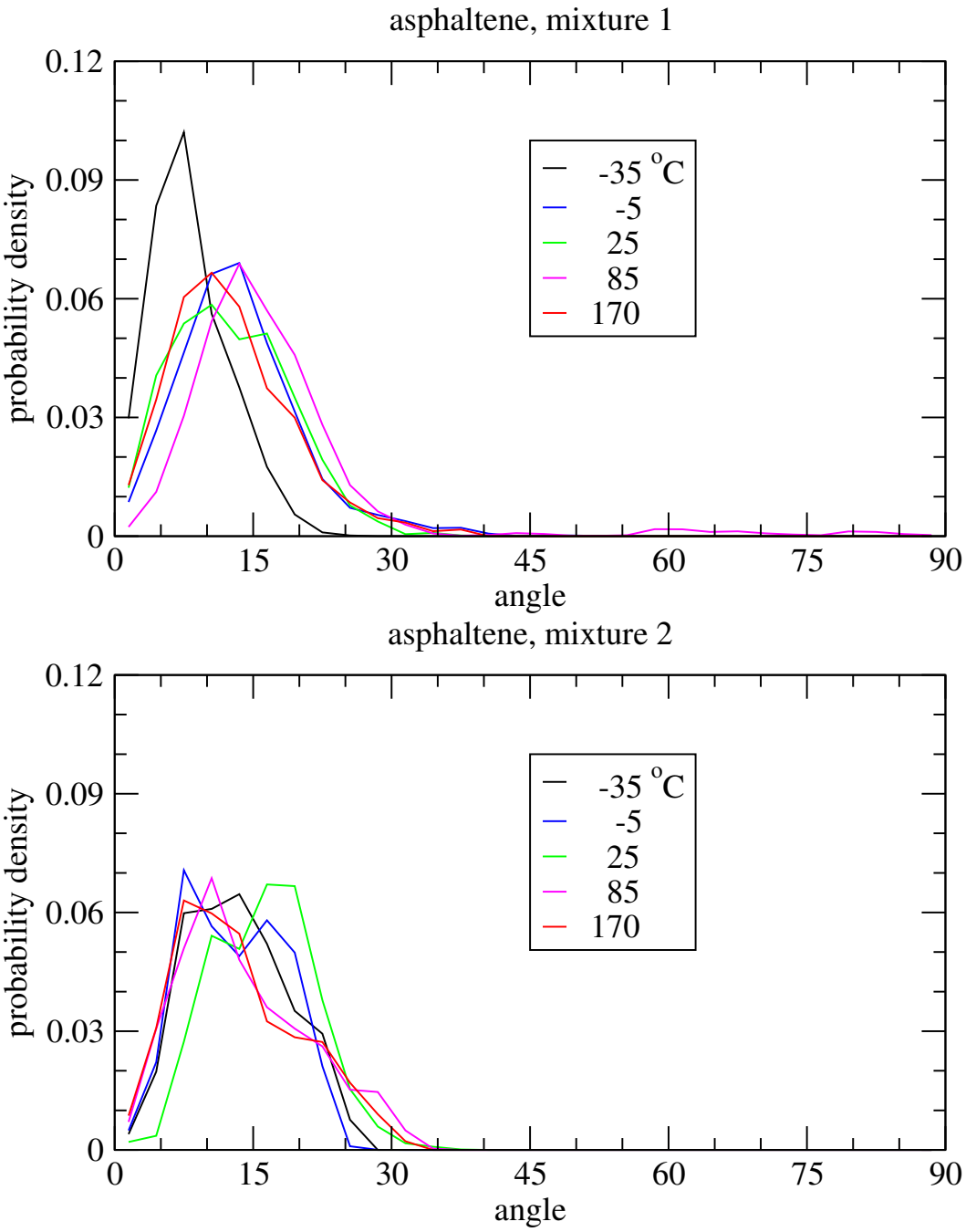

Figure 6.15: Intramolecular orientation for asphaltene molecules in mixture types 1 and 2; colors distinguish among different temperatures.

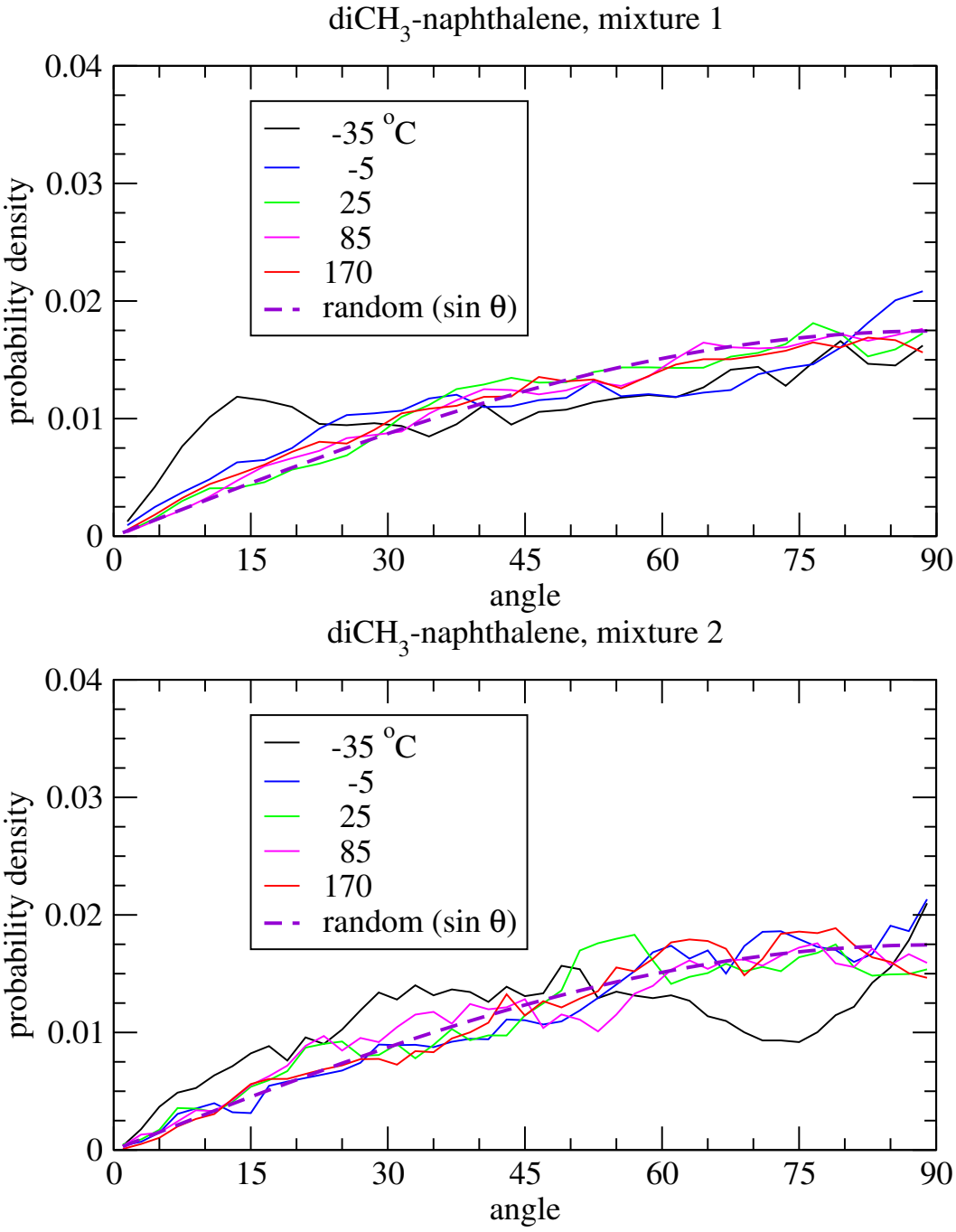

Figure 6.16: Intermolecular orientation for dimethylnaphthalene molecules in mixtures based on asphaltene 1 and 2; colors distinguish among different temperatures.

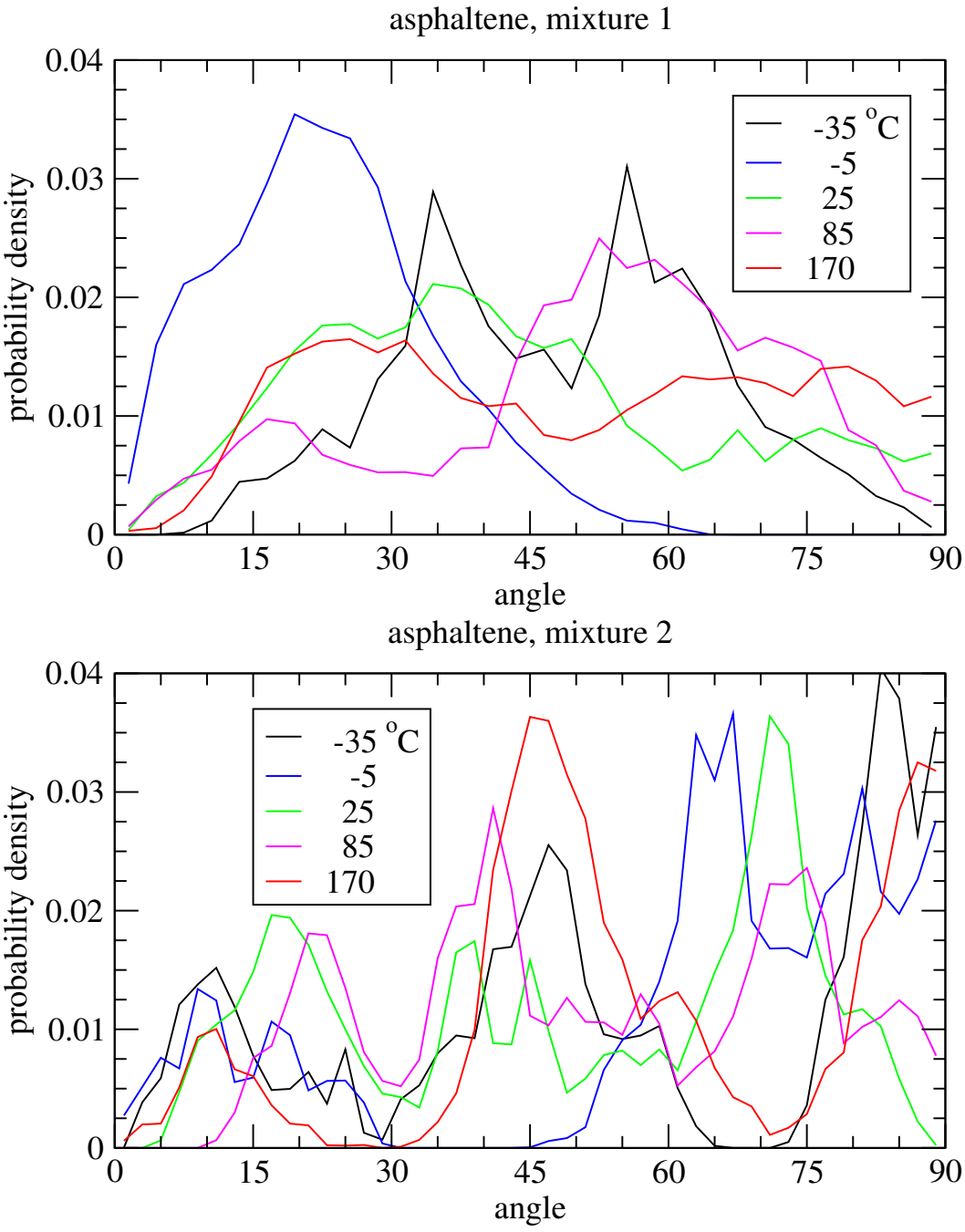

Figure 6.17: Intermolecular orientation for asphaltene molecules in mixtures 1 and 2.

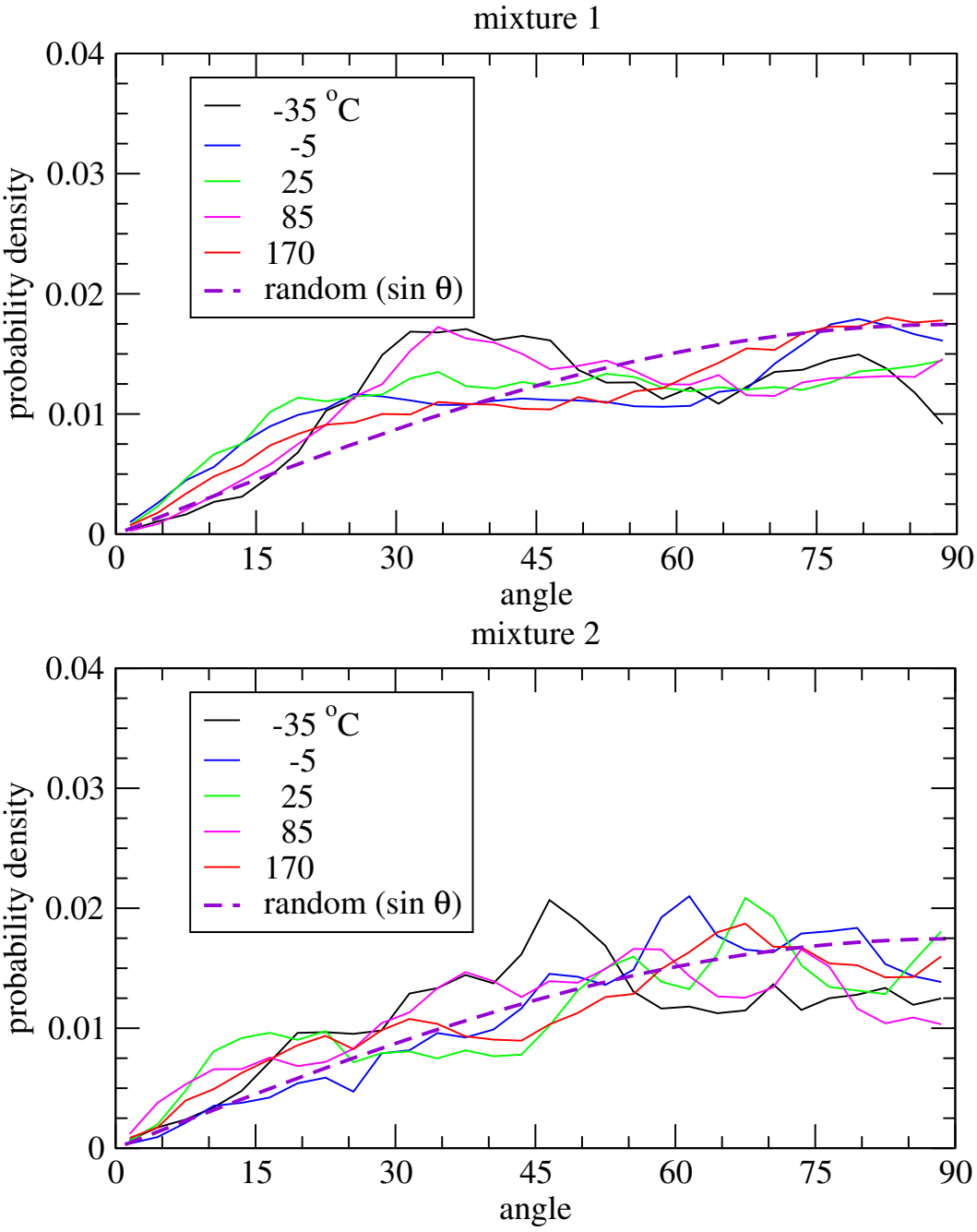

Figure 6.18: Intermolecular orientation between molecules of dimethylnaphthalene and asphaltene in mixtures based on asphaltene 1 and 2.

brand solubility parameter model [102] is based on the cohesive energy density: essentially the square root of the average stabilization energy for molecules to be randomly arranged and close together (liquid) or far apart (gas), per unit volume. This leads to

$$\delta^2 = (\Delta H^{\text{vap}})/v^L \; [=] \; (\text{energy per mol})/(\text{volume per mol}) \tag{6.2}$$

The heat of vaporization ΔH^{vap} equals the energy change upon boiling a liquid, and the specific volume v^L equals the molecular weight (g/mol) divided by the density (g/volume). The net result is a model that assigns a single value of δ to each compound. Subsequent developments, called Hansen parameters, combine nonpolar (also called dispersion), polar, and hydrogen bonding separately [103]. This leads to three solubility parameters $(\delta_d, \delta_p, \delta_h)$ per compound. Liquids with similar δ or $(\delta_d, \delta_p, \delta_h)$ values can dissolve one another, and disparate values lead to phase separation.

Standard literature sources [102, 103] cite solubility parameter values for many small molecules, including the solvents used in asphalt separations (see Table 6.5). Data for larger, more complex molecules are scarce. Experiments conducted by dissolving asphalts in different solvents [104] (described in [94]) have suggested ranges of 15.3 to 23 $(\text{J/cm}^3)^{1/2}$ for overall asphalts. Not all solvents in that range are equally good (or even good at all) at dissolving asphalts, however, for reasons concerning differences in polarity and hydrogen bonding [94]. Hansen solubility parameters [103] for chemical families within asphalts were also reported by Redelius [101].

We have turned to correlations to estimate the solubility parameters of the compounds used in this study. For molecules such as polymers that have a repeating chemical structure, correlations have been developed [105] that are based on the repeat unit. The molar volume v^L and solubility parameter δ are estimated by group contribution:

$$v^L = \sum_i n_i V_i \tag{6.3}$$

$$F = \sum_i n_i F_i \tag{6.4}$$

$$\delta = F/v^L \tag{6.5}$$

where n_i equals the number of groups i in the repeat unit or molecule, and volume V_i and free energy F_i are parameters for each chemical group (see page 320 in ref [105]). The units of F $(\text{cal}^{1/2}\text{cm}^{3/2}/\text{mol})$ and v^L (cm^3/mol) cancel so δ has proper units of $(\text{cal/cm}^3)^{1/2}$. We applied those same correlations here for the different asphaltenes and small molecules.

The accuracy of this correlation can be estimated for the small molecules for which solubility parameter values are available in the literature. These are also listed in Table 6.5. Agreement is within approximately 0.2 $(\text{J/cm}^3)^{1/2}$, except for a larger error for methylcyclohexane, a cyclic alkane. More advanced correlations, such as those for Hansen solubility parameters, are being conducted in the next phase of this work.

The original correlation does not contain values for sulfur, which can occur in asphaltene molecules as either a thiophene or sulfide. Thus we used solubility parameters listed in the literature for thiophene and

Table 6.5: Comparison of solubility parameters calculated using the correlation of Painter and Coleman [105] with local extensions, compared to experimental values [103, 107].

	δ in $(\text{cal/cm}^3)^{1/2}$		δ in $(\text{J/cm}^3)^{1/2}$	
compound	expt	correlation	expt	correlation
n-heptane	7.4	7.5	15.1	15.3
n-octane	7.5	7.55	15.3	15.45
toluene	8.9		18.2	
n-C_{22}	7.9	7.8	16.2	16.0
methylcyclohexane	7.8	6.1	16.0	12.45
naphthalene	9.9	9.7	20.3	19.3
1-methylnaphthalene			20.3	20.1
1,7-dimethylnaphthalene		9.4		19.3
phenanthrene		10.6		21.7
asphaltene 1		10.6		21.7
asphaltene 2		9.0		18.3

dimethyl sulfide [106] to estimate the required parameters. We solved the correlation equations for molar volume (6.3) and solubility parameter (6.4) for the unknown group volume and energy parameters. Thus we assumed that the correlation would be perfect for these two compounds. This imposed constraint is not likely correct, since the correlation is not precisely correct for any single compound; it is only sufficiently close for many of them. Neglecting such averaging, after substituting the literature values for v^L and F and applying the Painter–Coleman correlation for other groups, we obtained $F_i = 333$ $(\text{cal cm}^3)^{1/2}$/mol, $V_i = 24.7$ cm^3/mol (thiophene S) and $F_i = 235.1$ $(\text{cal cm}^3)^{1/2}$/mol, $V_i = 10.2$ cm^3/mol (sulfide S).

The Hildebrand solubility parameter for each model asphalt mixture can be estimated by combining the solubility parameters of each component. Normally the volume fraction is used as an appropriate weighting factor [105]. Here we achieve that via

$$\overline{\delta} = \sum_i \frac{w_i v_i^L / M_i}{\sum_j w_j v_j^L / M_j} \delta_i \tag{6.6}$$

The combination $w_i v_i^L / M_i$ converts to volume fraction from mass fraction w_i in the mixture (g/total), volume parameter v^L for compound i (cm^3/mol), and inverse of the molecular weight M_i (thus mol/g), leading to units of (cm^3/total) for each term. The net results for model asphalt mixtures are $\overline{\delta} = 17.2$ $(\text{J/cm}^3)^{1/2}$ (mixture 1) and $\overline{\delta} = 16.9$ $(\text{J/cm}^3)^{1/2}$ (mixture 2). These are towards the more alkane/dispersion-focused end of the range quoted by Redelius (15.3 to 23 $(\text{J/cm}^3)^{1/2}$). This feature is strongly influenced by the high mass fraction (and higher volume fraction) of the saturate component.

6.7 Discussion

The idea of asphalt consisting of different molecule types mixed over length scales of order 5–10nm is consistent with recent notions inferred from experiments [1, 94] that counter the older micellar model of asphalts. A resin-stabilized micelle of asphaltenes, suspended in saturate, would require larger length scales: 10–1000 nm for a single micelle, with solvent then surrounding it. Representing asphalt as a mixture of molecules with a range of polarities and chemical structures can still lead to microphase separation, but it also allows for mixing over the smaller length scales available in current molecular simulations.

We hypothesize that by comparing the behavior of the different asphaltenes in mixtures, it will be possible to learn what kinds of physical property differences can be traced to different asphaltene molecules. The results shown here already indicate that different asphaltenes at the same mass fraction can lead to different dilatometry (Figure 6.9) and heat capacity (Figure 6.10) results. The differences in molecule orientation indicate that such differences occur because different asphaltenes, such as those with long vs. short side chains, will pack together differently.

The low molecular weight recently surmised for asphaltenes [45] suggested to Groenzin and Mullins that the chemical diversity present in an asphaltene fraction must result in a wide range of different asphaltene molecules, each with a different key functionality (sulfur, nitrogen, oxygen, metal, etc.). Multiple groups on the same molecule were unlikely, since that would lead to each single asphaltene molecule being too large [45]. This is consistent with earlier suggestions of there being many types of asphaltenes [33] and of 10^5–10^6 total molecule types in petroleum [97, 108]. For the studies here, that suggests that it is important in follow-up work to chose a number of different types of asphaltene molecules for use within the same simulation. The real asphalt includes many different types of asphaltene molecules interacting together, and the simulations may be able to indicate how such packings and interactions lead to different physical behaviors than those that would be present if only 1 kind of asphaltene was employed.

The model compositions identified in this report are not yet optimal for representing asphalt properties accurately on the molecular level. The overall balance among saturate (oil), resin, and asphaltene was chosen in support of one study, but the overall hydrogen-to-carbon ratio is slightly high compared to measured values for SHRP asphalts (Table 7 in ref [9]). In contrast, the fractions of aromatic carbon are consistent with values listed in Table 2 of that report, while the fractions of aromatic hydrogen are slightly high (9.4 or 8% here, compared to 6.4–7.6, with one measurement of 8.7%). The total amount of asphaltene in the model mixtures (21 mass%) is consistent with the range 10.2%–27.4% reported more recently (Tables 3-4 and 4-6 of ref [97]). We conclude that the asphaltene concentration is reasonable, while the amount of linear saturated maltene is far in excess (59% vs 5–12% in experiment [97]). Adding cyclic alkanes is one way to decrease both H/C and the fraction of aromatic hydrogen atoms simultaneously. Making an explicit presence of naphthene aromatics and polar aromatics, at the expense of *n*-C_{22} and dimethylnaphthalene, will be pursued in future work. The low overall density (of order 0.9 g/cm^3 in comparison to 1.0 for SHRP asphalts [2]) follows from this composition difference, since asphaltenes have higher densities than saturated alkanes (straight or branched). Chemical distinctions between vacuum residue and asphalt could also lead

to differences in mole fraction between the results of Storm et al. [33] and SHRP asphalts [9]. For example, molecules in vacuum residue that can be degraded to liquids may be removed prior to the use of resid for producing asphalts for road materials, leaving a more aromatic residue.

Simulated densities lower than experimental values were also found by Rogel and Carbognani [95], who conducted molecular dynamics simulations of 12 different asphaltene structures. Each average asphaltene structure was chosen to match a different Venezuelan crude oil, and their architectures combine aspects of asphaltenes 1 and 2 (large cores of 8–20 condensed aromatic rings, with alkane side chains of *n*-C_4 to *n*-C_9). They ran their calculations using only asphaltene molecules, with 100 ps of sampling after extensive simulated annealing at constant volume. The predicted densities were of order 0.1–0.2 g/cm^3 lower than experimental values.

The size of individual molecules in the system is reasonable to a large extent. The asphaltene molecules, copied from recent hypotheses drawn from experimental molecular characterizations [31,45], have molecular weights of 885.25 and 995.6 g/mol (see Table 6.2). These are lower than those estimated using osmometry at higher concentrations but are consistent with mass spectroscopy [32] and fluorescence depolarization [44,45] experiments. The side group lengths (C_1 to C_3 for asphaltene 1, up to C_{12} for asphaltene 2) are within the ranges observed by RICO [27,28] in studies of Alberta asphaltenes.

The resin molecule (1,7-dimethylnaphthalene) is arguably both too small and insufficiently polar. Its aromatic:alkane balance also differs from that observed in NMR studies (Table 6.1). Groenzin and Mullins [45] report some overlap in molecular weight between asphaltenes and resins, and dimethylnaphthalene is significantly smaller than the asphaltene range. Dimethylnaphthalene also lacks heteroatom functionality. More polar resin molecules suggested by Masson and co-workers [109] will be investigated in future work. They alone will not necessarily correct the imbalance in aromatic:alkane ratio, however.

The *n*-C_{22} length is a compromise among the different sizes that can be inferred from NMR, as discussed at the beginning of this chapter. A range of sizes and structures (e.g. branches, rings) is likely present in real asphalts. Indeed, the reference [55] that showed *n*-C_{22} at the highest concentration also listed many other linear and branched alkanes being at only slightly concentrations.

The glass transition temperatures of SHRP core asphalts are mostly in the range of -20 to -25°C [51,97]. The glass transition occurs over a window of approximately $\Delta T_g \approx 30$°C, as measured in DSC experiments [51,97]. The simulation predictions of T_g for the simple mixtures are inconclusive at this time. The much smaller number of compounds makes it more likely that the glass transition should be sharper in the model systems than in real asphalts. The calculations here provide hints of a transition near 0°C, but the signal:noise ratio of those results is insufficient to quote a precise value. Measurements of asphaltene concentration effects on T_g [51] will provide useful future tests of the synergy between model and real asphalt mixtures.

6.7.1 MD vs MC

Unfortunately for the project, the need for the change in chosen method (from Monte Carlo to molecular dynamics) took away from time that could have been otherwise spent on improving mixture composition.

The advantages of molecular dynamics over Monte Carlo for equilibrating and sampling the average properties of asphalt mixtures is now recognized for use in future molecular modeling studies. Both methods should work in theory. We hypothesize that MD is more effective for these systems because of the difficulty of moving such complicated molecules closer to one another. MD rearranges all molecules at once, while MC is usually limited to moves that affect one (or a few) molecules at a time. The probability of consecutive MC motions being chosen that replicate a small set of MD steps is relatively low, given the many possible moves.

6.7.2 Ongoing Issues

Two flaws in the molecular dynamics simulations were recognized after the project end date was reached. One is that the settings for the neighbor list update (which atoms are near to which others) were not set to optimal values. The result is that some interatomic energies were neglected during the course of integrating the differential equations defined by the equations of motion. These energies were most likely small, since they correspond to the most distant atom pairs that would still interact. They likely lead to inaccuracy in the energy fluctuations, however, and thus to incorrect heat capacity predictions. Better choices for these settings have been employed in followup work. The second flaw is that so-called "improper" torsion angles were employed for the dimethylnaphthalene but not for the asphaltenes. This angle creates a contribution to the total energy that helps to ensure that so-called sp2 carbons — those that occur when there are double bonds or aromatic rings — maintain a planar configuration. As a result, the asphaltene molecules were more flexible (perpendicular to the plan of aromatic rings) than would be expected. This flexibility is a potential cause of the wide range of intramolecular orientation angles experienced by the asphaltene. The required improper torsion angles have been restored for subsequent calculations.

Chapter 7

Conclusions

The calculations described in this report constitute one of the first attempts to conduct fully atomistic molecular simulations on a multicomponent mixture whose chemical composition is chosen to be reflective of compounds found in real asphalts. Different molecules were chosen to reflect the maltene, resin, asphaltene components, and the ultimate mixtures displayed properties that were similar to those of real asphalts, but not exactly the same.

The overall outcomes of this work are best described in the context of the original tasks. Subtle issues that came to light only as the work was being completed created unanticipated noise in the simulation results (see sections 6.7 and 6.7.2). Those issues are summarized here and are being addressed in follow-up work.

7.1 Conclusions by Task

Task 1. Method Validation

These calculations were described in chapter 4. Monte Carlo methods for simulating small molecules were found to lead to reasonable agreement in the predicted density and coefficient of thermal expansion (change in density with temperature). Heat capacity predictions were approximately 2–3 times too high, but the extent of the overprediction via Monte Carlo was consistent across many different molecules. Glass transition data could not be found in the literature for the kinds of small molecules chosen to reflect subsets of asphalt chemistry, and measurements on experimental realizations of the model systems were not possible during the project. The simulation data (density vs. temperature) showed a single slope, rather than the break in slope that is characteristic of a glass transition. This single slope is consistent with the absence of experimental T_g data. In total, we conclude that the OPLS all-atom force field [74] is sufficiently accurate for the current project.

Task 2. Initial Mixture Simulations

An initial mixture of three small molecules was constructed. Detailed experimental results in the literature provided an opportunity to confirm the ability of the simulation method to predict mixture properties. Monte Carlo calculations at several compositions, temperatures, and pressures were conducted (chapter 5).

The overall volume increased with increasing temperature and increasing methylcyclohexane content, and it decreased with increased pressure. Overall agreement with experimental results was better than simple estimates using an ideal mixing rule. We conclude that the Monte Carlo simulation methods are capable of describing mixtures.

Tasks 3. Mixture Composition Iteration and 4. Other SHRP Core Asphalts

Model asphalt mixtures were constructed using two different asphaltene models at comparable mass fractions of asphaltene, resin, and maltene. The two asphaltenes differed significantly in their underlying chemistry (section 6.1) and slightly in size, leading to different sizes for the two mixtures. Despite its success with smaller molecules, the Monte Carlo approach was inadequate for equilibrating the overall asphalt mixture, and molecular dynamics simulations needed to be used instead.

Averaged estimates of density and heat capacity were found to depend on temperature in different ways for the two mixtures (sections 6.3 and 6.4). Mixture 2 shows some evidence of a glass transition below 0°C, while noise in mixture 1 makes the T_g location hard to define. Orientation calculations indicate that molecules pack together differently in the two mixtures. Both asphaltenes pack together in mixtures at angles that deviate from a random distribution. Asphaltene 1 molecules are more likely to pack parallel to one another, while asphaltene 2 molecules show a broader range of characteristic packing angles. The 1,7-dimethylnaphthalene molecules in mixture 1 also show an enhanced tendency to pack parallel to one another, while in mixture 2 they tend to pack randomly except for a decreased probability of being perpendicular. Similar trends were found for intermolecular packing between both asphaltenes and 1,7-dimethylnaphthalene. In total, both systems contained many molecule pairs in which packing was at angles far from parallel.

7.2 Issues Resolved in Subsequent Work

Several weaknesses in the calculations were identified when writing this final report. Section 6.7 describes inadequacies in the overall composition. The overall saturate concentration is too high, leading to a lower mixture density since saturates are lower in mass density than aromatics. The 1,7-dimethylnaphthalene acts more as a naphthene aromatic than as a resin, and (looking towards future work) it is now considered part of the maltene, with *n*-C_{22}. A gap thus exists in the polarity range of the mixture, which can be identified by the solubility parameters (section 6.6).

Several molecular dynamics simulation parameters were found to be set to non-optimal values, as discussed in section 6.7.2. A consequence of one parameter choice was inaccurate heat capacity estimation due to excessively large energy fluctuations. Another parameter choice led to asphaltene molecules that were too "floppy" due to a lack of improper torsion angle potentials, which are intended to maintain planarity. The relatively larger intramolecular orientation angles for the asphaltenes compared to dimethylnaphthalene (Figures 6.14 and 6.15) are a result of these settings. Corrected parameters and revised calculations are being used in the next phases of the research.

Appendix D: Research Exchanges

The following research exchanges and presentations occurred as direct results of this project.

- Prof. Greenfield visited Turner-Fairbanks Highway Research Center in Virginia, as part of an October 2004 tour sponsored by the URI Transportation Center, and discussed the project with Dr. Ernest Bastian and Dr. Jack Youtcheff of TFHRC. Both were enthusiastic about the possible outcomes, and Dr. Youtcheff in particular provided excellent suggestions about additional chemical considerations (see solubility parameter discussion in chapter 6, for example).

- A poster presentation entitled "Developing Model Asphalt Systems Using Molecular Simulation" was presented at the Annual Meeting of the American Institute of Chemical Engineers (AIChE), November 7-12, 2004 in Austin, TX. Ms. Zhang made the presentation and was accompanied by Prof. Greenfield. She received several good questions and was encouraged about her research direction. A petroleum researcher from Institut de Petrole in France was particularly interested.

- One followup item from the TFHRC visit was that Prof. Greenfield was invited to observe the annual review of the FHWA-funded asphalt research programs conducted at the Western Research Institute. This full-day meeting, conducted immediately after the Transportation Research Board conference, provided an opportunity for Greenfield to meet the WRI researchers in person for the first time. WRI Principal Investigator Dr. Ray Robertson had become aware of the research project described here via the TFHRC scientists, and he included it in his summary at TRB of new research directions in asphalts.

- Prof. Greenfield delivered a presentation entitled *Towards Design of Model Asphalts by Molecular Simulation* at the Petersen Asphalt Conference (June 20–22, Cheyenne, WY). This conference "brings together top researchers, highway officials, producers and others who are working to advance the specification and performance of petroleum asphalts. For more than 40 years, research presented and discussed at the Petersen Asphalt Research Conference has led to safer, longer-lasting and more cost-effective highways throughout the world." (Quote taken from the conference web page at `http://www.petersenasphaltconference.org/`.) The presentation was well received and led to discussions of potential research collaborations.

Bibliography

[1] J. C. Petersen, R. E. Robertson, J. F. Branthaver, P. M. Harnsberger, J. J. Duvall, S. S. Kim, D. A. Anderson, D. W. Christiansen, and H. U. Bahia, Binder characterization and evaluation, volume 1, Technical Report SHRP-A-367, Strategic Highway Research Program, 1994, Available on-line from http://gulliver.trb.org/publications/shrp/SHRP-A-367.pdf.

[2] J. F. Branthaver, J. C. Petersen, R. E. Robertson, J. J. Duvall, S. S. Kim, P. M. Harnsberger, T. Mill, E. K. Ensley, F. A. Barbour, and J. F. Schabron, Binder characterization and evaluation, volume 2: Chemistry, Technical Report SHRP-A-368, Strategic Highway Research Program, 1994, Available on-line from http://gulliver.trb.org/publications/shrp/SHRP-A-368.pdf.

[3] David A. Anderson, Donald W. Christiansen, Hussain U. Bahia, Raj Dongre, M. G. Sharma, Charles E. Antle, and Joe Button, Binder characterization and evaluation, volume 3: Physical characterization, Technical Report SHRP-A-369, Strategic Highway Research Program, 1994, Available on-line from http://gulliver.trb.org/publications/shrp/SHRP-A-369.pdf.

[4] J. C. Petersen, R. E. Robertson, J. F. Branthaver, P. M. Harnsberger, J. J. Duvall, S. S. Kim, D. A. Anderson, D. W. Christiansen, H. U. Bahia, R. Dongre, C. E. Antle, M. G. Sharma, J. W. Button, and C. J. Glover, Binder characterization and evaluation, volume 4: Test methods, Technical Report SHRP-A-370, Strategic Highway Research Program, 1994, Available on-line from http://gulliver.trb.org/publications/shrp/SHRP-A-370.pdf.

[5] Arthur M. Usmani, *Asphalt Science and Technology*, New York: Marcel Dekker, 1997.

[6] Thomas W. Kennedy, Gerald A. Huber, Edward T. Harrigan, Ronald J. Cominsky, Charles S. Hughes, Harold Von Quintus, and James S. Moulthrop, Superior performing asphalt pavements (Superpave): The product of the SHRP asphalt research program, Technical Report SHRP-A-410, Strategic Highway Research Program, 1994, Available on-line from http://gulliver.trb.org/publications/shrp/SHRP-A-410.pdf.

[7] Michael L. Greenfield, George A. Lavoie, Carol S. Smith, and Eric W. Curtis, Macroscopic model of the D86 fuel volatility procedure, *SAE paper 982724*, (1998).

[8] Michael L. Greenfield, Development of model fuels with volatilities that resemble those of real fuels, *Fuel Chemistry Division Preprints (American Chemical Society)*, **47**:209–210 (2002).

[9] P. W. Jennings, J. A. Pribanic, M. A. Desando, M. F. Raub, F. Stewart, J. Hoberg, R. Moats, J. A. Smith, T. M. Mendes, M. McGrane, B. Fanconi, D. L. VanderHart, and W. F. Manders, Binder characterization and evaluation by nuclear magnetic resonance spectroscopy, Technical Report SHRP-A-335, Strategic Highway Research Program, 1993, Available on-line from http://gulliver.trb.org/publications/shrp/SHRP-A-335.pdf.

[10] Thomas P. Turner and Jan F. Branthaver, DSC studies of asphalts and asphalt components, in Arthur M. Usmani, editor, *Asphalt Science and Technology*, pages 59–101, New York: Marcel Dekker, 1997.

[11] Liqun Zhang and Michael L. Greenfield, Relaxation time, diffusion, and viscosity analysis of model asphalt systems using molecular simulation, *J. Chem. Phys.*, **127**:194502 (2007).

[12] John D. Ferry, *Viscoelastic Properties of Polymers*, New York: John Wiley & Sons, 3rd edition, 1980.

[13] Joel R. Fried, *Polymer Science and Technology*, Upper Saddle River, NJ: Prentice-Hall PTR, 1995.

[14] Robert Q. Kluttz and Raj Dongré, Effect of SBS polymer modification on the low-temperature cracking of asphalt pavements, in Arthur M. Usmani, editor, *Asphalt Science and Technology*, pages 217–233, New York: Marcel Dekker, 1997.

[15] Fred N. Finn, Margot T. Yapp, John S. Coplantz, and Amer Z. Durrani, Asphalt properties and relationship to pavement performance: Literature review, Technical Report SHRP-A-314, Strategic Highway Research Program, 1990, Available on-line from http://gulliver.trb.org/publications/shrp/SHRP-A-314.pdf.

[16] P. W. Jennings, Jacqueline Fonnesbeck, Jennifer Smith, and J. A. S. Pribanic, Asphalt chemistry: An NMR investigation of the benzylic hydrogens and oxidation, in Arthur M. Usmani, editor, *Asphalt Science and Technology*, pages 1–10, New York: Marcel Dekker, 1997.

[17] *Superpave Performance Graded Asphalt Binder Specification and Testing*, Lexington, KY: Asphalt Institute, manual series SP-1 edition, 1995.

[18] J. W. H. Oliver and P. F. Tredrea, Relationships between asphalt rut resistance and binder rheological properties, *J. Assoc. Asphalt Pav. Technol.*, **67**:623–643 (1998).

[19] S. C. Huang, J. F. Branthaver, R. E. Robertson, and S. S. Kim, Effect of film thickness on the rheological properties of asphalts in contact with aggregate surface, *Transportation Research Record*, **1638**:31–39 (1998).

[20] Aroon Shenoy, Developing unified rheological curves for polymer-modified asphalts – Part I. Theoretical analysis, *Mater. Struct.*, **33**:425–429 (2000).

[21] Aroon Shenoy, Developing unified rheological curves for polymer-modified asphalts – Part II. Experimental verification, *Mater. Struct.*, **33**:430–437 (2000).

[22] J. C. Petersen, Chemical composition of asphalt as related to asphalt durability: State of the art, *Transp. Res. Rec.*, **999**:13–30 (1984).

[23] R. Edgar, Ten year performance of asphalt additive test sections: Lava Butte Road — Fremont highway junction section, Technical Report Report OR-RD-99-08, FHWA, U.S. Department of Transportation, 1998.

[24] Freddy L. Roberts, Prithvi S. Kandhal, E. Ray Brown, Dah-Yinn Lee, and Thomas W. Kennedy, *Hot Mix Asphalt Materials, Mixture Design, and Construction*, Lanham, Maryland: National Asphalt Pavement Association, 2nd edition, 1996.

[25] J. G. Speight, *The Chemistry and Technology of Petroleum*, New York: Marcel Dekker, 1999.

[26] James W. Bunger and Norman C. Li, *Chemistry of Asphaltenes*, Washington, DC: American Chemical Society, advances in chemistry series, no 195 edition, 1981.

[27] Otto P. Strausz, Thomas W. Mojelsky, and Elizabeth M. Lown, The molecular structure of asphaltene: an unfolding story, *Fuel*, **71**:1355–1363 (1992).

[28] Otto P. Strausz, Thomas W. Mojelsky, Farhad Faraji, Elizabeth M. Lown, and Ping'an Peng, Additional structural details on Athabasca asphaltene and their ramifications, *Energy Fuels*, **13**:207–227 (1999).

[29] Otto P. Strausz, Thomas W. Mojelsky, Elizabeth M. Lown, Isabelle Kowalewski, and Françoise Behar, Structural features of Boscan and Duri asphaltenes, *Energy Fuels*, **13**:228–247 (1999).

[30] Ping'an Peng, Angelina Morales-Izquierdo, Elizabeth M. Lown, and Otto P. Strausz, Chemical structure and biomarker content of Jinghan asphaltenes and kerogens, *Energy Fuels*, **13**:248–265 (1999).

[31] Levent Artok, Yan Su, Yoshihisa Hirose, Masahiro Hosokawa, Satoru Murata, and Masakatsu Nomura, Structure and reactivity of petroleum-derived asphaltene, *Energy Fuels*, **13**:287–296 (1999).

[32] David A. Storm, Stephen J. DeCanio, Maureen M. DeTar, and Vincent P. Nero, Upper bound on number average molecular weight of asphaltenes, *Fuel*, **69**:735–738 (1990).

[33] D. A. Storm, J. C. Edwards, S. J. DeCanio, and E. Y. Sheu, Molecular representations of Ratawi and Alaska north slope asphaltenes based on liquid- and solid-state NMR, *Energy Fuels*, **8**:561–566 (1994).

[34] Stéphane Gillet, Patrice Rubini, Jean-Jacques Delpuech, Jean-Claude Escalier, and Patrice Valentin, Quantitative carbon-13 and proton nuclear magnetic resonance spectroscopy of crude oil and petroleum products. I Some rules for obtaining a set of reliable structural parameters, *Fuel*, **60**:221–225 (1981).

[35] Stéphane Gillet, Patrice Rubini, Jean-Jacques Delpuech, Jean-Claude Escalier, and Patrice Valentin, Quantitative carbon-13 and proton nuclear magnetic resonance spectroscopy of crude oil and petroleum products. 2. Average structure parameters of representative samples, *Fuel*, **60**:226–230 (1981).

[36] Sara Pekerar, Teresa Lehmann, Bernardo Méndez, and Sócrates Acevedo, Mobility of asphaltene samples studied by ^{13}C NMR spectroscopy, *Energy Fuels*, **13**:305–308 (1999).

[37] Z. Frakman, T. M. Ignasiak, E. M. Lown, and O. P. Strausz, Oxygen compounds in Athabasca asphaltene, *Energy Fuels*, **4**:263–270 (1990).

[38] Thomas K. Green, Paul Whitley, Kanning Wu, William G. Lloyd, and Li Zhui Gan, Structural characterization of sulfur compounds in petroleum by S-methylation and ^{13}C NMR spectroscopy, *Energy Fuels*, **8**:244–248 (1994).

[39] Eric Y. Sheu, K. S. Liang, S. K. Sinha, and R. E. Overfield, Polydispersity analysis of asphaltene solutions in toluene, *J. Coll. Int. Sci.*, **153**:399–410 (1992).

[40] P. Thiyagarajan, Jerry E. Hunt, Randall E. Winans, Ken B. Anderson, and Jeffrey T. Miller, Temperature-dependent structural changes of asphaltenes in 1-methylnaphthalene, *Energy Fuels*, **9**:829–833 (1995).

[41] Eric Y. Sheu, D. A. Storm, and M. B. Shields, Dielectric response of asphaltenes in solvent, *Energy Fuels*, **8**:552–556 (1994).

[42] D. A. Storm, E. Y. Sheu, M. M. DeTar, and R. J. Barresi, A comparison of the macrostructure of Ratawi asphaltenes in toluene and vacuum residue, *Energy Fuels*, **8**:567–569 (1994).

[43] J. T. Miller, R. B. Fisher, P. Thiyagarajan, R. E. Winans, and J. E. Hunt, Subfractionation and characterization of Mayan asphalt, *Energy Fuels*, **12**:1290–1298 (1998).

[44] Henning Groenzin and Oliver C. Mullins, Asphaltene molecular size and structure, *J. Phys. Chem. A*, **103**:11237–11245 (1999).

[45] Henning Groenzin and Oliver C. Mullins, Molecular size and structure of asphaltenes from various sources, *Energy Fuels*, **14**:677–684 (2000).

[46] Karen Schou Pedersen, Ann Lisbeth Blilie, and Knut Kristian Meisingset, PVT calculations of petroleum reservoir fluids using measured and estimated compositional data for the plus fraction, *Ind. Eng. Chem. Res.*, **31**:1378–1384 (1992).

[47] Aroon Shenoy, Unifying asphalt rheological data using the material's volumetric flow rate, *J. Mater. Civ. E.*, **13**:260–273 (2001).

[48] Aroon Shenoy, Validating the generality and predictive ability of unified rheological curves for unmodified paving asphalts, *Constr. Build. Mater.*, **14**:325–339 (2000).

[49] Aroon Shenoy, Prediction of high temperature rheological properties of aged asphalts from the flow data of the original unaged samples, *Constr. Build. Mater.*, **16**:509–517 (2002).

[50] D. A. Netzel, T. F. Turner, F. P. Miknis, and J. Soule, Molecular dynamics and the structure of asphalts and modified asphalts at low temperatures, *Am. Chem. Soc., Fuel Chem. Div. Prepr.*, **41**:1260–1261 (1996).

[51] Daniel A. Netzel, Francis P. Miknis, Kenneth P. Thomas, J. Calhoun Wallace Jr., and Clinton H. Butcher, Molecular motions and rheological properties of asphalts: An NMR study, in Arthur M. Usmani, editor, *Asphalt Science and Technology*, pages 11–58, New York: Marcel Dekker, 1997.

[52] Christopher H. Domke, Richard R. Davison, and Charles J. Glover, Effect of asphaltenes on SHRP superpave specifications, *Energy Fuels*, **13**:340–345 (1999).

[53] Martin H. Sadd, Qingli Dai, Venkitanarayanan Parameswaran, and Arun Shukla, Microstructural simulation of asphalt materials: Modeling and experimental studies, *J. Mater. Civ. E.*, **16**:107–115 (2004).

[54] Z. You and W. G. Buttlar, Discrete element modeling to predict the modulus of asphalt concrete mixtures, *J. Mater. Civ. E.*, **16**:140–146 (2004).

[55] I. Kowalewski, M. Vandenbroucke, A. Y. Huc, M. J. Taylor, and J. L. Faulon, Preliminary results on molecular modeling of asphaltenes using structure elucidation programs in conjunction with molecular simulation programs, *Energy Fuels*, **10**:97–107 (1996).

[56] Michael T. Klein, Monte Carlo simulation of asphaltene structure and reactivity, *Am. Chem. Soc., Petrol. Chem. Div. Prepr.*, **39**:208–209 (1994).

[57] Juan Murgich, Jesús Rodríguez M., Alejandro Izquierdo, Lante Carbognani, and Estrella Rogel, Interatomic interactions in the adsorption of asphaltenes and resins on kaolinite calculated by molecular dynamics, *Energy Fuels*, **12**:339–343 (1998).

[58] Jianzhong Wu, John M. Prausnitz, and Abbas Firoozabadi, Molecular-thermodynamic framework for asphaltene-oil equilibria, *AIChE J.*, **44**:1188–1199 (1998).

[59] Jianzhong Wu, John M. Prausnitz, and Abbas Firoozabadi, Molecular thermodynamics of asphaltene precipitation in reservoir fluids, *AIChE J.*, **46**:197–209 (2000).

[60] Matthew Neurock and Michael T. Klein, Monte Carlo simulation of asphaltene structure, reactivity and reaction pathways, in T.F. Yen and G. V. Chilingarian, editors, *Asphalts and Asphaltenes (Developments in Petroleum Science Series)*, volume 40B, pages 59–101, New York: Elsevier, 2000.

[61] Estrella Rogel and Olga León, Study of the adsorption of alkyl-benzene-derived amphiphiles on an asphaltene surface using molecular dynamics simulations, *Energy Fuels*, **15**:1077–1086 (2001).

[62] S. Li, Y. Li, and J. B. Metcalf, Enhancement of asphalt pavement evaluation using Monte Carlo simulation and accelerated pavement testing, *J. Testing Eval.*, **30**:392–399 (2002).

[63] Matthew Neurock, Christian Libanati, Abhash Nigam, and Michael T. Klein, Monte Carlo simulation of complex reaction systems: Molecular structure and reactivity in modeling heavy oils, *Chem. Eng. Sci.*, **45**:2083–2088 (1990).

[64] Thomas F. Petti, Daniel M. Trauth, Scott M. Stark, Matthew Neurock, Muzaffer Yasar, and Michael T. Klein, CPU issues in the representation of the molecular structure of petroleum resid through characterization, reaction, and Monte Carlo modeling, *Energy Fuels*, **8**:570–575 (1994).

[65] Daniel M. Trauth, Scott M. Stark, Thomas F. Petti, Matthew Neurock, and Michael T. Klein, Representation of the molecular structure of petroleum resid through characterization and Monte Carlo modeling, *Energy Fuels*, **8**:576–580 (1994).

[66] Gary A. Carlson and Jean-loup Faulon, Applications of molecular modeling in coal research, *Am. Chem. Soc., Fuel Chem. Div. Prepr.*, **39(1)**:18–21 (1994).

[67] Juan Murgich, Jesús Rodríguez M., and Yosslen Aray, Molecular recognition and molecular mechanics of micelles of some model asphaltenes and resins, *Energy Fuels*, **10**:68–76 (1996).

[68] Juan Murgich, José A. Abanero, and Otto P. Strausz, Molecular recognition in aggregates formed by asphaltene and resin molecules from the Athabasca oil sand, *Energy Fuels*, **13**:278–286 (1999).

[69] Alexey I. Victorov and Abbas Firoozabadi, Thermodynamic micellization model of asphaltene precipitation from petroleum fluids, *AIChE J.*, **42**:1753–1764 (1996).

[70] Alexey I. Victorov and Natalia A. Smirnova, Description of asphaltene polydispersity and precipitation by means of thermodynamic model of self-assembly, *Fluid Phase Equilib.*, **158–160**:471–480 (1999).

[71] Daan Frenkel and Berend Smit, *Understanding Molecular Simulation*, San Diego: Academic Press, second edition, 2002.

[72] M. P. Allen and D. J. Tildesley, *Computer Simulation of Liquids*, New York: Oxford University Press, 1987.

[73] Michael Kotelyanskii and Doros N. Theodorou, *Simulation Methods for Polymers*, New York: Marcel Dekker, 2004.

[74] W. L. Jorgensen, D. S. Maxwell, and J. Tirado-Rives, Development and testing of the OPLS all-atom force field on conformational energetics and properties of organic liquids, *J. Am. Chem. Soc.*, **118**:11225–11236 (1996).

[75] N. A. McDonald and W. L. Jorgensen, Development of an all-atom force field for heterocycles. Properties of liquid pyrrole, furan, diazoles, and oxazoles, *J. Phys. Chem. B*, **102**:8049–8059 (1998).

[76] Doros N. Theodorou, Travis D. Boone, Lawrence R. Dodd, and Kevin F. Mansfield, Stress tensor in model polymer systems with periodic boundaries, *Makromol. Chem. Theory Simul.*, **2**:191–238 (1993).

[77] Suchira Sen, Sanat K. Kumar, and Pawel Keblinski, Viscoelastic properties of polymer melts from equilibrium molecular dynamics simulations, *Macromolecules*, **38**:650–653 (2005).

[78] O. Byutner and Grant D. Smith, Viscoelastic properties of polybutadiene in the glassy regime from molecular dynamic simulations, *Macromolecules*, **35**:3769–3771 (2002).

[79] Marcus G. Martin and J. Ilja Siepmann, Transferable potentials for phase equilibria. 1. United-atom description of n-alkanes, *J. Phys. Chem. B*, **102**:2569–2577 (1998).

[80] Marcus G. Martin and J. Ilja Siepmann, Novel configurational-bias Monte Carlo method for branched molecules. Transferable potentials for phase equilibria. 2. United-atom description of branched alkanes, *J. Phys. Chem. B*, **103**:4508–4517 (1999).

[81] Bin Chen and J. Ilja Siepmann, Transferable potentials for phase equilibria. 3. Explicit-hydrogen description of normal alkanes, *J. Phys. Chem. B*, **103**:5370–5379 (1999).

[82] Collin D. Wick, Marcus G. Martin, and J. Ilja Siepmann, Transferable potentials for phase equilibria. 4. United-atom description of linear and branched alkenes and alkylbenzenes, *J. Phys. Chem. B*, **104**:8008–8016 (2000).

[83] Bin Chen, Jeffrey J. Potoff, and J. Ilja Siepmann, Monte Carlo calculations for alcohols and their mixtures with alkanes. Transferable potentials for phase equilibria. 5. United-atom description of primary, secondary, and tertiary alcohols, *J. Phys. Chem. B*, **105**:3093–3104 (2001).

[84] Gustav Egloff, *Physical Constants of Hydrocarbons*, New York: Reinhold Publishing Corporation (American Chemical Society Monograph Series), 1947.

[85] Frederick D. Rossini, Kenneth S. Pitzer, Raymond L. Arnett, Rita M. Braun, and George C. Pimentel, *Selected Values of Physical and Thermodynamic Properties of Hydrocarbons and Related Compounds*, Pittsburgh: Carnegie Press, 1953.

[86] A. Baylaucq, C. Boned, P. Dauge, and B. Lagourette, Measurements of the viscosity and density of three hydrocarbons and the three associated binary mixtures versus pressure and temperature, *Int. J. Thermophys.*, **18**:3–23 (1997).

[87] A. Baylaucq, P. Daugé, and C. Boned, Viscosity and density of the ternary mixture heptane + methylcyclohexane + 1-methylnaphthalane, *Int. J. Thermophys.*, **18**:1089–1107 (1997).

[88] Robert C. Reid, John M. Prausnitz, and Bruce E. Poling, *The Properties of Gases and Liquids*, New York: McGraw-Hill, 4th edition, 1987.

[89] John A. Dean, *Lange's Handbook of Chemistry*, New York: McGraw-Hill, 13th edition, 1985.

[90] P.J. Linstrom and W.G. Mallard, *NIST Chemistry WebBook, NIST Standard Reference Database Number 69*, Gaithersburg MD: National Institute of Standards and Technology, 2005, http://webbook.nist.gov.

[91] H. L. Finke, J. F. Messerly, S. H. Lee, A. G. Osborn, and D. R. Rouslin, Comprehensive thermodynamic studies of seven aromatic hydrocarbons, *J. Chem. Thermodynamics*, **9**:937–956 (1977).

[92] J. K. Holzhauer and W. T. Ziegler, Temperature dependence of excess thermodynamic properties of *n*-heptane–toluene, methylcyclohexane–toluene, and *n*-heptane–methylcyclohexane systems, *J. Phys. Chem.*, **79**:590–604 (1975).

[93] Yogesh Srivastava and Michael L. Greenfield, Development of OPLS-style force field parameters for aromatic ketones, aromatic ethers, and substituted thiophenes, *J. Comput. Chem.*, (2005), in preparation.

[94] P. G. Redelius, Solubility parameters and bitumen, *Fuel*, **79**:27–35 (2000).

[95] E. Rogel and L. Carbognani, Density estimation of asphaltenes using molecular dynamics simulations, *Energy Fuels*, **17**:378–386 (2003).

[96] Liqun Zhang and Michael L. Greenfield, Effects of polymer modification on properties and microstructure of model asphalt systems, *Energy Fuels*, **22**:3363–3375 (2008).

[97] Raymond E. Robertson, Jan F. Branthaver, P. Michael Harnsberger, J. Claine Petersen, Samuel M. Dorrence, John F. McKay, T. Fred Turner, A. Troy Pauli, Shin-Che Huang, Jung-Do Huh, Jane E. Tauer, Kenneth P. Thomas, Daniel A. Netzel, Francis P. Miknis, Theresa Williams, John J. Duvall, F. Alan Barbour, and Christine Wright, Fundamental properties of asphalts and modified asphalts

volume I: Interpretive report, Technical Report FHWA-RD-99-212, Federal Highway Administration, 2001.

[98] Lawrence J. Lowden and David Chandler, Theory of intermolecular pair correlations for molecular liquids. Applications to the liquids carbon tetrachloride, carbon disulfide, carbon diselenide, and benzene, *J. Chem. Phys.*, **61**:5228–5241 (1974).

[99] A. H. Narten, X-ray diffraction pattern and models of liquid benzene, *J. Chem. Phys.*, **67**:2102–2108 (1977).

[100] Liqun Zhang and Michael L. Greenfield, Molecular orientation in model asphalts using molecular simulation, *Energy Fuels*, **21**:1102–1111 (2007).

[101] Per Redelius, Bitumen solubility model using Hansen solubility parameter, *Energy Fuels*, **18**:1087–1092 (2004).

[102] J. M. Prausnitz, R. Lichtenthaler, and E. G. Azevedo, *Molecular Thermodynamics of Fluid Phase Equilibria*, Englewood Cliffs, NJ: Prentice-Hall, 1986.

[103] Allan F. M. Barton, *CRC Handbook of Solubility Parameters and Other Cohesion Parameters*, Boca Raton, FL: CRC Press, 1983.

[104] Iradj Rahimian and Günther Zenke, organischer Lösemittel gegenüber Bitumen, *Bitumen*, **1**:2–8 (1986).

[105] Paul C. Painter and Michael M. Coleman, *Fundamentals of Polymer Science*, Boca Raton, FL: CRC Press, 2nd edition, 1997.

[106] J.-L. M. Abboud and R. Notario, Critical compilation of scales of solvent parameters. Part I. Pure, non-hydrogen bond donor solvents, *Pure Appl. Chem*, **71**:645–718 (1999).

[107] T. E. Daubert, R. P. Danner, H. M. Sibal, C. C. Stebins, R. L. Rowley, W. V. Wilding, J. L. Oscarson, M. E. Adams, and T. L. Marshall, *Physical and Thermodynamic Properties of Pure Chemicals: Evaluated Process Design Data*, Philadelphia: Taylor & Francis, 1999.

[108] I. A. Wiehe and K. S. Liang, Asphaltenes, resins, and other petroleum macromolecules, *Fluid Phase Equilib.*, **117**:201–210 (1996).

[109] J.-F. Masson and M. A. Lacasse, A review of adhesion mechanisms at the crack sealant/asphalt concrete interface, in A. T. Wolf, editor, *3rd International RILEM Symposium on Durability of Building and Construction Sealants*, pages 259–274, Paris: RILEM, 2000.